



**Faculty of Graduate Studies**

**Synthesis, Characterization and Biological Applications of  
Transition Metals (II) Levofloxacin Complexes with  
Different Bioactive Nitrogen Based Ligands.**

تحضير، تشخيص ودراسة الفعالية الحيوية لمركبات تحتوي عناصر انتقالية ثنائية الشحنة ومادة الليفوفلوكساسين مع بعض القواعد النيتروجينية النشطة حيوياً.

This Thesis was submitted in partial fulfillment of the requirements for the Master's Degree in Applied Chemistry, at the Faculty of Graduate Studies, Birzeit University, Ramallah, Palestine.

**Asem Mubarak**

**Under Supervision of**

**Prof. Hijazi Abu Ali**

**August, 2020**

**Synthesis, Characterization and Biological Applications of  
Transition Metals (II) Levofloxacin Complexes with  
Different Bioactive Nitrogen Based Ligands.**

**By**

**Asem Mubarak**

This thesis was defended successfully on 29/08/2020 and approved by:

Committee Members

Signature

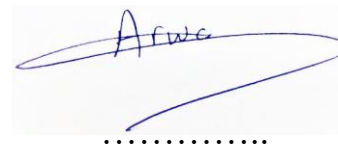
Prof. Hijazi Abu Ali



.....

Supervisor

Department of Chemistry, Birzeit University



.....

Dr. Arwa Abu Khweek

Member of thesis committee

Department of Biology and Biochemistry, Birzeit University



.....

Dr. Wadie Sultan

Member of thesis committee

Department of Chemistry, Al-Quds University

## Acknowledgements

I want to begin by thanking Allah the Almighty for giving me the strength to complete this work. I would like to express my deepest gratitude and appreciation to my supervisor Prof. Hijazi Abu Ali for his endless encouragement throughout my research period. I benefited greatly from his critique, instructions, advice and supervision.

I also would like to thank the thesis committee; Dr. Wadie Sultan and Dr. Arwa Abu Khweek for their valuable time and efforts in reading and discussing the thesis.

To my colleagues in the Chemistry Department, thank you for your continuous support, especially Dr. Ibrahim Shalash, Mr. Azmi Dudin, Dr. Saleh Suliman and Mr. Amer Jafar, as well as Fatima Hamdan and Sabreen Tawafsha. Also, my utmost appreciation goes out to Mr. Munther Matani and Mr. Rateb Mohammad for their patience, support and help in completing the biological activity part of my thesis.

My deepest gratitude and indebtedness go out to my dear friend Mr. Ibrahim Elian, for his support throughout my educational journey. I also

would like to thank my friends Dr. Mohanad Darawsheh and Mr. Ayamn Barghouti for their encouragement and help.

Special appreciation to, Birzeit Pharmaceutical Company, Pharmacare and Jerusalem Pharmaceutical Company for providing us with some necessary chemicals and supplies to complete the present work.

My wife Ruba Mubarak, thank you for your endless patience and support, I could not have achieved this without you.

I would like to deeply thank my father, mother, daughters (Layan, Lana and Tala), brothers, sisters and friends for their encouragement and support.

Finally, I would like to dedicate this work to my beloved family

Asem Mubarak

August, 2020

## Table of Contents

<b>Acknowledgements.....</b>	<b>III</b>
<b>Table of Contents .....</b>	<b>V</b>
<b>List of Figures .....</b>	<b>IX</b>
<b>List of Tables.....</b>	<b>XIII</b>
<b>List of Schemes .....</b>	<b>XV</b>
<b>Abbreviations.....</b>	<b>XVI</b>
<b>Abstract .....</b>	<b>XVII</b>
<b>ملخص بالعربية .....</b>	<b>XIX</b>
<b>1. Introduction .....</b>	<b>1</b>
<i>1.1. Theoretical background.....</i>	<i>1</i>
<i>1.2 Metals in biological systems .....</i>	<i>3</i>
<i>1.3 Zinc.....</i>	<i>4</i>
1.3.1 Zinc as an element .....	4
1.3.2 Zinc in biological systems .....	5
1.3.3 Zinc metal in medicine .....	8
<i>1.4 Copper.....</i>	<i>9</i>
1.4.1 Copper as an element.....	9

1.4.2 Copper in biological systems .....	10
1.4.3 Copper in medicine: .....	13
<i>1.5 Metal carboxylates chemistry .....</i>	<i>15</i>
1.5.1 Coordination modes of carboxylates .....	16
1.5.2 Infrared spectra of carboxylate complexes .....	18
1.5.3 Zn carboxylates .....	20
1.5.4 Cu carboxylates.....	21
<i>1.6 Levofloxacin.....</i>	<i>23</i>
<i>1.7 Nitrogen-donor ligands.....</i>	<i>25</i>
<i>1.8 Metal levofloxacin complexes with N-base ligands.....</i>	<i>29</i>
<i>1.9 Aims of the research: .....</i>	<i>32</i>
<b>2. Experimental.....</b>	<b>33</b>
2.1 Materials .....	33
2.2 Characterization techniques .....	33
2.3 Synthesis and characterization of zinc and copper complexes.....	34
2.3.1 Synthesis of [Zn(levo) <sub>2</sub> (MeOH) <sub>2</sub> ] ( <b>1</b> ).....	34
2.3.2 Synthesis of [Zn(levo) <sub>2</sub> (2-ampy) <sub>2</sub> ] ( <b>2</b> ).....	35
2.3.3 Synthesis of [Zn(levo) <sub>2</sub> (2,2-bipy)].H <sub>2</sub> O ( <b>3</b> ).....	36
2.3.4 Synthesis of [Cu(levo) <sub>2</sub> (2-ampy)] .6.25H <sub>2</sub> O ( <b>4</b> ).....	37
2.3.5 Synthesis of [Cu(levo)(H <sub>2</sub> O)(2,2-bipy)](NO <sub>3</sub> ).2.5H <sub>2</sub> O ( <b>5</b> ) .....	38
2.4 single X-ray crystal diffraction .....	39

2.5. <i>Anti-bacterial activity</i> .....	42
<b>3. Results and discussion</b> .....	<b>44</b>
3.1.1 Synthesis of zinc levofloxacin complexes .....	44
3.1.2 Synthesis of copper levofloxacin complexes.....	46
3.2 <i>Electronic absorption spectroscopy</i> .....	47
3.3 <i>IR vibrational assignments</i> .....	50
3.4 <sup>1</sup> H Nuclear Magnetic Resonance .....	55
3.4 <i>Crystal structure description</i> .....	57
3.4.1 Crystal structure of [Cu(levo) <sub>2</sub> (2-ampy)].6.25H <sub>2</sub> O ( <b>4</b> ) .....	58
3.4.2 Crystal structure of [Cu(levo)(H <sub>2</sub> O)(2,2-bipy)](NO <sub>3</sub> ).2.5H <sub>2</sub> O ( <b>5</b> ).....	62
3.5 <i>Anti-bacterial activity</i> .....	68
<b>4. Conclusion</b> .....	<b>77</b>
<b>5. References</b> .....	<b>79</b>
<b>6. Appendices</b> .....	<b>88</b>
<i>Appendix A: Electronic spectra of complexes 1, 3 and 4.</i> .....	88
<i>Appendix B: Infrared spectra of complexes 1, 3 and 4</i> .....	89
<i>Appendix C: <sup>1</sup>H-NMR spectral data of complexes 1 and 2 and their     parent ligands.</i> .....	91
<i>Appendix D: In-vitro anti-bacterial activity data for complexes 1-5.</i> ...	93

<i>Appendix E: Crystal structure data of [Cu(lev<sub>o</sub>)<sub>2</sub>(2-ampy)].6.25H<sub>2</sub>O (4)</i> .....	95
<i>Appendix F: Crystal structure data of [Cu(lev<sub>o</sub>)(H<sub>2</sub>O)(2,2-bipy)](NO<sub>3</sub>).2.5H<sub>2</sub>O (5)</i> .....	104



## List of Figures

Figure 1: Essential elements for life in the Periodic Table.....	2
Figure 2: Backbone structure of matrix metalloproteinase inhibitors. ....	9
Figure 3: Copper is essential for a competent immune system. ....	12
Figure 4: The carboxylate functional group showing <i>syn</i> - and <i>anti</i> -lone pairs .....	16
Figure 5: Different binding modes of metal carboxylates; (I) Ionic, (II) monodentate, (III) bidentate ( <i>sym</i> ), (IV) bidentate bridging. ....	17
Figure 6: Bridging binding modes in metal carboxylates.....	18
Figure 7: Molecular structure of $[\text{Zn}(\text{valp})_2(1,10\text{-phen})(\text{H}_2\text{O})]$ .....	20
Figure 8: Tetrahedral structure of $[\text{Cu}(\text{neocuproine})(\text{salH})_2]$ . ....	21
Figure 9: Square planar geometry of $[\text{Cu}(\text{O}_2\text{CMe})_2(\text{bipy})]$ . ....	22
Figure 10: Square pyramidal geometry of $[\text{Cu}(\text{neocuproine})(5\text{-chloro-2-}$ $\text{hydroxybenzoate})_2]$ .....	23
Figure 11: Levofloxacin structure and 3D model view. The model shows the (-)-(S)- enantimer of $(\text{OCH}_2)\text{C}^*\text{H}(\text{CH}_3)$ group with $\text{CH}_3$ in the axial position. The six-membered ring is in the chair conformation. ....	24

Figure 12: Schematic representation of an imine group. ....	25
Figure 13: Nitrogen donor-ligands. (I) monodentate ligand, (II) bidentate ligand (III) tetradentate ligand. ....	26
Figure 14: Nitrogen donor-ligands: 1) 1,10-phenanthroline 2) 2,9-dimethyl-1,10-phenanthroline, 3) 4,4-bipyridine, 4) 2,2-bipyridine, 5) 2-aminopyridine, 6) 2-aminomehtylpyridine. ....	27
Figure 15: Molecular structure of [W(bpy)(CO) <sub>4</sub> ]. ....	28
Figure 16: Main coordination modes of levofloxacin. ....	30
Figure 17: Molecular structure of Cu(II) levofloxacin complex with 1,10-phenanthroline. ....	31
Figure 18: Agar diffusion plates. ....	43
Figure 19: UV-Vis. spectra of complex <b>2</b> with parent ligands. ....	49
Figure 20: UV-Vis. spectra of complex <b>5</b> with parent ligands ....	50
Figure 21: IR spectra of complex <b>2</b> and levo ligand. ....	54
Figure 22: IR spectra of complex <b>5</b> and levo ligand. ....	54
Figure 23: <sup>1</sup> H-NMR spectra of complex <b>1</b> . ....	55
Figure 24: <sup>1</sup> H-NMR spectra of complex <b>2</b> . ....	57

Figure 25: (a) Molecular structure of complex **4** showing the labeling atom scheme. (b) the distorted square-pyramidal [CuNO<sub>4</sub>] center.58

Figure 26: Number of molecules per unit cell of complex **4** indicating the hydrogen bonds.....59

Figure 27: (a) Molecular structure of complex **5** showing the labeling atom scheme. (b) The distorted square-pyramidal [CuN<sub>2</sub>O<sub>3</sub>] center.....63

Figure 28: Number of molecules per unit cell of complex **5** .....64

Figure 29: Inhibition zone diameter of complexes **1-5** and their parent ligands against G<sup>-</sup> bacteria; the data stated as average ± standard deviation (N = 3), 6 mg/ml of all species.....70

Figure 30: Inhibition zone diameter of complexes **1-5** and their parent ligands against G<sup>+</sup> bacteria; the data stated as average ± standard deviation (N = 3), 6 mg/ml of all species.....70

Figure 31: Inhibition zone diameter of complexes **1-5** and their parent ligands against G<sup>-</sup> bacteria; the data stated as average ± standard deviation (N = 3), 6 mg/ml of complexes **1-5**, 4 mg/ml of levo and 1.34 mg/ml of 2,2-bipy. ....71

- Figure 32: Inhibition zone diameter of complexes **1-5** and their parent ligands against G<sup>+</sup> bacteria; the data stated as average ± standard deviation (N = 3), 6 mg/ml of complexes **1-5**, 4 mg/ml of levo and 1.34 mg/ml of 2,2-bipy. .... 71
- Figure 33: Correlation between inhibition zone diameter and different concentrations of levofloxacin..... 74

## List of Tables

Table 1: The daily intake of some essential TE needed for adults. ....	<b>4</b>
Table 2: Zinc content in typical food. ....	<b>6</b>
Table 3: Typical copper content of various food types.....	<b>11</b>
Table 4: Examples of copper-dependent enzymes.....	<b>13</b>
Table 5: Cu(II) complexes that exhibit biological activities.....	<b>15</b>
Table 6: Infra-red spectral data ( $\Delta(\text{OCO})$ ) for coordinated carboxylate ligands .....	<b>19</b>
Table 7: Crystal data and structure refinement for complexes <b>4</b> and <b>5</b> . ....	<b>41</b>
Table 8: Physical properties and % yields of complexes ( <b>1-5</b> ).....	<b>47</b>
Table 9: UV-visible spectral data for complexes ( <b>1-5</b> ) and their parent ligands. ....	<b>49</b>
Table 10: IR absorption frequencies (in $\text{cm}^{-1}$ ) of $\text{Na}_{\text{levo}}$ and complex <b>1</b> ..	<b>51</b>
Table 11: IR absorption frequencies (in $\text{cm}^{-1}$ ) of complexes <b>2-5</b> . ....	<b>53</b>
Table 12: Selected bond distances ( $\text{\AA}$ ) and bond angles ( $^{\circ}$ ) of complex <b>4</b>	<b>60</b>
Table 13: Hydrogen bond distances ( $\text{\AA}$ ) and bond angles ( $^{\circ}$ ) of complex <b>4</b> .....	<b>62</b>
Table 14: Selected bond distances ( $\text{\AA}$ ) and bond angles ( $^{\circ}$ ) of complex <b>5</b> ..	<b>65</b>

Table 15: Hydrogen bond distances ( $\text{\AA}$ ) and bond angles ( $^\circ$ ) of complex

**5.....67**

Table 16: Anti-bacterial activity data of different levo concentrations. ....**73**

## List of Schemes

Scheme 1: Synthesis of $[\text{Zn}(\text{levo})_2(\text{MeOH})_2]$ ( <b>1</b> ), proposed structure.....	<b>44</b>
Scheme 2: Synthesis of complexes <b>2</b> and <b>3</b> , proposed structures. ....	<b>45</b>
Scheme 3: Synthesis of complexes <b>4</b> and <b>5</b> . ....	<b>46</b>

## Abbreviations

Levo	Levofloxacin
2-ampy	2-Aminopyridine
2,2-bipy	2,2-Bipyrdine
<sup>1</sup> H-NMR	Proton Nuclear Magnetic Resonance
IR	Infrared
UV-Vis	Ultraviolet-Visible
IZD	Inhibition Zone Diameter
MeOH	Methanol
DMSO	Dimethyl sulfoxide
Rt	Room Temperature
H	Hour
m.p.	Melting point
NMR multiplicities	s = Singlet d = Doublet t = Triplet m = Multiplet
G <sup>+</sup>	Gram-positive
G <sup>-</sup>	Gram-negative
TE	Trace elements
UTE	Ultra-trace elements
Hex	Hexanoate
Hep	Heptanoate
Sal-Trp	N-salicylidene-tryptophanato



## Abstract

New zinc and copper levofloxacin complexes with different nitrogen based ligands with the following molecular structures; [Zn(levo)<sub>2</sub>(MeOH)<sub>2</sub>] (**1**), [Zn(levo)<sub>2</sub>(2-ampy)<sub>2</sub>] (**2**), [Zn(levo)<sub>2</sub>(2,2-bipy)].H<sub>2</sub>O (**3**), [Cu(levo)<sub>2</sub>(2-ampy)].6.25H<sub>2</sub>O (**4**) and [Cu(levo)(H<sub>2</sub>O)(2,2-bipy)](NO<sub>3</sub>).2.5H<sub>2</sub>O (**5**) were synthesized and characterized using various techniques such as IR, UV-Vis, <sup>1</sup>H-NMR, single crystal X-ray diffraction and other physical properties. The crystal structure of complexes **4** and **5** were determined using single crystal X-ray diffraction.

*In-vitro* anti-bacterial activities for the prepared complexes were investigated against four gram-negative bacteria (*Proteus mirabilis*, *Escherichia coli*, *Pseudomonas aeruginosa* and *Klebsiella pneumonia*) and four gram-positive bacteria (*Staphylococcus aureus*, *Staphylococcus epidermidis*, *Bacillus subtilis* and *Enterococcus faecalis*) by using the agar diffusion method. All complexes showed high anti-bacterial activity against different Gram-positive and Gram-negative bacteria. Complexes

**1-5** showed high inhibition activity against all G<sup>-</sup> and G<sup>+</sup> bacteria with IZD values between 29- 46 mm.

## ملخص بالعربية

تم تحضير وتشخيص مركبات جديدة تحتوي على أيون الزنك أو النحاس ثنائي الشحنة المرتبطين كلٌّ على حدا بدواء الليفوفلوكساسين مع بعض القواعد النيتروجينية المختلفة التالية:

[Zn(levo)<sub>2</sub>(MeOH)<sub>2</sub>] (1), [Zn(levo)<sub>2</sub>(2-ampy)<sub>2</sub>] (2), [Zn(levo)<sub>2</sub>(2,2-bipy)].H<sub>2</sub>O (3), [Cu(levo)<sub>2</sub>(2-ampy)].6.25H<sub>2</sub>O (4) and [Cu(levo)(H<sub>2</sub>O)(2,2-bipy)](NO<sub>3</sub>).2.5H<sub>2</sub>O (5)

حيث تم تشخيص المركبات بطرق وأجهزة مختلفة مثل جهاز طيف الأشعة فوق البنفسجية والمرئية وطيف الأشعة تحت الحمراء وجهاز الرنين المغناطيسي وجهاز حيود الأشعة السينية البلورية (X-Ray) بالإضافة الى خصائص فيزيائية أخرى. ومن خلال جهاز حيود الأشعة السينية البلورية تم تحديد البنية البلورية للمركبين 4 و5.

تمت دراسة الأنشطة الحيوية للمركبات باستخدام طريقة الانتشار في الآجار ضد أربعة أنواع من البكتيريا سلبية الغرام ( *Proteus mirabilis*, *Escherichia coli*, *Pseudomonas aeruginosa* and *Klebsiella pneumonia* ) وأربعة أنواع من البكتيريا إيجابية الغرام ( *Staphylococcus aureus*, *Staphylococcus epidermidis*, *Bacillus subtilis* ) (and *Enterococcus faecalis*). أظهرت جميع المركبات فعالية كبيرة ضد أنواع البكتيريا المستخدمة مقارنة مع القواعد النيتروجينية التي تم استخدامها. كما وأنها أظهرت نشاطاً حيوياً متشابهاً الى حد كبير مقارنة مع الليفوفلوكساسين لوحده.

أظهرت المركبات 5-1 نشاطاً تشبيطياً عاليًا ضد جميع أنواع البكتيريا المستخدمة سلبية وموجبة الغرام بقيم IZD بين 29-46 مم.

# **1. Introduction**

## **1.1. Theoretical background**

Metals are inorganic substances, exist in all tissues and body fluids.<sup>1</sup> The presence of these elements is necessary to maintain various physiochemical functions in living organisms which are essential to life.<sup>1,2</sup> They play important roles humans.<sup>2</sup> The essential elements to the various aspects of life in plant, human and animals can be divided into four major categories:

- (a) bulk elements like hydrogen, oxygen, carbon, sulfur and phosphorus.<sup>3</sup>
- (b) macrominerals and ions such as sodium, potassium, calcium, magnesium, chloride and sulfate.
- (c) trace elements enzymatic activities such as copper, iron and zinc.<sup>3</sup>
- (d) ultratrace elements contain metals like lithium, cadmium, nickel, chromium, molybdenum, and manganese and nonmetals like boron, fluorine, silicon, arsenic and selenium.<sup>3</sup>

Some of these chemical elements, such as Fe, Cu and Zn, are exist in all organisms and have physiological activities in human body as shown in Figure 1.<sup>4,5</sup>

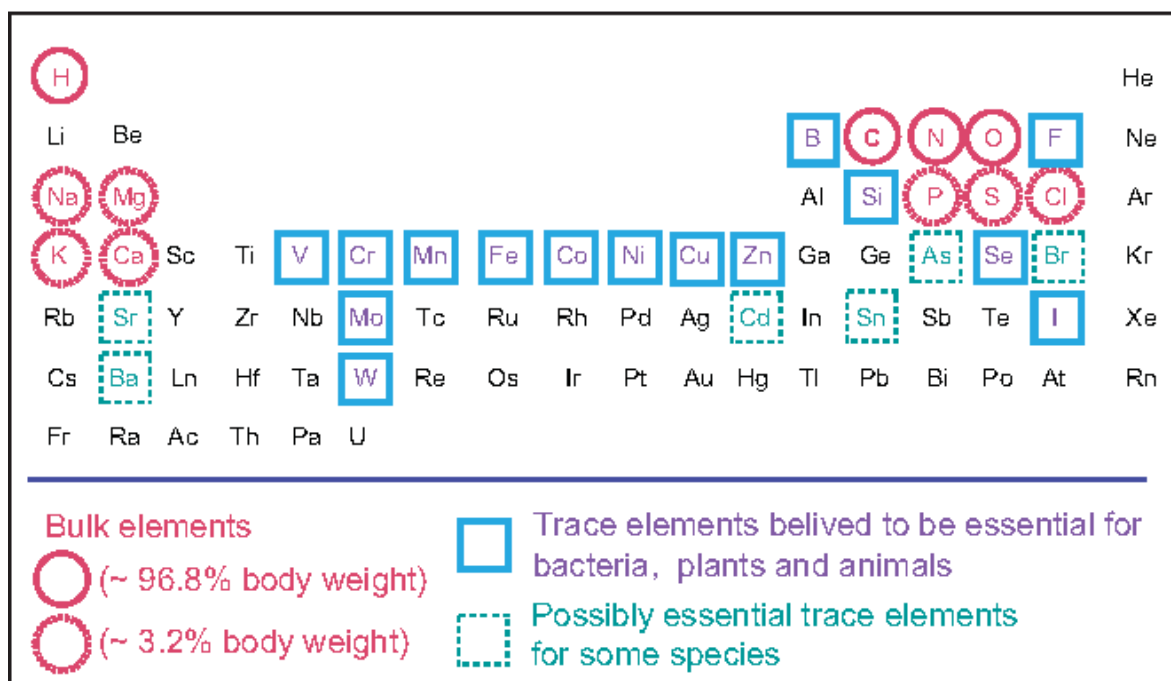


Figure 1: Essential elements for life in the Periodic Table.<sup>5</sup>

Essential trace elements (TE) and ultra-trace elements (UTE) of the human body include zinc, copper, cobalt, chromium, selenium, iodine, manganese, and molybdenum. These elements play significant roles as active centers of enzymes or as trace bioactive substances.<sup>6</sup> They are required in varied concentration, the TE and UTE are needed in less than 100 mg/dl while the macro-minerals are needed in amounts greater than 100 mg/dl.<sup>6</sup>

## 1.2 Metals in biological systems

Trace elements such as iron, copper and zinc play important roles in specific functions related to various life processes. In addition, they were used as dioxygen transport in metalloproteins<sup>7</sup> and serve as cofactor and activators of enzyme reactions. Metalloenzymes, most RNA and DNA polymerases are important sources of zinc.<sup>7,8</sup>

Many transition elements showed potent biological roles, but larger/lower amounts than normal can cause serious health effects.<sup>9</sup> For example, copper is essential for iron mobilization,<sup>9</sup> is a catalyst in the peroxidation of membrane lipids,<sup>10</sup> and is important to cardiovascular health.<sup>11</sup> Zinc is essential for many biological functions, and is the most abundant transition metal in the human body after iron.<sup>12</sup> Zinc acts as an important constituent in vitamin A metabolism, protein synthesis and cellular division.<sup>13</sup>

Transition elements can be toxic when their concentration in the body become in excess, whereas their deficiency will result in serious problems,<sup>14</sup> as shown in Table 1

Table 1: The daily intake of some essential TE and UTE needed for adults.

Element	Intake (mg/day)
Zn	15
Mn	2.5 - 5.0
Fe	10
Cu	2.0 - 3.0
Cr	0.05 - 0.2
I	0.5
Mo	0.15 - 0.5
F	1.5 - 4.0

## 1.3 Zinc

### 1.3.1 Zinc as an element

Zinc is a transition metal with atomic mass  $65.37 \text{ g}\cdot\text{mol}^{-1}$ , atomic number equal 30, electronic shell  $[\text{Ar}]3d^{10}4s^2$  with five stable natural isotopes ( $^{64}\text{Zn}$ ,  $^{66}\text{Zn}$ ,  $^{67}\text{Zn}$ ,  $^{68}\text{Zn}$ , and  $^{70}\text{Zn}$ ), but the major isotopes are  $^{64}\text{Zn}$ ,  $^{66}\text{Zn}$  and  $^{68}\text{Zn}$  with percentages 48.6%, 27.9% and 18.8% respectively.<sup>15</sup> Because zinc has a completely filled  $d$  shell with 10 electrons, zinc can lose two electrons from  $s$  orbital and form  $\text{Zn}^{2+}$  ion.

When coordinated with ligands,  $\text{Zn(II)}$  has zero ligand field stabilization energy in all geometries.<sup>16</sup>  $\text{Zn}^{2+}$  is a borderline acid, according to hard-soft



acid-base concept. Thus, zinc can bind strongly with different types of ligands including sulfur, nitrogen, oxygen, halides and  $\text{CN}^-$ . Also zinc cyanide complexes may gain their stability from the  $\sigma$  rather than  $\pi$  bonding.<sup>17</sup>

Zn(II) does not undergo oxidation/reduction reactions; neither Zn(III), nor Zn(I), are stable under normal conditions.<sup>17,18</sup>

The geometry and the coordination number are influenced mainly by the charge and ligands size. Zn(II) usually formed complexes with 4-coordination numbers with a tetrahedral geometry. As a consequence, zinc can binds easily in tetra- or penta-coordination modes which are more acidic than high coordination sites.<sup>19</sup>

### **1.3.2 Zinc in biological systems**

Zinc ion is one of the most essential trace elements which play important role in biological processes in humans and animals. Normal serum level of Zn is 84-159  $\mu\text{g}/\text{dl}$ .<sup>20</sup> Zinc ion plays extensive roles in enzymes function, nucleic acid, proteins metabolism and apoptosis.<sup>21</sup> It is found in the structure of approximately 300 enzymes and large number of other proteins.<sup>22</sup> Foods recognized as good sources of zinc such as red meat, eggs,

fish and dairy products. Furthermore, low zinc amounts can be obtained from vegetables and fruits.<sup>23</sup> However, meat and dairy products are considered as the richest sources of zinc. Table 2 below shows the amount of zinc in food.<sup>24</sup>

Table 2: Zinc content in typical food.\*

<b>Food</b>	<b>Zinc content (mg/kg)</b>
Meat	52
Offal	52
Nuts	30
Milk	4
Potatoes	3.3
Eggs	13
Fish	8
Bread	9.8

\*Adapted from references.<sup>23,24</sup>

Humans have approximately 2-4 grams of zinc that are localized mainly in the liver, prostate, bones, muscle, kidney, eye and brain.<sup>25</sup> Zn is considered as the second most abundant trace elements in organisms after iron and it's the only metal present in all enzyme.<sup>26</sup>

Zinc binds to 10% of human proteins, required for immune functions<sup>27</sup>, protein synthesis, DNA synthesis, cell division<sup>28</sup> and developments during

pregnancy.<sup>29</sup> At low concentrations, Zinc possesses anti-microbial activities.

Gastroenteritis and stomach inflammation is strongly reduced by zinc intake or by absorption of zinc and releasing it from the immune cells.<sup>30</sup> Moreover, it plays a role in cellular communication and signaling.<sup>31</sup>

Zinc deficiencies are related to the reduced anti-oxidant potential in organisms, which is associated with several infectious diseases such as shigellosis, malaria, human immune deficiency virus (HIV), tuberculosis, and pneumonia.<sup>32</sup>

Zn deficiency occurs when the serum level of Zn becomes less than 83  $\mu\text{g}/\text{dl}$ .<sup>6</sup> Zinc has recommended value of 8-11 mg for an adult male and female daily.<sup>33</sup> Zn deficiency demonstrated broad range of diseases including impaired growth, anemia, dwarfism, impaired sexual development, dermatitis, loss of hair and slow wound healing.<sup>33</sup>

### 1.3.3 Zinc metal in medicine

Biomedical inorganic chemistry is an important branch of chemistry. It is essential in understanding diseases and designing therapeutics. Inorganic elements play important roles in biological and biomedical processes.<sup>34</sup>

The field of medicinal inorganic chemistry was established in 1960s, following the discovery and development of the anti-cancer compound *cis*-platin, *cis*-[PtCl<sub>2</sub>(NH<sub>3</sub>)<sub>2</sub>].<sup>35</sup>

Metal ions play an essential function in the mechanism of action of organic drugs, for example, galardin, batimastat (BB-94), and BB-2516 are being diagnosed in clinical trials for the treatment of diseases such as arthritis, tumor, cardiovascular disease, and prostate disorder. Zinc-dependent enzymes are good inhibitors of matrix metalloproteinases (MMPs), have been responsible for several diseases including cancer, multiple sclerosis, and arthritis. Usually, inhibitors of these enzymes occur when Zn(II) bind in a chelating mode to their active-site, and a peptide backbone as shown in Figure 2.<sup>34</sup>

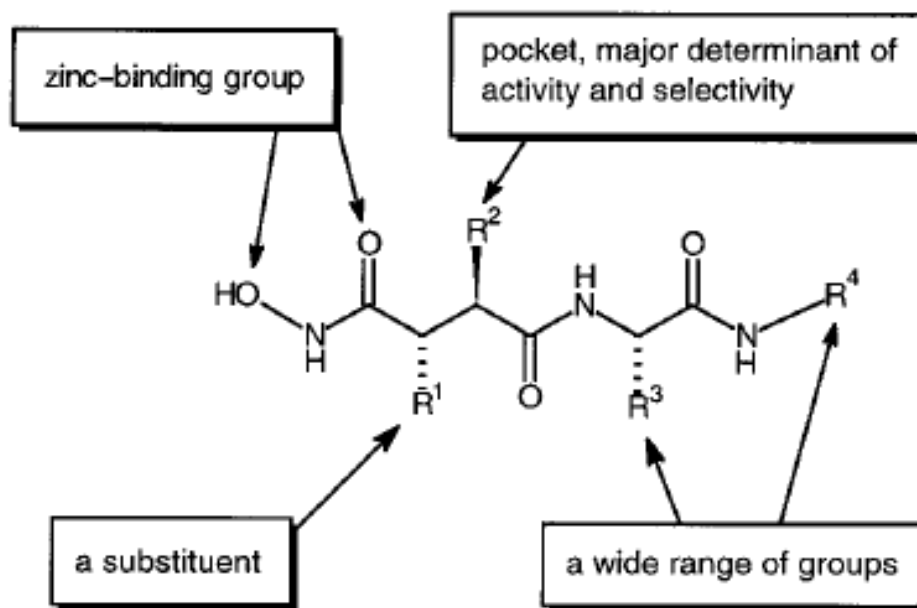


Figure 2: Backbone structure of matrix metalloproteinase inhibitors.<sup>34</sup>

The most important health uses of zinc are as prostate disorder, enzymes regulation, chronic fatigue, alopecia, bone loss and wound healing.<sup>36</sup>

## 1.4 Copper

### 1.4.1 Copper as an element

Copper is the 29<sup>th</sup> element in the Periodic Table with an electronic configuration  $[\text{Ar}]3d^{10}4s^1$ . It has a reddish brown color, melting point of

1083.4 °C and a boiling point of 2567 °C. Copper is a good thermal and electrical conductor.<sup>37</sup>

There are many oxidation states of copper, the common oxidation states are the cuprous Cu(I) or the cupric (Cu(II)), and the other two oxidation states: metallic Cu (Cu<sup>0</sup>) and trivalent ion (Cu<sup>3+</sup>). Cu<sup>3+</sup> is found in few compounds and is a strong oxidizing agent.<sup>38</sup>

Cu(I) complexes are diamagnetic and rapidly oxidized by any oxidizing agent. Cu(I) has no *d-d* transitions so the color of Cu(I) complexes is due to inter-ligands transitions. The Cu(II) complexes are colored and most stable with 4, 5 and 6 coordination numbers. The colors of these complexes are mainly due to the *d-d* transitions in addition to the inter-ligands transitions .<sup>38</sup>

### **1.4.2 Copper in biological systems**

Copper is one of the essential trace elements for human body, that can be considered as the third most abundant essential transition metal found in biological systems after iron and zinc.<sup>39</sup> The total amount of copper needed

for the body is 75-100 mg. Copper is present in the brain, heart and muscles, but is stored primarily in the liver.<sup>39</sup> It cannot be formed by the human body so must be get from daily dietary sources, 1–3 milligrams per day of copper are required to prevent any symptoms deficit according to the World Health Organization.<sup>40</sup> Copper is obtained from food such as grains, nuts, meats, fish, legumes and chocolate,<sup>41</sup> as shown in Table 3.

Table 3: Typical copper content of various food types.\*

<b>Food</b>	<b>Copper (mg/100g)</b>	<b>Comments</b>
<b>Chicken</b>	0.06	Roasted, meat only
<b>Liver</b>	4.51	Beef, braised
<b>Tuna</b>	0.04	White, canned in water, drained solids
<b>Oysters</b>	0.57	Battered or breaded, fried
<b>Potato</b>	0.22	Baked, without salt, flesh only
<b>Potato</b>	0.17	Boiled, no skin, no salt
<b>Mushrooms</b>	0.24	Canned
<b>Green Peas</b>	0.14	Frozen, cooked, drained, no salt
<b>Banana</b>	0.1	Raw
<b>Raisins</b>	0.36	Golden, seedless
<b>Peanuts</b>	0.67	Dry roasted, no salt
<b>Peanuts</b>	1.14	Raw
<b>Brazil Nuts</b>	1.77	Dried, unblanched
<b>Chick Peas</b>	0.17	Canned
<b>Chick Peas</b>	0.85	Raw
<b>Chocolate (Dark)</b>	0.8	Dark chocolate bar

\*Adapted from reference.<sup>40</sup>

In humans, copper is essential for the normal functions of the immune system, nervous systems, and cardiovascular systems. It is necessary for the maintenance of a normal white blood cells count; because copper deficiency can lead to immune system disorder, and increased incidence of pneumonia,<sup>40,41</sup> Figure 3.

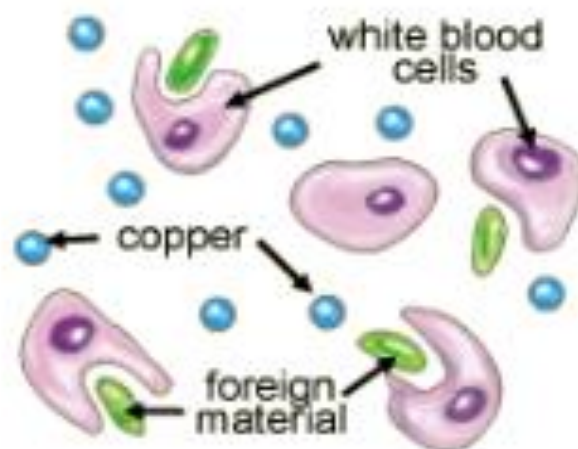


Figure 3: Copper is essential for a competent immune system.<sup>40</sup>

Copper is absorbed in the upper small intestine and transported to the liver through a carrier protein.<sup>42</sup> Copper is in the catalytic center of many enzymes, especially those involved in neurotransmitter synthesis. In



humans body there are 12 cupro-enzymes, Table 4 shows examples of copper-dependent enzymes.<sup>25,42</sup>

Table 4: Examples of copper-dependent enzymes.\*

Enzyme	Role in metabolism
Cytochrome c oxidase	Electron transport, energy metabolism
Amine oxidase	Deamination of primary amines
Ceruloplasmin, GPI-ceruloplasmin, hephaestin, zyklopen (multi-copper ferroxidases)	Iron metabolism ferroxidases
Cu/Zn superoxide dismutase (SOD)	Superoxide dismutation
Lysyl oxidase	Collagen and elastin cross-linking
Tyrosinase	Melanin synthesis
Peptidylglycine $\alpha$ -amidating monooxygenase	$\alpha$ -Amidation of neuropeptides
Dopamine $\beta$ -monooxygenase	Dopamine to noradrenaline conversion

---

\*Adapted from reference.<sup>42</sup>

### 1.4.3 Copper in medicine:

Metal ions play important roles in the biological and biomedical processes, such as breathing, metabolism, growth, reproduction, muscle contraction. Essential metal ions, especially zinc and copper, are cofactors in

metalloproteins. They modulate enzymetic, catalytic activities and regulatory functions.<sup>4,43</sup>

Copper is connected with several metalloenzymes in hemoglobin formation.<sup>44</sup>

Many metal complexes are used in the treatment of some diseases, including different kind of cancers, rheumatoid arthritis, diabetes, Wilson's disease, and Alzheimer's disease.<sup>43</sup>

Copper (II) complexes gained many advantages through the years such as anti-microbial, anti-inflammatory, anticancer, enzyme inhibitor, and they are also useful against many diseases such as rheumatoid and stomach ulcers.<sup>45</sup>

Cu(II) can form many complexes with non-steroidal anti-inflammatory drugs (NSAIDs) and show enhanced anti-inflammatory and anti-ulcerogenic activities, as well as decrease in the gastrointestinal toxicity compared to the uncomplexed drug. Different biological activity applications of Cu(II) complexes with different N, S, or O biological ligands have been tested as shown in Table 5.<sup>46</sup>

Table 5: Cu(II) complexes that exhibit biological activities.\*

Ligand	Type of complex	Biological Activity
2,6-bis (benzimidazo-2-yl) pyridine	LCuCl <sub>2</sub>	Protease mimetic
Pyridyl-2-carboxamidrazone	LCuCl <sub>2</sub>	Anticancer
2,4-diiodo-6-(pyridine-2-yl methylamino) methyl phenolate	(L-H)CuCl or [L(L-H)Cu] <sup>+</sup>	Proteasome inhibitor, Apoptosis inducer
[(5-bromo-2 hydroxyphenyl)methylidene] amino-N-(pyrimidin-2-yl)benzene sulfonamides	(L-H) <sub>2</sub> Cu	Antibacterial
6-(2-chlorobenzyl amino) purine	[(LH) <sub>2</sub> CuCl <sub>3</sub> ] <sup>+</sup>	Potent anticancer, inhibiting cell growth of various types of cancer

\*Adapted from reference.<sup>46</sup>

## 1.5 Metal carboxylates chemistry

Carboxylates are important compounds in organometallic and inorganic chemistry, which play a vital role in various medicinal and pharmaceutical applications. Different therapeutic areas contain the carboxyl group such as valproic acid, levofloxacin, piroxicam and ibuprofen. Being versatile (RCOO<sup>-</sup>) ligands, they can adopt a wide range of coordination modes.<sup>47</sup>

### 1.5.1 Coordination modes of carboxylates

The functional carboxylate group can bind in different coordination modes with metal ions. It has two lone pairs of electrons on each of the oxygen atoms which are available for metal binding. These lone pairs can be divided into *syn*- and *anti*-lone pairs, Figure 4. Carboxylate group exhibits different basicity between *syn*- and *anti*- position, where the *syn*-lone pairs are more basic than those in the *anti*- position.<sup>48</sup>

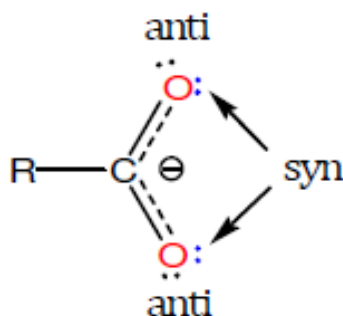


Figure 4: The carboxylate functional group showing *syn*- and *anti*-lone pairs

The various different coordination modes are shown below:

1. **Ionic:** This mode is formed by electrostatic attraction between the metal and the carboxylic oxygen anions, like sodium carboxylate.
2. **Monodentate:** Only one oxygen atom in the carboxylate group interacts with metal and the other oxygen atom remains free without interaction.

**3. Bidentate:** The carboxylate ion coordinates to metal ion through two oxygen forming four members ring.

**4. Bridging:** The carboxylate group can form bridging, when it interact with two metal atoms.

The bridging coordination mode may occur in *syn-syn*, *anti-syn*, and *anti-anti* interactions depending on the orientation of the pair of electrons on each of the oxygen atoms.<sup>49,50</sup> Figures 5 and 6 show the various binding modes of the carboxylate ligands.

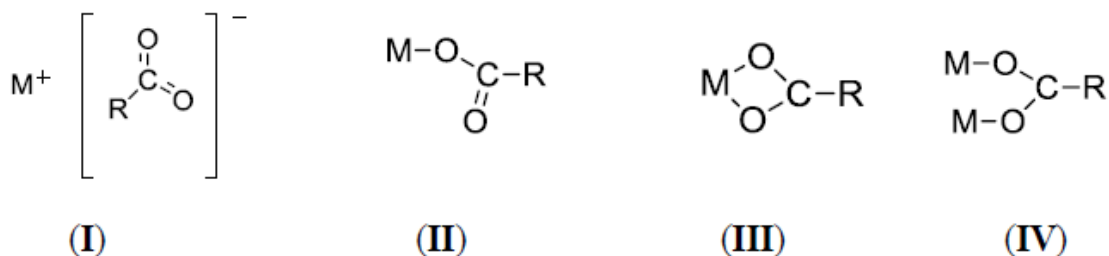


Figure 5: Different binding modes of metal carboxylates; (I) Ionic, (II) monodentate, (III) bidentate (sym), (IV) bidentate bridging.

**5. Monodentate terminal bridging:** Monodentate terminal bridging mode is rare and can be considered as an intermediate between other bridging

modes.<sup>50</sup> It occurs when two metal atoms coordinate to one oxygen atom in carboxylate group.

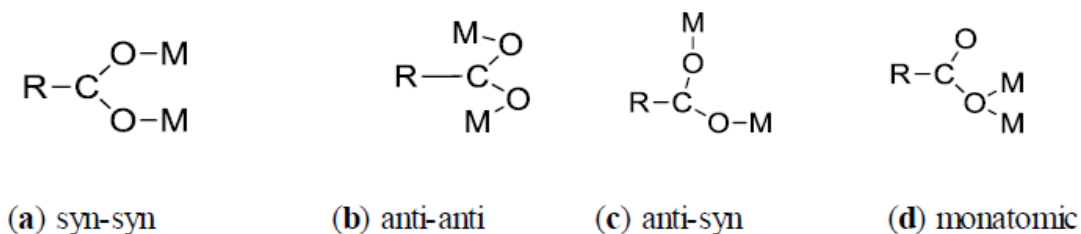


Figure 6: Bridging binding modes in metal carboxylates.

### 1.5.2 Infrared spectra of carboxylate complexes

Infrared spectroscopy was usually used to identify the functional groups and molecular structure of both organic and inorganic compounds including metal containing compounds. In free carboxylic acid, the carbonyl group, C=O absorption band occurs at 1760-1680  $\text{cm}^{-1}$ . Two IR bands can be assigned in metal carboxylate complexes, asymmetric and symmetric stretching of  $\text{COO}^-$  group which are generally absorbed at 1620-1530  $\text{cm}^{-1}$  region for  $\nu_{as}(\text{COO}^-)$  and around 1400  $\text{cm}^{-1}$  for  $\nu_s(\text{COO}^-)$ .

The absence of a carbonyl peak around 1700  $\text{cm}^{-1}$  and its replacement by absorptions in the region of 1600 and 1400  $\text{cm}^{-1}$  indicates that there was

complete resonance in the C–O bonds of the carbonyl group as a result of coordination with the metal. The difference in asymmetric and symmetric frequencies,  $\Delta = \nu_{as}(\text{COO}^-) - \nu_s(\text{COO}^-)$  has been used to determine the nature of the carboxylate coordination modes.

According to Deacon and Philips, based on acetate complexes the following series can be used to demonstrate the difference between metal carboxylate coordination modes.<sup>51-55</sup> Table 6 shows the coordination modes of carboxylate groups based on  $\Delta$  (COO-) values.

$$\Delta (\text{chelating}) < \Delta (\text{bridging}) < \Delta (\text{ionic}) < \Delta (\text{monodentate})$$

Table 6: Infra-red spectral data ( $\Delta(\text{OCO})$ ) for coordinated carboxylate ligands.\*

$\Delta(\text{OCO}), (\text{cm}^{-1})$	Coordination mode
< 105	Symmetric chelating or short bridging
< 150	Chelating or bridging
~165	Ionic
>200	Monodentate

\*Adapted from reference.<sup>50</sup>

### 1.5.3 Zn carboxylates

Zinc carboxylates have important role in synthetic chemistry and biological activities.<sup>56</sup> Carboxylate group can bind with metal ions through the versatility of RCOO<sup>-</sup> ligand that can form a wide range of coordination modes. Recently, there are many zinc carboxylate compounds with different applications. For example, Zn valproate with 1,10-phenanthroline complexes showed anti-bacterial activity and zinc naproxen complexes showed different anti-ulcer and anti-inflammatory activities.<sup>57,58</sup>

Figure 7 shows an ortip of single crystal X-ray structure of Zn valproate and 1,10-phenanthroline complex.

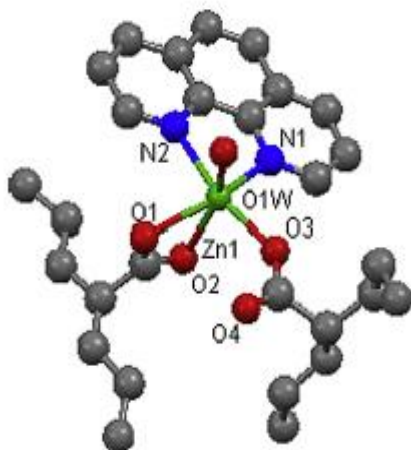


Figure 7: Molecular structure of  $[\text{Zn}(\text{valp})_2(1,10\text{-phen})(\text{H}_2\text{O})]$ .<sup>58</sup>



### 1.5.4 Cu carboxylates

A versatile carboxylate anion can adopt a wide range of coordination modes with metals, including monodentate, bidentate and bridging.<sup>59</sup>

Copper carboxylate can assume a variety of coordination modes and numbers with different geometries, such as tetrahedral and square planar four coordination numbers, square pyramidal and trigonal bipyramidal five coordination numbers and octahedral six coordination numbers. Copper (II) complex of salicylic acid with 2,9-dimethyl-1,10-phenanthroline [Cu(neocuproine)(salH)<sub>2</sub>] is an example of distorted tetrahedral geometry as shown in Figure 8.<sup>49,60</sup>

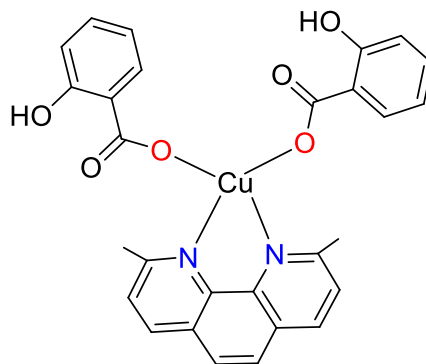


Figure 8: Tetrahedral structure of [Cu(neocuproine)(salH)<sub>2</sub>].

Another example of square planar Cu(II) acetate complex with 2,2'-bipyridine ligand  $[\text{Cu}(\text{O}_2\text{CMe})_2(\text{bipy})]$  is shown in Figure 9.<sup>61</sup>

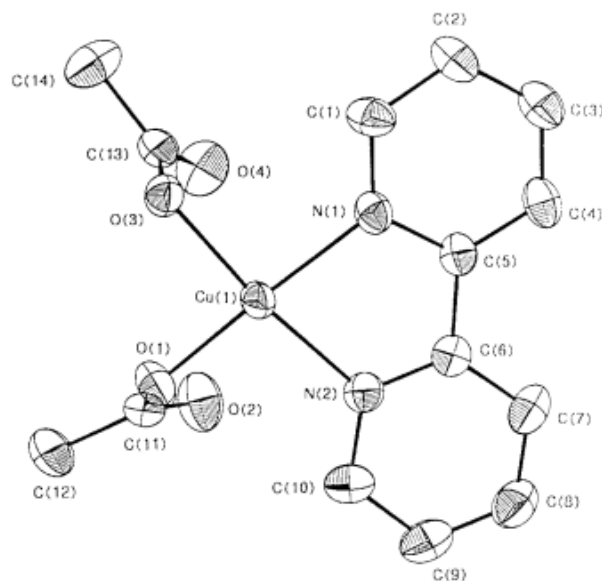


Figure 9: Square planar geometry of  $[\text{Cu}(\text{O}_2\text{CMe})_2(\text{bipy})]$ .

Lenka Kucková et al. determined the structure of  $[\text{Cu}(\text{neocuproine})(5\text{-chloro-2-hydroxybenzoate})_2]$  which is an example of five coordination complex with square pyramidal geometry as shown in Figure 10.<sup>62</sup>

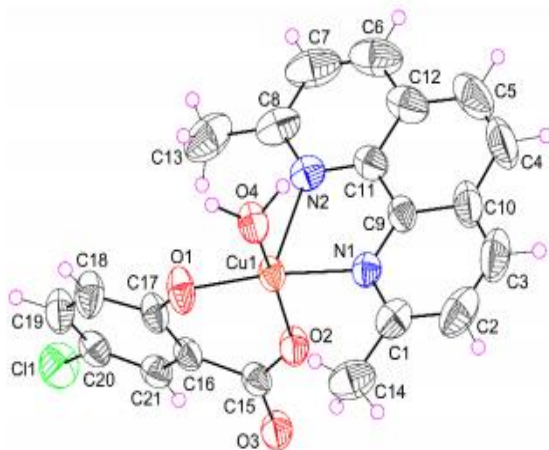


Figure 10: Square pyramidal geometry of  $[\text{Cu}(\text{neocuproine})(5\text{-chloro-2-hydroxybenzoate})_2]$

Dinuclear copper carboxylate complexes usually exhibit bridging coordination modes. The complexes  $[\text{Cu}_2(\text{bipy})_2(\text{OAc})_3]$  and  $[\text{Cu}(\text{Neo})(\text{sal})]_2$  are examples of this mode of interaction.<sup>49</sup>

## 1.6 Levofloxacin

Quinolones, also known as fluoroquinolones are anti-bacterial agents with broad-spectrum activity. For instance, ofloxacin, norfloxacin, ciprofloxacin, and moxifloxacin are some examples of such fluoroquinolone compounds.<sup>63,64</sup> Levofloxacin (Figure 11) is a pure chiral S-enantiomer of the racemic drug substance ofloxacin. The chemical name of levofloxacin

(levo) is (-)-(S)-9-fluoro-2,3-dihydro-3-methyl-10-(4-methylpiperazin-1-yl)-7-oxo-7H-pyrido[1,2,3-de]-1,4-benzoxazine-6-carboxylic acid and the common name is levaquin with a light yellowish crystalline powder. The solubility of levofloxacin is the same at pH 0.6 to 5.8. It's soluble in acetic acid, chloroform and methanol with moderate solubility in water. Levofloxacin can form stable complexes with many metal ions.<sup>65,66</sup>

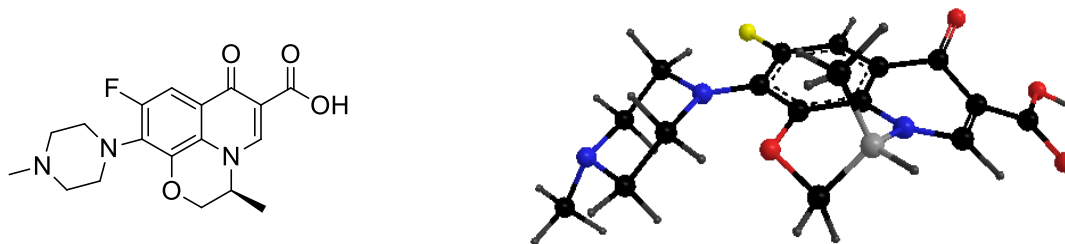


Figure 11: Levofloxacin structure and 3D model view. The model shows the (-)-(S)- enantiomer of  $(\text{OCH}_2)\text{C}^*\text{H}(\text{CH}_3)$  group with  $\text{CH}_3$  in the axial position. The six-membered ring is in the chair conformation.

Levofloxacin as a third-generation of quinolone has wide-spectrum of bactericidal anti-biotics and is active against both Gram-positive and Gram-negative bacteria. The proposed mechanism of action might be by inhibiting the deoxyribonucleic acid (DNA) gyrase (topoisomerase II) enzymes, that is necessary for bacterial DNA replication, in the treatment of many bacterial infections, such as, respiratory tract infections, chronic bronchitis,

acute bacterial sinusitis, acute pneumonia, skin infections, post-inhalational anthrax, genitourinary infections, urinary tract infections and chronic prostatitis, by using once-daily dosages of 250, 500 or 750 mg depending on the indication.<sup>65,67-70</sup>

### 1.7 Nitrogen-donor ligands

In coordination chemistry, ligands containing nitrogen atoms have been widely used in pharmaceutical industries. The nitrogen based ligands were described by Hugo Schiff in 1864. Figure 12.<sup>71,72</sup>

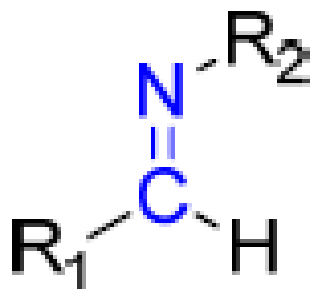


Figure 12: Schematic representation of an imine group.<sup>71</sup>

Schiff bases have been also showed a broad range of biological activities such as, anti-fungal, anti-bacterial, anti-malarial, anti-inflammatory, anti-viral and anti-pyretic properties.<sup>72</sup>

Schiff bases are classified into bidentate, tridentate, tetradentate or multidentate ligands, which are able to form complexes with transition metal ions.<sup>73</sup> Figure 13, description of the classes of coordination modes of nitrogen base ligands.

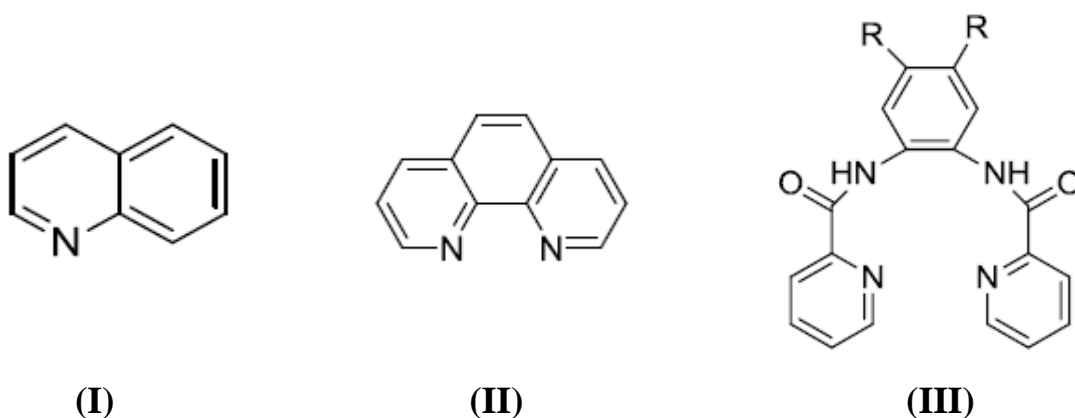


Figure 13: Nitrogen donor-ligands. (I) monodentate ligand, (II) bidentate ligand (III) tetradentate ligand.<sup>73</sup>

Heterocyclic organic compounds contain carbon and hydrogen atoms with one or more different kinds of atoms such as nitrogen, sulfur and oxygen. Pyridine and its derivatives play a vital role in biological activities and pharmaceutical industries.<sup>74</sup> Derivatives of pyridine exhibit wide variety of biological activities like antitumor, anti-bacterial, anti-inflammatory, anti-malarial, anti-HIV, and anti-fungal.<sup>74</sup>

Pyridine has a lone pair of electrons located on imine group which give it the ability to interact both as base and nucleophile with transition metals. So, pyridines are very important N-donor ligands in coordination chemistry.<sup>74</sup>

There are many bioactive nitrogen base ligands related to pyridine such as 2-aminopyridine, 2,2-bipyridine, 1,10-phenanthroline 2-aminomehtylpyridine, 2,9-dimethyl-1,10-phenanthroline and 4,4-bipyridine as shown in Figure 14. 2,2-Bipyridine (2,2-bipy) and 2-aminopyridine (2-ampy) compounds were chosen in the present work.<sup>75</sup>

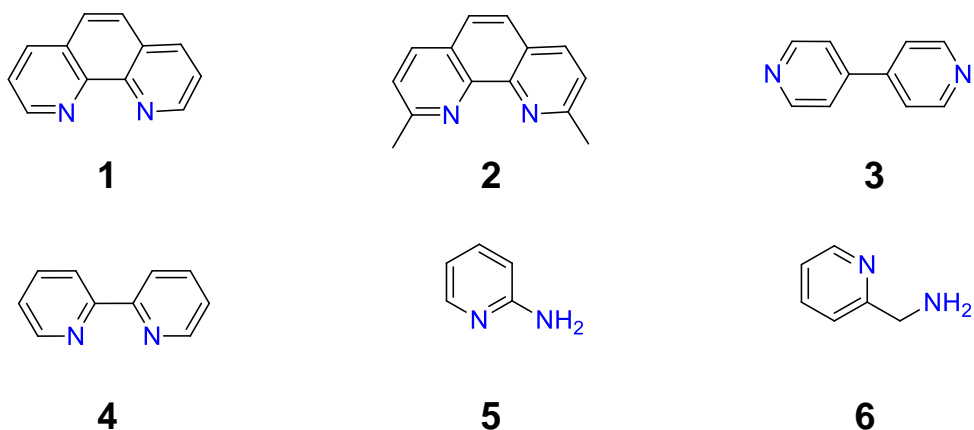


Figure 14: Nitrogen donor-ligands: 1) 1,10-phenanthroline 2) 2,9-dimethyl-1,10-phenanthroline, 3) 4,4-bipyridine, 4) 2,2-bipyridine, 5) 2-aminopyridine, 6) 2-aminomehtylpyridine.

Metal complexes with nitrogen ligands are used in medicinal chemistry and have important roles in biological applications.<sup>76</sup> There are many examples in previous studies that contain metal complexes with 2,2'-bipy ligand and their biological activities.<sup>77</sup> Figure 15 shows the molecular structure of tungsten complex containing 2,2'-bipy ligand.<sup>77</sup>

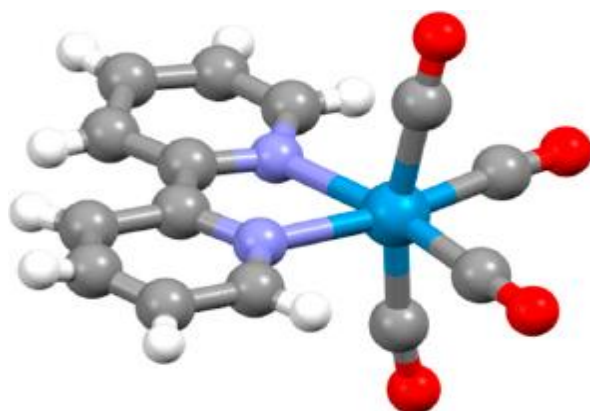


Figure 15: Molecular structure of  $[W(bpy)(CO)_4]$ .

Complexes of 2-ampy with various anti-inflammatory compounds such as piroxicam showed important applications in the medical field and the pharmaceutical industries. This ligand can interact with various metal ions in different binding modes, 2-ampy acts as chelating monodentate only through pyridine nitrogen atom or bidentate through the  $NH_2$  amine group and the pyridine nitrogen atom.<sup>78</sup>



## 1.8 Metal levofloxacin complexes with N-base ligands

Levofloxacin is a zwitterion by nature, with two functional groups carboxylic acid and piperazinyl ring. Both functional groups support its solubility in acidic or basic media and allow the levo compound to interact with bacterial enzymes-DNA forming a drug-enzyme-DNA matrix that blocks the progression and the replication processes.<sup>70,79</sup>

The interaction between metal ions and different anti-biotic drugs can alter their potential anti-microbial activities such as anti-bacterial, anti-fungal and anti-viral. The levo ligand can complex with metal ions as bidentate, monodentate and bridging ligands. Rarely, the levo can act as bidentate ligand through two carboxyl oxygen atoms (Figure 16 A), or via two piperazinic nitrogen atoms (Figure 16 B). Frequently, levo can be coordinated as bidentate, through one of the oxygen atoms of deprotonated carboxylic group and the ring carbonyl oxygen atom (Figure 16 C). Levo can also act as monodentate ligands coordinated to the metal ion through terminal piperazinyl nitrogen atom, (Figure 16 D).<sup>80</sup>

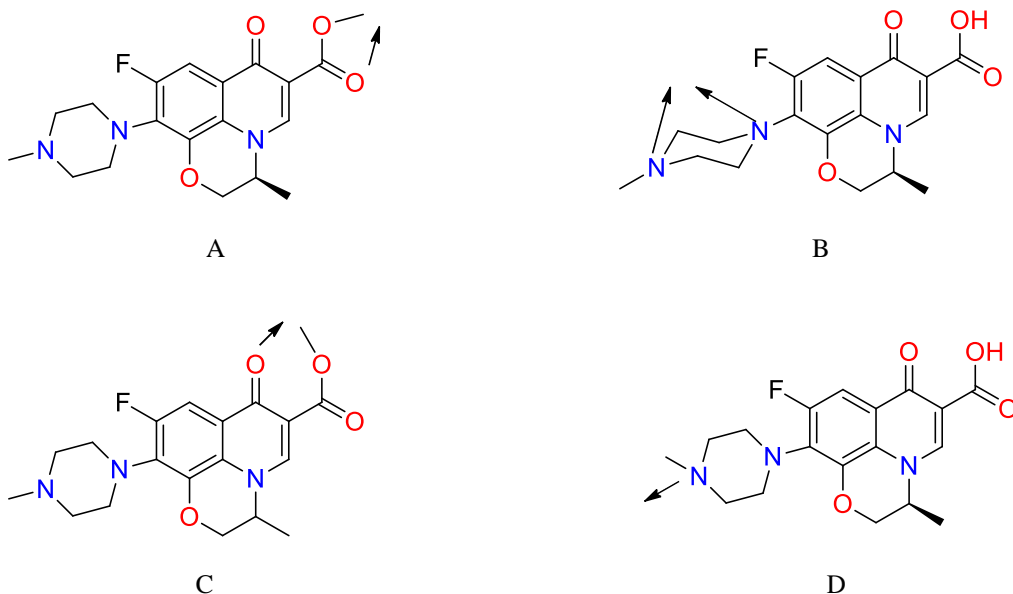


Figure 16: Main coordination modes of levofloxacin.

The carbonyl group and carboxylic acid of levo are the most common sites of metal chelate formation. Levo can bind divalent cations ( $\text{Mg}^{2+}$ ,  $\text{Ca}^{2+}$ ,  $\text{Cu}^{2+}$ ,  $\text{Zn}^{2+}$ ,  $\text{Fe}^{2+}$ ,  $\text{Co}^{2+}$ ), forming chelates with ratio 1:1 or 1:2 (metal:ligand) stoichiometry or with ( $\text{Al}^{3+}$ ,  $\text{Fe}^{3+}$ ) trivalent cations forming chelates with 1:1, 1:2 or 1:3 ratios. The number of coordinated ligands depends on the metal ion, relative concentration of the levo and the pH. Thus, in more acidic media 1:1 complexes are favorable, whereas 1:2 complexes are predominant at basic pH values.<sup>70,81,82</sup>

Copper and Zinc levofloxacin complexes with nitrogen base donor ligands have an interesting potential biological activity. Sadeek et al. prepared zinc levofloxacin complex with glycine as nitrogen donor ligand.<sup>83</sup> Isabel et al. prepared copper complex with levofloxacin and 1,10-phenanthroline nitrogen donor ligands and showed that the anti-bacterial activity was enhanced upon complexation compared with the free levofloxacin, Figure 17.<sup>84</sup>

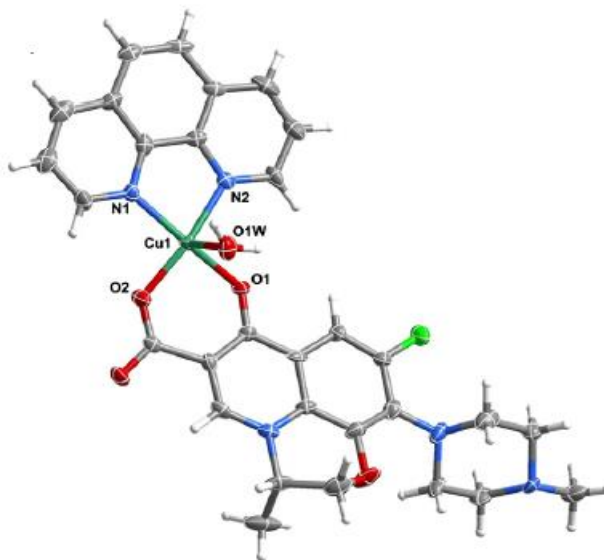


Figure 17: Molecular structure of Cu(II) levofloxacin complex with 1,10-phenanthroline.

### **1.9 Aims of the research:**

This work will focus on the synthesis and characterization of zinc and copper levofloxacin complexes with different nitrogen base ligands using 2-aminopyridine and 2,2'-bipyridine. The general formula of these complexes is  $\{M(\text{levofloxacin})_n(L)_m\}$ , ( $M = \text{Zn or Cu}$ ;  $n = 1, 2, \dots$ ;  $m = 1, 2, \dots$ ;  $L = \text{nitrogen base ligands}$ ). The new synthesized complexes will be characterized to investigate their structure and formula using different techniques. Then, the biological activities of these complexes will be screened and evaluated.

## 2. Experimental

### 2.1 Materials

Levofloxacin were kindly donated by Al-Quds Pharmaceutical Company. All metal salts and nitrogen based ligands were purchased from Fluka, Sigma Aldrich and Merck chemical companies. Solvents used were of analytical grade and were used as obtained. The Department of Biology and Biochemistry at Birzeit University generously provided us with all bacteria strains (*Proteus mirabilis*, *Escherichia coli*, *Pseudomonas aeruginosa*, *Klebsiella pneumonia*, *Staphylococcus aureus*, *Staphylococcus epidermidis*, *Bacillus subtilis* and *Enterococcus faecalis*).

### 2.2 Characterization techniques

Various techniques were utilized to characterize the levofloxacin complexes. FT-IR spectra in the region 4000-200  $\text{cm}^{-1}$  were obtained in Bruker TENSOR II Spectrometer using KBr disc. 300 MHz  $^1\text{H}$ -NMR, 75 MHz  $^{13}\text{C}$ -NMR and 282 MHz  $^{19}\text{F}$ -NMR spectra were collected on a Varian Unity Spectrometer. Molecular structures determination was recorded on

Bruker SMART APEX CCD X-ray diffractometer. Melting points were determined using EZ-Melt melting point apparatus and electronic spectra were recorded on Agilent 8453 UV-Vis spectrophotometer.

## 2.3 Synthesis and characterization of zinc and copper complexes

All complexes were prepared at ambient conditions.

### 2.3.1 Synthesis of $[\text{Zn}(\text{levo})_2(\text{MeOH})_2]$ (**1**)

Levofloxacin (27.6 mmol, 10 g) and sodium hydroxide (30 mmol, 1.2 g) were added to 150 ml MeOH with continuous stirring until dissolved. Zinc chloride (13.8 mmol, 1.88 g) was added to the solution and the mixture was stirred for additional 3 h. The yellowish solution was then evaporated on a rotavapor and the product was collected and extracted by dichloromethane. After evaporated the solvent, the product was washed with ether to obtain a yellow precipitate.

$[\text{Zn}(\text{levo})_2(\text{MeOH})_2]$  (**1**). 79% yield, m.p. = 268.3 °C (d);  $^1\text{H}$  NMR (DMSO):  $\delta$  (ppm) 1.39 (d, 3H,  $\text{CH}_3$ ,  $^3J_{\text{H-H}} = 5.25$  Hz), 2.22 (s, 3H,  $\text{CH}_3$ ), 2.42 (s, 4H,  $\text{CH}_2$ ), 3.25 (s, 4H,  $\text{CH}_2$ ), 4.34 (d, 1H,  $\text{OC}(\text{H}_a)\text{H}$ ,  $^3J_{\text{H-H}} = 10.11$

Hz), 4.54 (d, 1H, OC(H<sub>b</sub>)H,  $^3J_{\text{H-H}} = 10.94$  Hz), 4.87 (bs, 1H, CH), 7.49 (d, 1H, CH,  $^3J_{\text{H-H}} = 11.64$  Hz), 8.96 (s, 1H, CH);  $^{19}\text{F-NMR}$  (DMSO):  $\delta$  (ppm) - 121.62; IR (cm<sup>-1</sup>): 3405, 2934, 2843, 2797, 1615, 1574, 1522, 1469, 1397, 1339, 1266, 1230, 1130, 1048, 1002, 981, 814, 689, 543, 501, 499, 367; UV-Vis (MeOH,  $\lambda$  (nm)): 198, 228, 257, 297, 325.

### 2.3.2 Synthesis of [Zn(levo)<sub>2</sub>(2-ampy)<sub>2</sub>] (2)

Complex **1** (8 mmol, 1.963 g) was dissolved in 30 ml MeOH, a solution of (16 mmol, 1.51 g) of 2-ampy in 15 ml MeOH was then added to the previous solution. Then the mixture was stirred for an additional 3 h. The solvent was then evaporated under vacuum to obtain a precipitate. The solid was washed with ether and petroleum ether and allowed to stand for air drying.

**[Zn(levo)<sub>2</sub>(2-ampy)<sub>2</sub>] (2)**. 73 % yield; m.p. = 228-231 °C;  $^1\text{H NMR}$  (DMSO):  $\delta$  (ppm) 1.33 (d, 3H, CH<sub>3</sub>,  $^3J_{\text{H-H}} = 4.5$  Hz), 2.18 (s, 3H, CH<sub>3</sub>), 2.38 (s, 4H, CH<sub>2</sub>), 3.21 (s, 4H, CH<sub>2</sub>), 4.28 (d, 1H, OC(H<sub>a</sub>)H,  $^3J_{\text{H-H}} = 10.5$  Hz), 4.48 (d, 1H, OC(H<sub>b</sub>)H,  $^3J_{\text{H-H}} = 10.8$  Hz), 4.80 (bs, 1H, CH), 5.88 (s, 2H, NH<sub>2</sub>), 6.37 (d, 1H, CH<sub>ampy</sub>,  $^3J_{\text{H-H}} = 7.8$  Hz), 6.5 (d, 1H, CH<sub>ampy</sub>,  $^3J_{\text{H-H}} = 7.2$  Hz), 7.28 (t, 1H, CH<sub>ampy</sub>,  $^3J_{\text{H-H}} = 5.7$  Hz), 7.45 (d, 1H, CH,  $^3J_{\text{H-H}} = 10.2$

Hz), 7.85 (d, 1H, CH<sub>ampy</sub>,  $^3J_{\text{H-H}} = 4.2$  Hz), 8.85 (s, 1H, CH);  $^{19}\text{F}$ -NMR (DMSO):  $\delta$  (ppm) -122.08 (d, 1F,  $^3J_{\text{H-F}} = 10.2$  Hz); IR (cm<sup>-1</sup>): 3337, 3044, 2933, 2843, 2797, 1613, 1574, 1524, 1470, 1446, 1398, 1366, 1265, 1229, 1130, 1094, 1048, 1003, 980, 816, 773, 540, 497, 418, 367. UV-Vis (MeOH,  $\lambda$  (nm)): 201, 231, 252, 297, 324.

### 2.3.3 Synthesis of [Zn(levo)<sub>2</sub>(2,2-bipy)].H<sub>2</sub>O (3)

2,2-Bipy (8 mmol, 1.25 g) was dissolved in 15 ml MeOH and slowly added to a stirred solution of **1** (8 mmol, 1.963 g) in 30 ml MeOH. Then the mixture was stirred for an additional 3 h. The solvent was evaporated under vacuum and the precipitate was then washed with ether and petroleum ether and allowed to stand for air drying.

**[Zn(levo)<sub>2</sub>(2,2-bipy)].H<sub>2</sub>O (3)**. 76 % yield; m.p. = 247-250 °C;  $^{13}\text{C}\{1\text{H}\}$ -NMR (DMSO):  $\delta$  (ppm) 18.389 (CH<sub>3(levo)</sub>), 46.51 (CH<sub>3(levo)</sub>), 50.56 (2CH), 55.73 (2CH) 68.54 (CH), 103.67 (CH), 114.53 (CH), 121.36 (2CH), 124.80 (2CH), 125.30 (2CH), 131.26 (CH), 138.67 (2CH), 140.02 (CH), 147.92 (CH), 149.59 (2CH), 153.95 (C), 167.72 (O-C=O), 175.71 (C=O);  $^{19}\text{F}$ -NMR (DMSO):  $\delta$  (ppm) -121.34 (d, 1F,  $^3J_{\text{H-F}} = 10.2$  Hz); IR( cm<sup>-1</sup>): 3363, 3047,



2934, 2843, 2797, 1617, 1582, 1520, 1463, 1391, 1265, 1137, 1047, 1002, 980, 817, 764, 685, 542, 498, 416, 365, 279; UV-Vis (MeOH,  $\lambda$  (nm)): 201, 232, 255, 296, 323.

### **2.3.4 Synthesis of [Cu(levofloxacin)<sub>2</sub>(2-ampy)] .6.25H<sub>2</sub>O (4)**

Levofloxacin (0.5 mmol, 0.1807 g) and sodium hydroxide 1 M (0.5 ml) were added to 25 ml of (1:1) water/ethanol with continuous stirring. Then 2-ampy (1 mmol, 0.0941 g) was added to the reaction mixture. After the mixture was dissolved, copper nitrate (0.5 mmol,  $\approx$  1 g) dissolved in minimum amount of water, was added. Then the reaction was stirred for 3 h. The solvent was evaporated under vacuum until the dark green solution was concentrated, and then kept at room temperature to afford. Green crystals which were suitable for single crystal X-ray structure determination.

**[Cu(levofloxacin)<sub>2</sub>(2-ampy)].6.25H<sub>2</sub>O (4).** 71 % yield; m.p. = 260-262 °C; IR (cm<sup>-1</sup>): 3383, 3036, 2944, 2808, 1612, 1577, 1519, 1446, 1400, 1368, 1340, 1265, 1200, 1136, 1002, 980, 895, 813, 769, 692, 637, 554, 515, 392, 301; UV-Vis (MeOH,  $\lambda$  (nm)): 201, 231, 257, 297, 329, 365.

### 2.3.5 Synthesis of $[\text{Cu}(\text{levo})(\text{H}_2\text{O})(2,2\text{-bipy})](\text{NO}_3)\cdot 2.5\text{H}_2\text{O}$ (5)

Levofloxacin (0.5 mmol, 0.1807 g) and sodium hydroxide 1 M (0.5 ml) were added to 25 ml of (1:1) water/ethanol solution with continuous stirring. Then, 2,2-bipy (0.5 mmol, 0.0781 g) was added to the clear reaction mixture solution, copper nitrate (0.5 mmol,  $\approx$  1 g) dissolved in minimum amount of water, was added followed by stirring the reaction for 3 h.

The solvent was evaporated under vacuum until the dark green solution was concentrated, and then kept at room temperature to obtain blue crystals which were suitable for single crystal X-ray structure determination.

**$[\text{Cu}(\text{levo})(\text{H}_2\text{O})(2,2\text{-bipy})](\text{NO}_3)\cdot 2.5\text{H}_2\text{O}$  (5).** 62 % yield; m.p. = 222-223 °C; IR(  $\text{cm}^{-1}$ ): 3356, 3045, 2947, 2912, 2853, 1614, 1583, 1517, 1470, 1445, 1362, 1323, 1273, 1229, 1162, 1128, 1050, 1000, 877, 809, 776, 693, 659, 597, 549, 513, 487, 417, 386, 262; UV-Vis (MeOH,  $\lambda$  (nm)): 203, 225, 250, 300, 327, 362.

## 2.4 single X-ray crystal diffraction:

Single crystal X-ray analysis of complexes **4** and **5** were carried out by attaching single crystal to a glass fiber with epoxy glue, and then it transferred to X-ray diffractometer system (Bruker SMART APEX CCD) which is controlled by using Pentium-based PC running the SMART software package. The three-circle goniometer of a single crystal which was mounted with  $\chi$  fixed at  $+54.76^\circ$ , was rapidly cooled to  $-150^\circ\text{C}$ . The diffracted graphite-monochromated ( $K\alpha$  radiation  $\lambda = 0.71073 \text{ \AA}$ ) was detected on a phosphor screen at  $-44^\circ\text{C}$  and it held at 6.0 cm from the crystal. A detector array of 512 X 512 pixels (a pixel size  $\sim 120 \mu\text{m}$ ) was used to collect data. The calibration of detector centroid and crystal to detector distance were applied by using least-squares analysis of the unit cell parameters, YLID was used as a reference crystal.

After the crystal of the compound was put in the cantered of the X-ray beam, a series of 30 data frames which measured at  $0.3^\circ$  increments of  $\omega$ , were collected with three different values ( $2\theta$  and  $\varphi$ ) to calculate a preliminary unit cell and to assess the overall crystal quality of the compound. The

intensity data was measured by put the detector at -28 °C but the intensity images were collected at 0.3° intervals of  $\omega$  through 2 sec.

After that, the raw data frames were transferred to another computer to integrate by using SAINT program package ((SAINT-NT V5.0, BRUKER AXS GMBH, D-76181 Karlsruhe). To update the background frame information was used this equation  $B' = (7B+C)/8$  where B' is the update pixel value, B is the background pixel value before updating and C is the pixel value through the current frame. The structure was refined and solved by using SHELXTL software package (SHELXTL-NT V6.1, BRUKER AXS GMBH, Karlsruhe).<sup>85-87</sup> Crystal data and structure refinements are summarized in Tables 7.

Table 7: Crystal data and structure refinement for complexes **4** and **5**.

	<b>Complex 4</b>	<b>Complex 5</b>
Empirical formula	<b>C<sub>41</sub>H<sub>44</sub>CuF<sub>2</sub>N<sub>8</sub>O<sub>8</sub> · 6.25(H<sub>2</sub>O)</b>	<b>C<sub>28</sub>H<sub>25</sub>CuFN<sub>5</sub>O<sub>5</sub> · NO<sub>3</sub> · 2.5(H<sub>2</sub>O)</b>
Formula weight	1046.74	701.21
Temperature/K	150.00(10)	99.9(5)
Crystal system	monoclinic	triclinic
Space group	P2 <sub>1</sub>	P1
a/Å	15.33240(10)	10.25000(10)
b/Å	16.8695(2)	10.42200(10)
c/Å	18.8099(2)	30.5150(3)
α/°	90	84.0340(10)
β/°	93.6570(10)	82.8630(10)
γ/°	90	70.4470(10)
Volume/Å <sup>3</sup>	4855.27(8)	3041.21(5)
Z	4	4
ρ <sub>calc</sub> /cm <sup>3</sup>	1.432	1.531
μ/mm <sup>-1</sup>	0.537	0.793
F(000)	2193.0	1451.0
Crystal size/mm <sup>3</sup>	0.304 × 0.238 × 0.134	0.206 × 0.088 × 0.068
Radiation	Mo Kα (λ = 0.71073)	Mo Kα (λ = 0.71073)
2θ range for data collection/°	4.11 to 64.002	4.044 to 63.134
Index ranges	-22 ≤ h ≤ 20, -24 ≤ k ≤ 24, -27 ≤ l ≤ 26	-14 ≤ h ≤ 15, -14 ≤ k ≤ 14, -44 ≤ l ≤ 43
Reflections collected	88332	83027
Independent reflections	28117 [R <sub>int</sub> = 0.0279, R <sub>sigma</sub> = 0.0352]	34154 [R <sub>int</sub> = 0.0174, R <sub>sigma</sub> = 0.0241]
Data/restraints/parameters	28117/1/1329	34154/7/1982
Goodness-of-fit on F <sup>2</sup>	1.036	1.026
Final R indexes [I ≥ 2σ (I)]	R <sub>1</sub> = 0.0467, wR <sub>2</sub> = 0.1276	R <sub>1</sub> = 0.0402, wR <sub>2</sub> = 0.1130
Final R indexes [all data]	R <sub>1</sub> = 0.0617, wR <sub>2</sub> = 0.1363	R <sub>1</sub> = 0.0428, wR <sub>2</sub> = 0.1152
Largest diff. peak/hole / e Å <sup>-3</sup>	0.86/-0.41	1.26/-0.66
Flack parameter	0.004(3)	0.0004(17)

$$^a R_1 = \sum ||F_o| - |F_c|| / \sum |F_o| \text{ and } wR_2 = \left\{ \frac{\sum [w(F_o^2 - F_c^2)^2]}{\sum [w(F_o^2)^2]} \right\}^{1/2}$$

## 2.5. Anti-bacterial activity

The Gram-negative bacteria (*P. mirabilis*, *E. coli*, *P. aeruginosa* and *K. pneumonia*) and Gram-positive bacteria (*S. aureus*, *S. epidermidis*, *B. subtilis* and *E. faecalis*) were used to investigate Zn and Cu complexes through Agar diffusion method.

*In-vitro*, single bacterial colonies was dissolved in sterile saline solution (0.9% of NaCl) until the suspended cells reached the turbidity of McFarland 0.5 Standard. Sterile cotton swab was used to spread the bacterial inocula on the surface of Muller Hinton nutrient agar. The wells (diameter 6 mm) in the agar plate were formed by using sterile glassy borer.<sup>88</sup>

Zinc and Cu complexes were dissolved in DMSO (6 mg/ml), then 25  $\mu$ L of the test complexes were added into the respective wells. After that, the plates were incubated at 37 °C for 12-24 h.

Levofloxacin and DMSO were used as positive, negative controls, respectively. Inhibition zone diameter (IZD) was used to measure the sensitivity of complexes toward the different kind of bacteria. Figure 18 shows agar diffusion.

The results were determined by calculating the average of three trials, and these results are stated as average  $\pm$  standard error.<sup>58,88,89</sup>

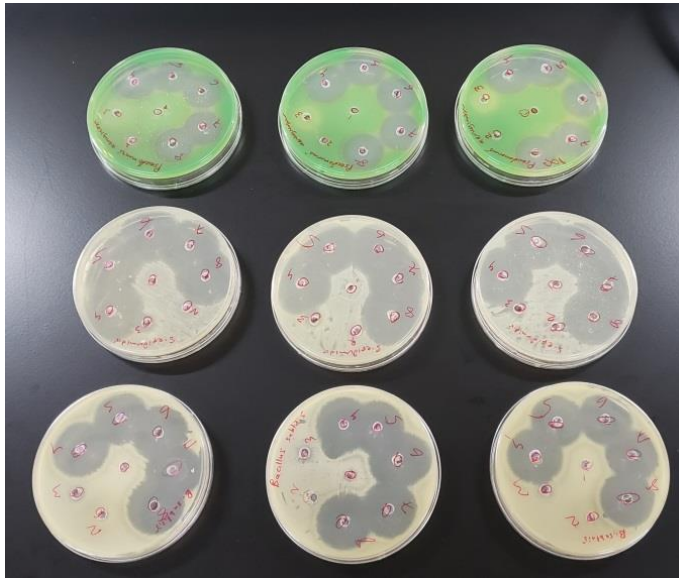


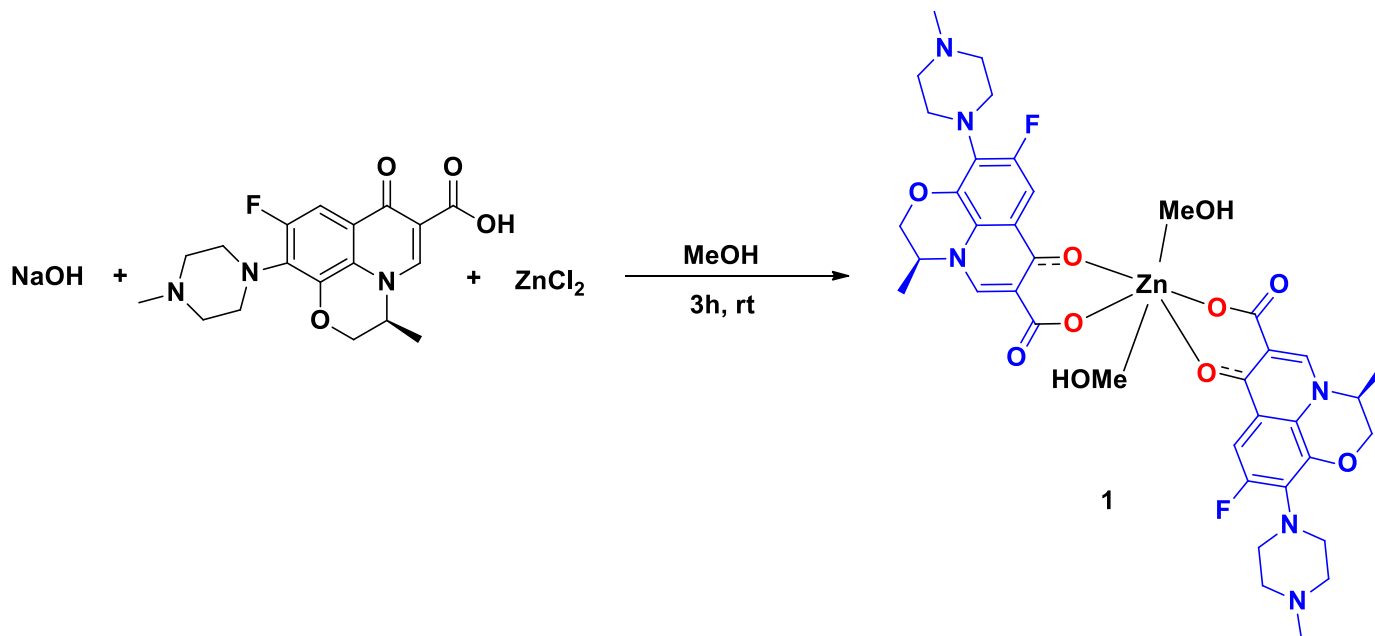
Figure 18: Agar diffusion plates.

### 3. Results and discussion

#### 3.1.1 Synthesis of zinc levofloxacin complexes

Zinc levofloxacin complex  $[\text{Zn}(\text{levo})_2(\text{MeOH})_2]$  (**1**) was prepared via reaction of 1 equivalent of  $\text{ZnCl}_2$  with 2 equivalents of levofloxacin and 2 equivalents of sodium hydroxide in methanol at ambient condition as shown in Scheme 1. The yellow solid complex was obtained in 79% yield.

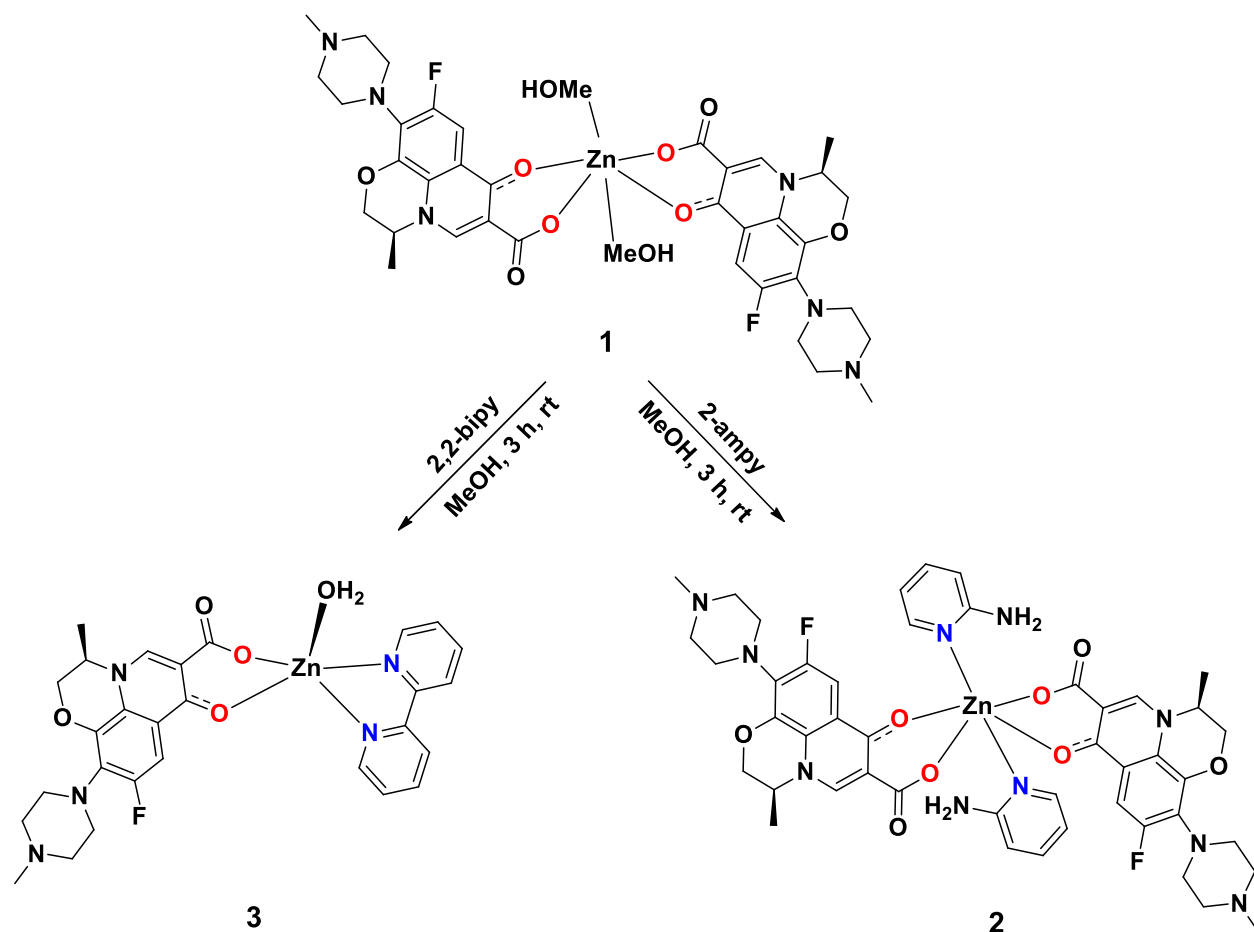
Scheme 1: Synthesis of  $[\text{Zn}(\text{levo})_2(\text{MeOH})_2]$  (**1**), proposed structure.





Zinc levofloxacin complex was reacted with different molar ratios of N-based ligands, (2-ampy and 2,2-bipy) to obtain zinc levofloxacin complexes **2** and **3** as shown in Scheme 2.

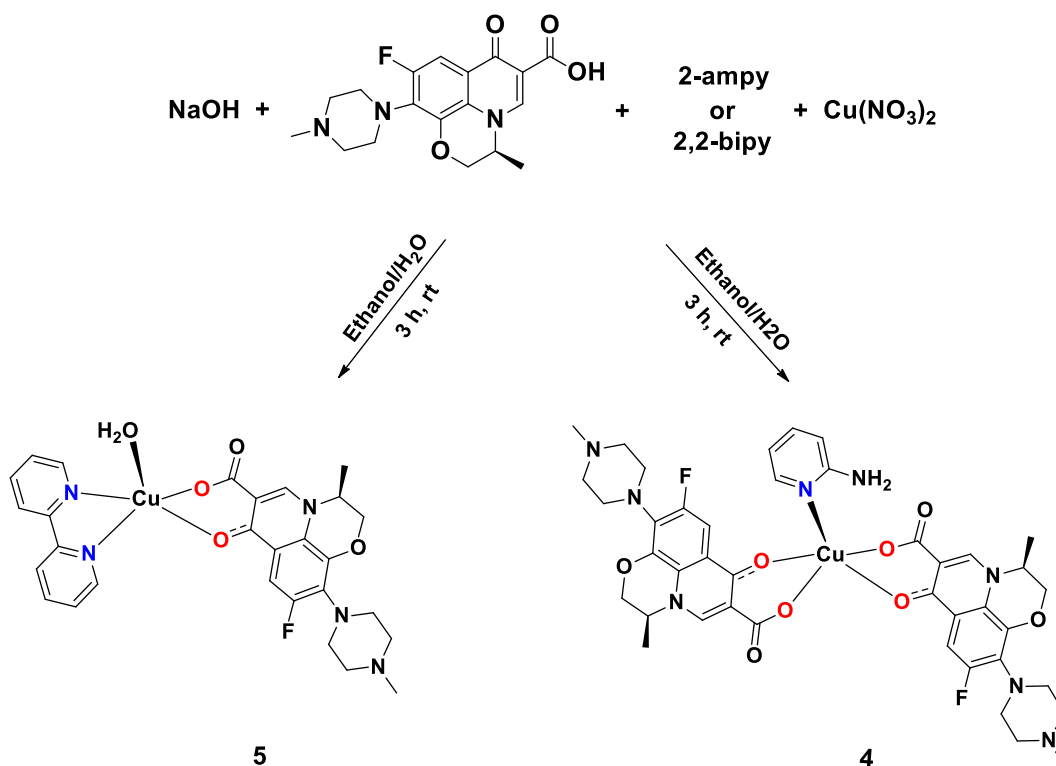
Scheme 2: Synthesis of complexes **2** and **3** proposed structures.



### 3.1.2 Synthesis of copper levofloxacin complexes

Copper levofloxacin complex  $[\text{Cu}(\text{levo})_2(2\text{-ampy})] \cdot 6.25\text{H}_2\text{O}$  (**4**) was obtained at room temperature by adding 1 equivalent of copper nitrate to a solution mixture of 1 equivalent of levofloxacin, 1 equivalent of sodium hydroxide and 0.5 equivalent of 2-ampy.  $[\text{Cu}(\text{levo})(\text{H}_2\text{O})(2,2\text{-bipy})](\text{NO}_3) \cdot 2.5\text{H}_2\text{O}$  (**5**) was prepared by the same procedure of **4** but with 2,2-bipy as the N-based ligand. Scheme 3 shows the synthesis of complexes **4** and **5**, respectively.

Scheme 3: Synthesis of complexes **4** and **5**.



The physical properties and the percent yields of complexes **1-5** are listed in Table 8.

Table 8: Physical properties and % yield of complexes (**1-5**).

Complex	Color	m.p (°C)	% Yield	Solubility
[Zn(lev <sub>o</sub> ) <sub>2</sub> (MeOH) <sub>2</sub> ] ( <b>1</b> )	Yellow	268 <sup>d</sup>	79	Water, methanol, dichloromethane, chloroform, DMSO and slightly soluble in ethanol.
[Zn(lev <sub>o</sub> ) <sub>2</sub> (2-ampy) <sub>2</sub> ] ( <b>2</b> )	Yellowish	228-231	73	Water, methanol, ethanol and DMSO
[Zn(lev <sub>o</sub> ) <sub>2</sub> (2,2-bipy)] ( <b>3</b> )	Yellowish	247-250	76	Water, methanol, ethanol, DMSO dichloromethane and chloroform
[Cu(lev <sub>o</sub> ) <sub>2</sub> (2-ampy)] ( <b>4</b> )	Green	260-262	71	Methanol, ethanol and DMSO.
[Cu(lev <sub>o</sub> )(H <sub>2</sub> O)(2,2-bipy)] (NO <sub>3</sub> ). 2.5H <sub>2</sub> O ( <b>5</b> )	Blue	222-223	62	Water, methanol, DMSO and slightly soluble in ethanol

### 3.2 Electronic absorption spectroscopy

In metal complexes, three types of electronic transition are generally described: (1) Intra-ligand transition bands. (2) Metal ion *d-d* electronic transition bands. (3) Metal to ligand (MLCT) or ligand to metal charge transfer (LMCT).<sup>90,91</sup>

Table 9 shows the UV-Vis. data of complexes **1-5** and their parent ligands in methanol as solvent. Zn(II) ion with  $d^{10}$  configuration has no  $d-d$  electronic transition bands. The observed bands at (198-325) nm of all complexes are due to the MLCT and intra-ligand transition bands e.g.,  $\pi-\pi^*$  and  $n-\pi^*$  transitions. In addition, no LMCT can be assigned for complexes **1, 2, and 3** due to the filled  $d$  orbital's of Zn(II) ion. However, complexes **4** and **5** can exhibit LMCT and  $d-d$  transitions due to the unfilled  $d^9$  electronic configuration of Cu(II) ion, so a less defined LMCT bands at 365 and 362 nm were assigned, respectively.

All bands between (198-325) nm for all complexes were similar to the bands of their parent ligands with slightly hypsochromic or bathochromic shifts indicating complex formation. Figures 19 and 20 show UV-Vis. Spectra of complexes **2, 5** and their parent ligands. Figures S1-S3 of complexes **1, 3** and **4** are shown in **Appendix A**.

Table 9: UV-visible spectral data for complexes (1-5) and their parent ligands.

Complexes	$\lambda_{\max}$ (nm)	Ligands	$\lambda_{\max}$ (nm)
[Zn(lev <sub>o</sub> ) <sub>2</sub> (MeOH) <sub>2</sub> ] (1)	198, 228 257, 297 325	Levo	198, 227 253, 299 324
[Zn(lev <sub>o</sub> ) <sub>2</sub> (2-ampy) <sub>2</sub> ] (2)	201, 231 252, 297 324	2-ampy	204, 233 295
[Zn(lev <sub>o</sub> ) <sub>2</sub> (2,2-bipy)].H <sub>2</sub> O (3)	201, 232 255, 296 323	2,2-bipy	203, 235 244, 281
[Cu(lev <sub>o</sub> ) <sub>2</sub> (2-ampy)].6.25H <sub>2</sub> O (4)	201, 231 257, 297 329, 365		
[Cu(lev <sub>o</sub> )(H <sub>2</sub> O)(2,2-bipy)](NO <sub>3</sub> ). 2.5H <sub>2</sub> O (5)	203, 225 250, 300 327, 362		

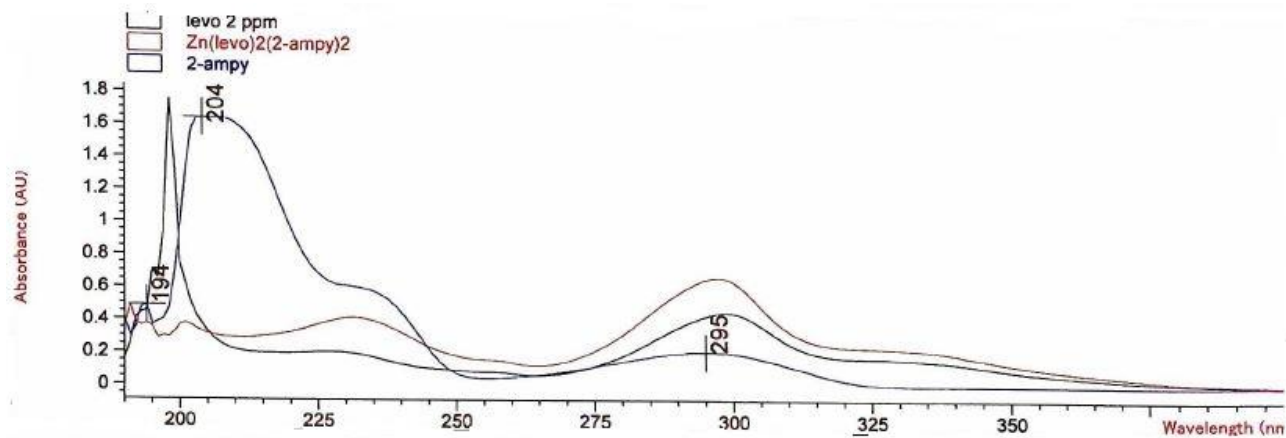


Figure 19: UV-Vis. spectra of complex 2 with parent ligands.

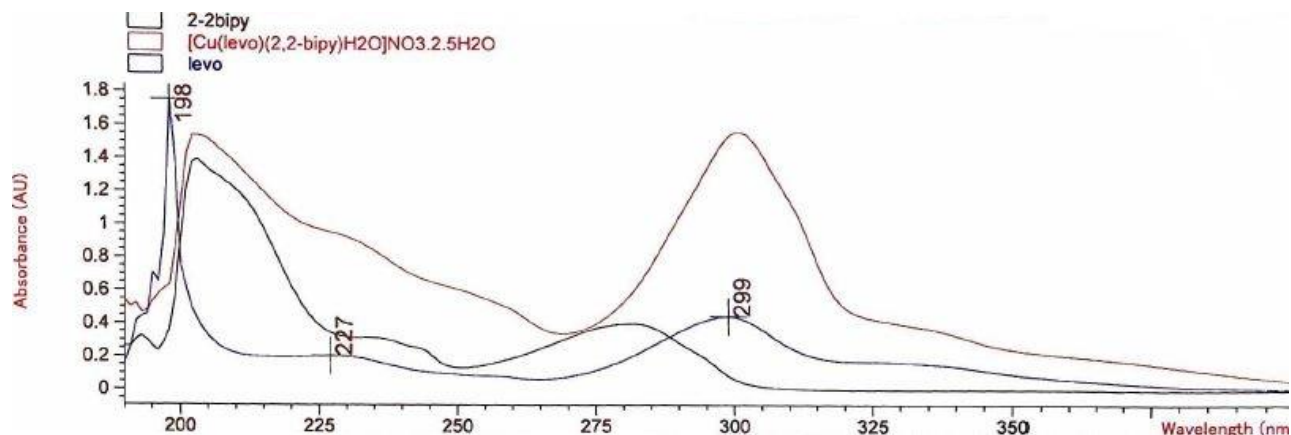


Figure 20: UV-Vis. spectra of complex **5** with parent ligands

### 3.3 IR vibrational assignments

FT-IR instrument was used to measure and assign the major functional groups as a characterization technique of the prepared Cu and Zn complexes to their parent ligands. IR spectra in the range of (200-4000  $\text{cm}^{-1}$ ) provide valuable information about the coordination mode between ligands and metal ions.<sup>84,92</sup> The IR frequencies for Na<sub>levO</sub> and complex **1** are summarized in Table 10. Na<sub>levO</sub> showed the absorption peak for the pyridone  $\nu(\text{C}=\text{O})_{\text{p}}$  at 1616  $\text{cm}^{-1}$  and the weak peak of the carboxylate stretch  $\nu(\text{C}=\text{O})_{\text{carb}}$  at 1721  $\text{cm}^{-1}$ .

Table 10: IR absorption frequencies (in  $\text{cm}^{-1}$ ) of  $\text{Na}_{\text{Levo}}$  and complex **1**.

Assignments	$\text{Na}_{\text{Levo}}$	Complex <b>1</b>
$\nu(\text{C-H})_{\text{alph}}$	2933, 2844	2934, 2843
$\nu(\text{C-H})_{\text{ar}}$	3081	3045
$\nu(\text{C=O})_{\text{p}}$	1616	1574
$\nu(\text{C=O})_{\text{carb}}$	1721	-
$\nu(\text{COO}^-)_{\text{asym}}$	1586	1615
$\nu(\text{COO}^-)_{\text{sym}}$	1392	1397
$\nu(\text{C-C})_{\text{ring}}$	1535	1522
$\Delta\nu(\text{COO}^-)$	194	218

In complex **1**, the peak of the carboxylic group,  $\nu(\text{C=O})_{\text{carb}}$  has disappeared upon binding and is replaced by two characteristic peaks at  $1615 \text{ cm}^{-1}$  and  $1397 \text{ cm}^{-1}$ , asymmetric  $\nu(\text{COO}^-)_{\text{asym}}$  and symmetric  $\nu(\text{COO}^-)_{\text{sym}}$  stretching vibrations, respectively. The difference between the two peaks  $\Delta\nu(\text{COO}^-) = 218 \text{ cm}^{-1}$  which is greater than in  $\text{Na}_{\text{Levo}}$   $\Delta\nu(\text{COO}^-) = 194 \text{ cm}^{-1}$  indicating monodentate coordination mode of the carboxylate group. The carbonyl pyridone  $\nu(\text{C=O})_{\text{p}}$  is shifted from  $1616 \text{ cm}^{-1}$  to  $1574 \text{ cm}^{-1}$  upon bonding.

The overall changes indicate that levofloxacin was binded to the metal through the pyridone oxygen atom and one of the oxygen atoms from the carboxylate group.<sup>80,92-99</sup>

The principal absorption peaks of complexes **2**, **3**, **4** and **5** were showed in Table 11,  $\Delta\nu(\text{COO}^-)$  values are 215, 226, 212 and 252  $\text{cm}^{-1}$ , respectively and all are greater than  $\text{Na}_{\text{levo}} \Delta\nu(\text{COO}^-) = 194 \text{ cm}^{-1}$ , which suggest monodentate coordination mode as also proved by X-ray single crystal structure determination of complexes **4** and **5**.

Generally, the  $\nu(\text{M-N})$  and  $\nu(\text{M-O})$  for metal complexes appear as weak bands in the range of (430 - 576)  $\text{cm}^{-1}$ .<sup>100-102</sup>

For all complexes, the broad split peak between 3500 and 3100  $\text{cm}^{-1}$  assigned to the O-H and N-H stretching of  $\text{H}_2\text{O}$  molecules and piperazinyl moiety, respectively.<sup>97</sup>



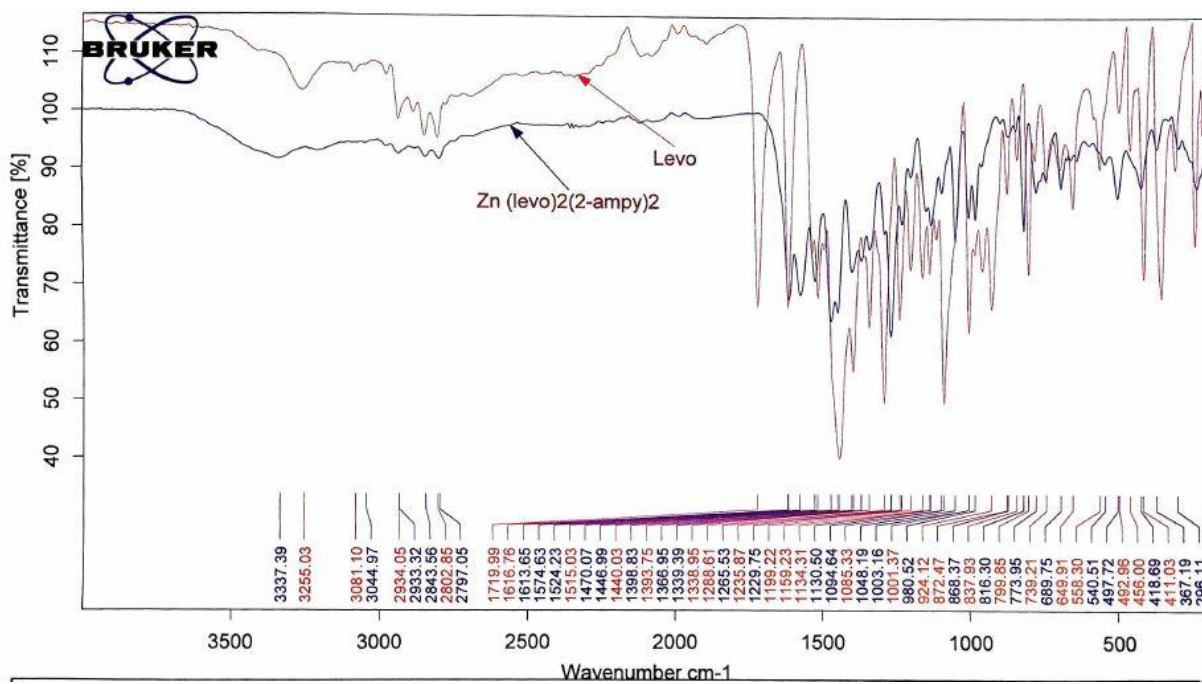
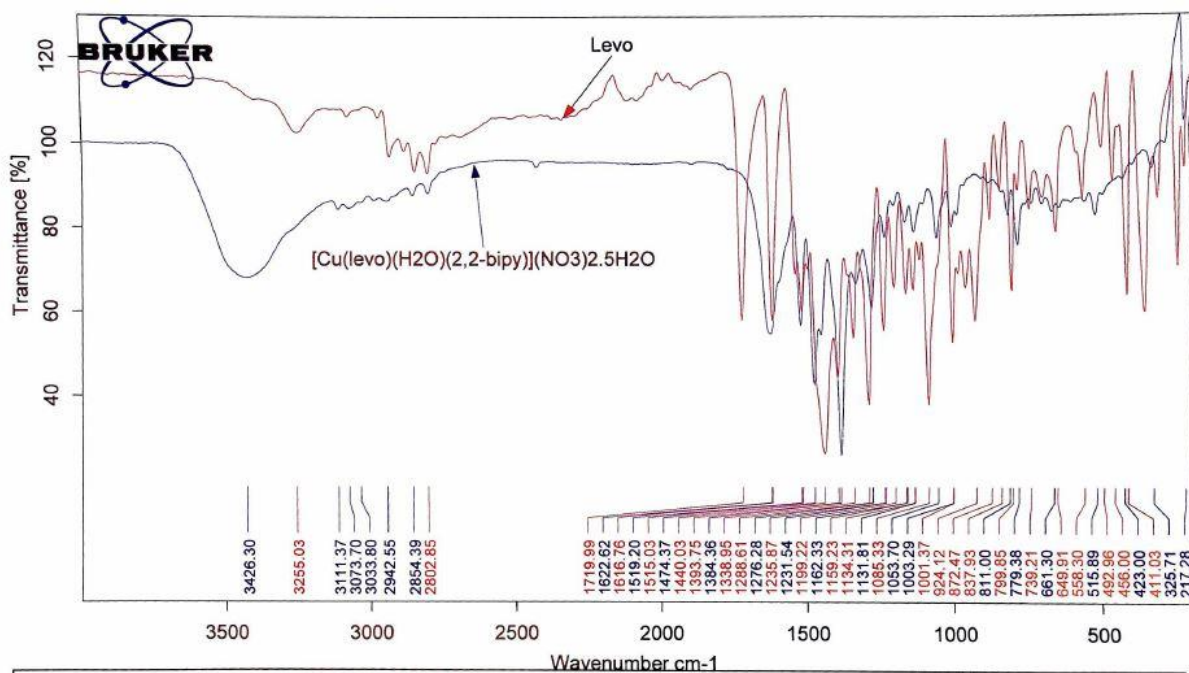
Table 11: IR absorption frequencies (in  $\text{cm}^{-1}$ ) of complexes **2-5**.

Assignments	Complex 2	Complex 3	Complex 4	Complex 5
$\nu(\text{C-H})_{\text{alph}}$	2933, 2843	2934, 2843	2944, 2849	2947, 2853
$\nu(\text{C-H})_{\text{ar}}$	3044	3047	3036	3045
$\nu(\text{C=O})_{\text{p}}$	1574	1582	1577	1583
$\nu(\text{COO}^-)_{\text{asym}}$	1613	1617	1612	1614
$\nu(\text{COO}^-)_{\text{sym}}$	1398	1391	1400	1362
$\nu(\text{C-C})_{\text{ring}}$	1524	1520	1519	1517
$\nu(\text{C-O})$	1130	1137	1136	1162
$\nu(\text{C-N})_{\text{ring}}$	1229	1230	1226	1229
$\Delta\nu(\text{COO}^-)$	215	226	212	252

Figures 21 and 22 show IR spectra of complexes **2, 5** and the levo ligand.

Figures S4-S6 of complexes **1, 3** and **4** IR spectra are found in **Appendix**

**B.**

Figure 21: IR spectra of complex **2** and levo ligand.Figure 22: IR spectra of complex **5** and levo ligand.

### 3.4 $^1\text{H}$ Nuclear Magnetic Resonance

The  $^1\text{H}$ -NMR spectral data of complex **1** and levofloxacin are shown in Figure 23 and the results are shown in in Table S 1 (**Appendix C**).

The relative intensities of  $^1\text{H}$ -NMR signals in complex **1** are supporting the proposed structure. In general, most  $^1\text{H}$ -NMR resonances showed slight upfield or down field shifts compared to the same resonances in the

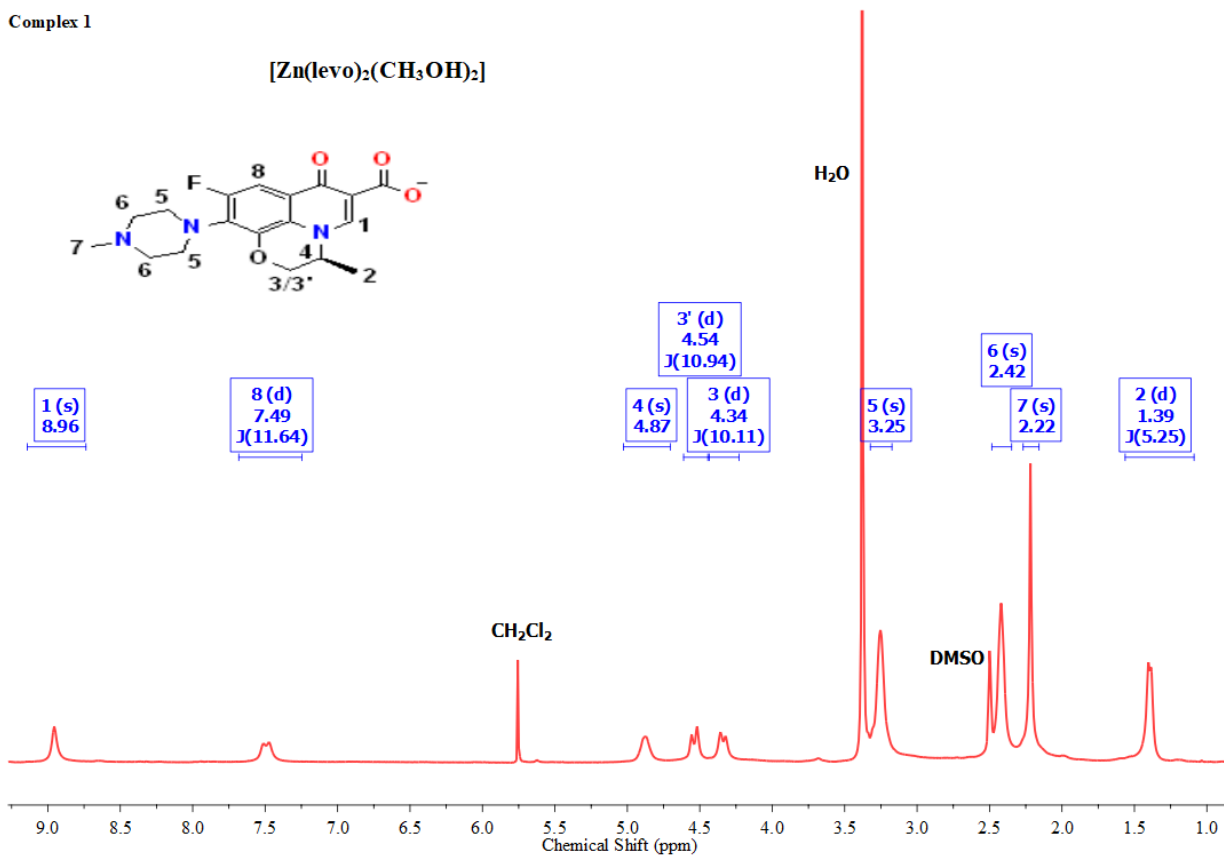


Figure 23:  $^1\text{H}$ -NMR spectra of complex **1**.

levofloxacin parent ligand which may be due to electron donation of the keto-carboxylate group to the zinc ion through  $\sigma$ -bond.

Figure 24 show the  $^1\text{H-NMR}$  spectra of complex **2** with relevant data and its parent ligand, the detailed resonances are also shown in Table S 2 (**Appendix C**). Slight upfield shifts compared to the same resonances in H-levo are pronounced which may be due to the complexation of the Zn cation with H-levo and the nitrogen donor ligand.

From the IR spectral analysis data we may conclude that the levofloxacin was coordinated to Zn(II) in a bidentate coordination mode through the pyridone oxygen atom and one of the carboxylate group oxygen atoms . In addition, the  $^1\text{H-NMR}$  spectral intensity data can be used to determine the coordination mode and the ratio between the levofloxacin ligand and the N-based ligand in the complex.

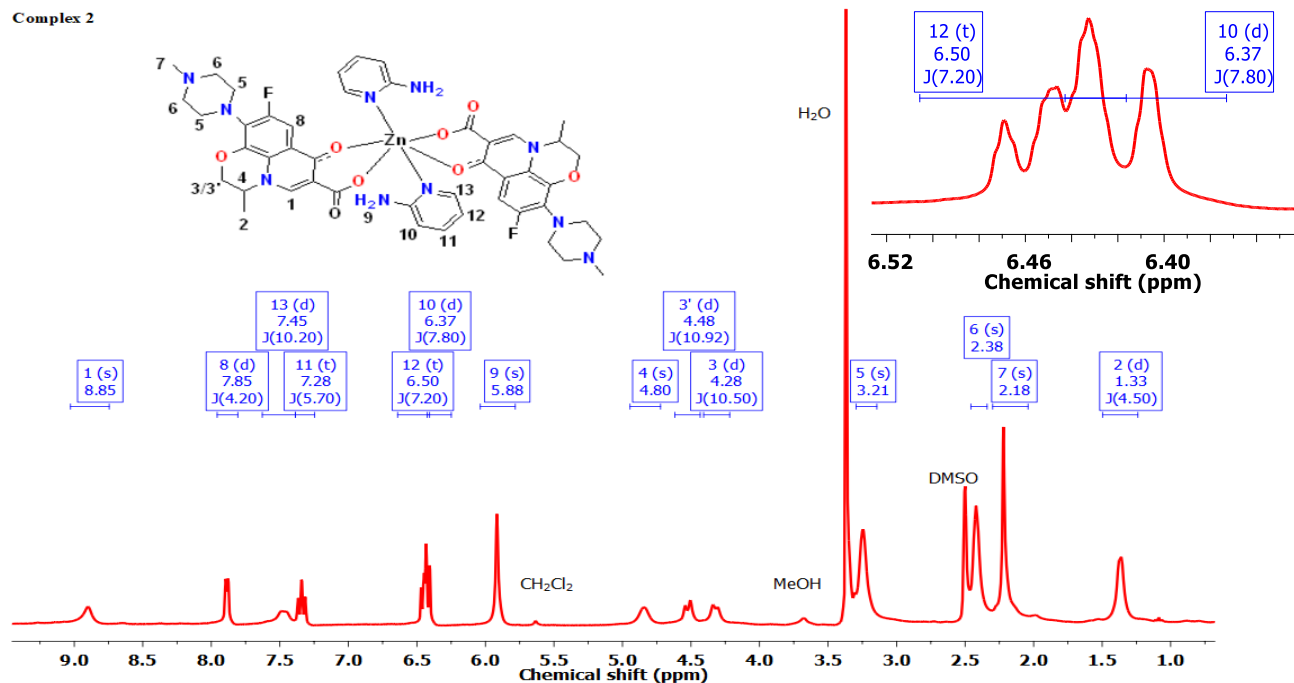


Figure 24:  $^1\text{H-NMR}$  spectra of complex 2.

### 3.4 Crystal structure description

Suitable crystals of complexes **4** and **5** were obtained by slow evaporation of an ethanol–water mixture and their molecular structures were determined. The crystal data and parameters are shown in Table 7. Crystallographic information files (CIF) are given in **Appendix E** and **Appendix F**.

### 3.4.1 Crystal structure of [Cu(levo)<sub>2</sub>(2-ampy)].6.25H<sub>2</sub>O (**4**)

The mononuclear molecular structure of complex **4** is shown in Figure 25a. According to this figure, Cu(II) is coordinated to two bidentate chelating levofloxacin molecules through the pyridone oxygen atom and one of the oxygen atoms from the carboxylato group forming a six-membered ring and one monodentate 2-ampy ligand forming slightly distorted square pyramidal geometry. The mononuclear complex **4** was crystallized in the monoclinic crystal system and the chiral space group  $P2_1$ . The monomeric units consist of (CuNO<sub>4</sub>) chromophore, Figure 25b.

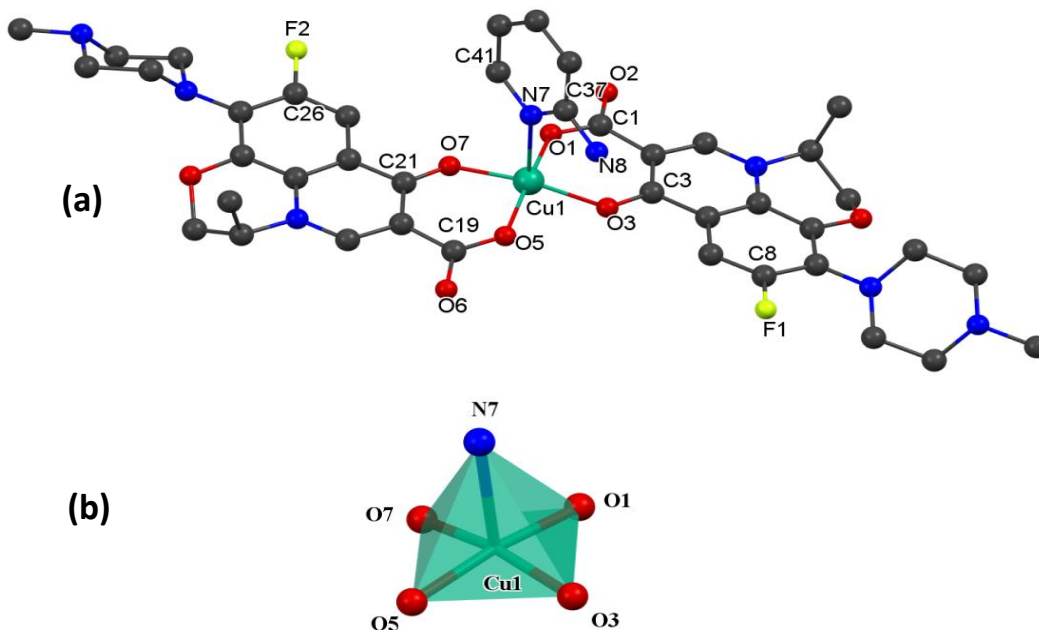


Figure 25: (a) Molecular structure of complex **4** showing the labeling atom scheme. (b) the distorted square-pyramidal [CuNO<sub>4</sub>] center.

The asymmetric unit contains two independent complexes with a distorted square pyramidal geometry in which the base of the pyramid composed of two *trans*- Levofloxacin ligands and the apex is a 2-aminopyridine molecule. In the first complex the chiral methyl group of levofloxacin ligands is in the same direction of the pyramid apex and in the second complex the chiral methyl group of levofloxacin ligands is in the opposite direction of the pyramid apex.

The unit cell contains four complexes and approximately twenty-five water molecules, in which some of them are badly disordered and these water molecules connected the complexes in a complicated web of hydrogen bonds as shown in Figure 26.

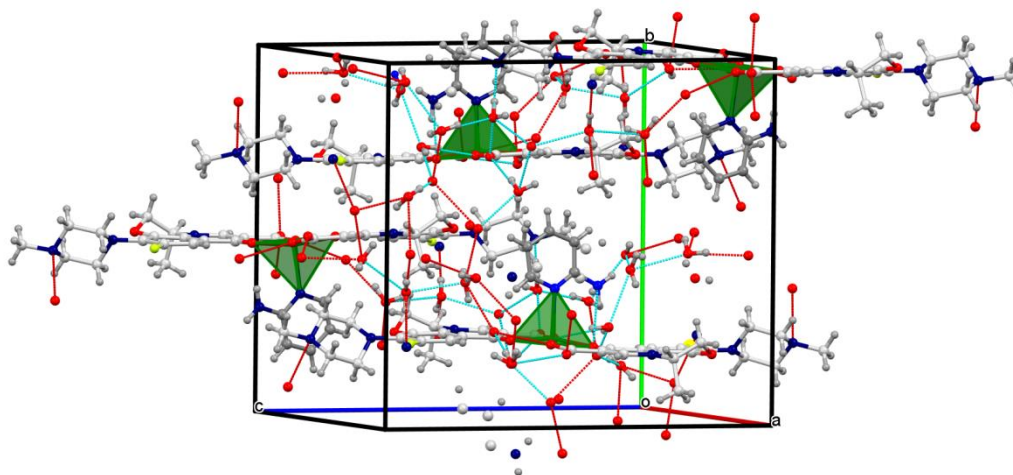


Figure 26: Number of molecules per unit cell of complex 4 indicating the hydrogen bonds.

Selected bond angles and distances are listed in Table 12 and the crystallographic information files (CIF) are given in **Appendix E**

Table 12: Selected bond distances (Å) and bond angles (°) of complex **4**

<b>Bond</b>	<b>Distance ( Å )</b>	<b>Bond</b>	<b>Angle (°)</b>
O(1)– Cu(1)	1.941(2)	O(1)– Cu(1)–N(7)	92.24(12)
O(3)– Cu(1)	1.940(2)	O(3)–Cu(1)–N(7)	99.65(13)
O(5)– Cu(1)	1.938(2)	O(5)–Cu(1)–N(7)	96.51(12)
O(7)– Cu(1)	1.931(2)	O(7)–Cu(1)–N(7)	93.92(12)
N(7)– Cu(1)	2.274(4)	O(3)–Cu(1)–O(1)	92.62(10)
		O(5)–Cu(1)–O(1)	171.22(14)
		O(5)–Cu(1)–O(3)	86.57(10)
		O(7)–Cu(1)–O(1)	85.29(10)
		O(7)–Cu(1)–O(3)	166.35(13)
		O(7)–Cu(1)–O(5)	93.44(10)

The bond distances of Cu-O [1.941(2), 1.940(2), 1.938(2) and 1.931(2) Å] which are slightly shorter than the distances found in previously reported [Cu(hex)<sub>2</sub>(2-apy)<sub>2</sub>] and [Cu(hep)<sub>2</sub>(2-apy)<sub>2</sub>] complexes.<sup>103</sup>



However, the observed bond distances of Cu-N [2.274(4) Å] for N(7)–Cu(1) is longer than the distance in [Zn(2-ampy)<sub>2</sub>Cl<sub>2</sub>], [Zn(2-ampy)<sub>2</sub>Br<sub>2</sub>] and [Cu(Sal-Trp)(2-aminopyridine)] complexes.<sup>103–106</sup>

Furthermore, [CuNO<sub>4</sub>] chromophore showed slightly distorted square pyramidal due to the following unsymmetrical bond angles: O(1)–Cu(1)–N(7) = 92.24(12)°, O(3)–Cu(1)–N(7) = 99.65(13)°, O(5)–Cu(1)–N(7) = 96.51(12)°, O(7)–Cu(1)–N(7) = 93.92(12)°, O(3)–Cu(1)–O(1) = 92.62(10)°, O(5)–Cu(1)–O(1) = 171.22(14)°, O(5)–Cu(1)–O(3) = 86.57(10)°, O(7)–Cu(1)–O(1) = 85.29(10)°, O(7)–Cu(1)–O(3) = 166.35(13)°, O(7)–Cu(1)–O(5) = 93.44(10)°.

Generally, the intermolecular and intramolecular hydrogen bonding play an important role in the enhancement of complex stability, for example, H-bonds give conformational stability of protein and other complex structures.<sup>107,108</sup>

Table 13, shows the various types of H-bonding, bond distances in (Å) and bond angles (°). The data show two intramolecular hydrogen bondings, (C32–H32B...O8 and C73–H73A...O16) and one intermolecular hydrogen bonding, C59–H59C...O23W<sup>1</sup>.

Table 13: Hydrogen bond distances (Å) and bond angles (°) of complex **4**.

D-H...A	d(D-H)/Å	d(H-A)/Å	d(D-A)/Å	D-H-A/°
C32-H32B...O8	0.97	2.27	2.887(4)	120.6
C59-H59C...O23W <sup>1</sup>	0.96	1.95	2.827(15)	150.5
C73-H73A...O16	0.97	2.28	2.902(4)	121.4

Symmetry transformations used to generate equivalent atoms: 1+X,-1+Y,+Z; <sup>2</sup>1+X,+Y,+Z; <sup>3</sup>1+X,-1+Y,+Z; <sup>4</sup>+X,1+Y,+Z

### 3.4.2 Crystal structure of [Cu(levO)(H<sub>2</sub>O)(2,2-bipy)](NO<sub>3</sub>).2.5H<sub>2</sub>O (**5**)

The crystal structure of complex **5** was depicted in Figure 27a. The mononuclear cationic complex [Cu(levO)(H<sub>2</sub>O)(2,2-bipy)]<sup>+</sup> was determined in the triclinic crystal system and the chiral space group *P1* with four molecules per unit cell as shown in **Error! Reference source not found.**

The Cu(II) cation is coordinated to one bidentate chelating levofloxacin through the pyridone oxygen atom and one of the oxygen atoms from the carboxylato group forming a six-membered ring, one bidentate 2,2-bipy and

one water molecule with a distorted square pyramidal geometry. The monomeric units consist of  $(\text{CuN}_2\text{O}_3)$  chromophore, Figure 27b.

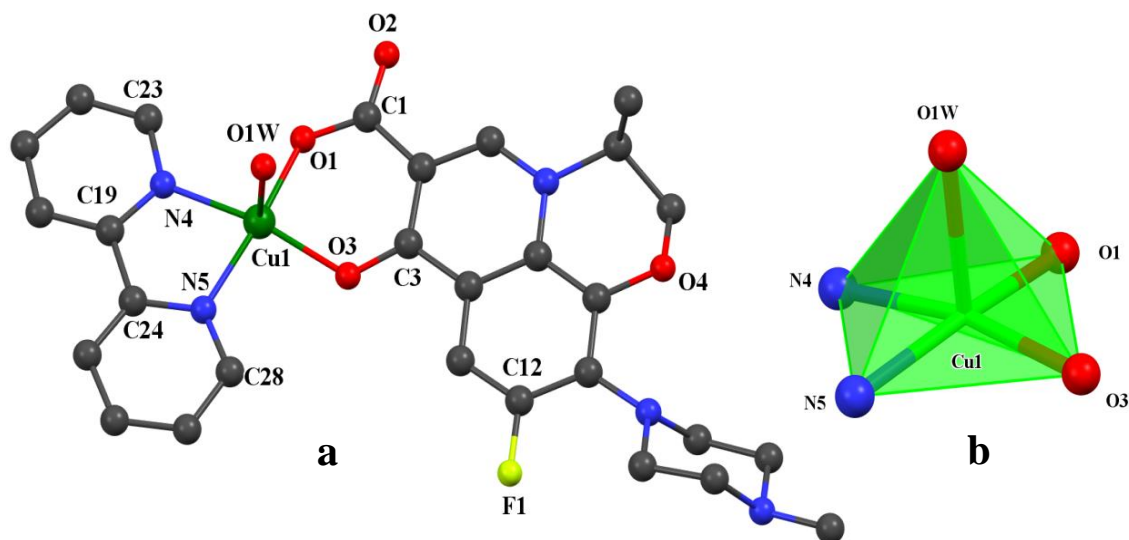


Figure 27: (a) Molecular structure of complex 5 showing the labeling atom scheme. (b) The distorted square-pyramidal  $[\text{CuN}_2\text{O}_3]$  center.

The crystallographic information files (CIF) are given in **Appendix F**. The unit cell contains four independent complexes, four nitrates and ten water molecules which are connected in a web of hydrogen bonds. The complexes are positively charged and have a nitrate anion to counter the charge. In addition the complexes are a distorted square pyramid with the base of the

pyramid composed of Levofloxacin ligand and 2,2'-Bipyridine and the apex is a water molecule. In two complexes the chiral methyl group of Levofloxacin ligands is in the same direction of the pyramid apex. In the other two complexes the chiral methyl is in the opposite direction of the pyramid apex and the levofloxacin is disordered.

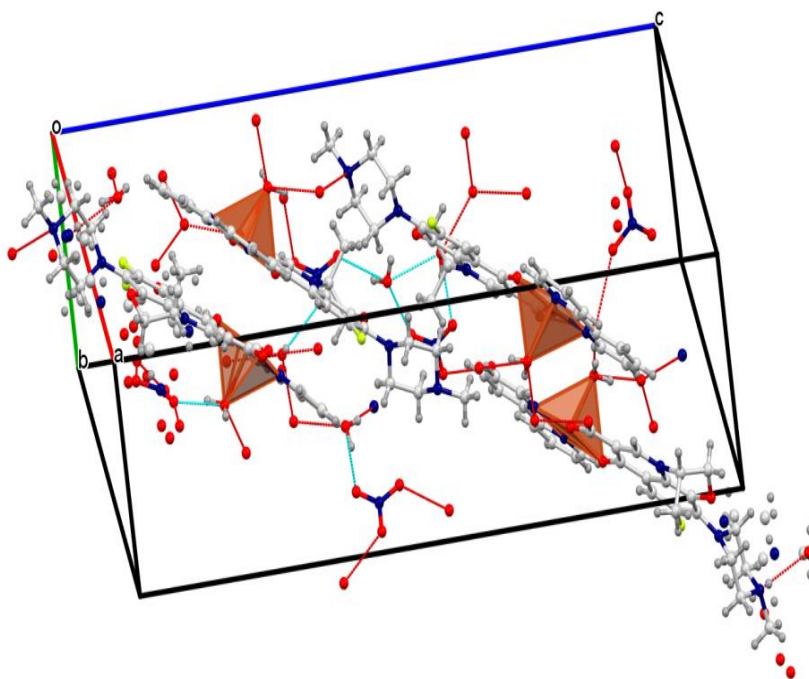


Figure 28: Number of molecules per unit cell of complex **5**

Selected bond angles and distances are listed in Table 14.

Table 14: Selected bond distances (Å) and bond angles (°) of complex 5.

Bond	Distance ( Å )	Bond	Angle (°)
N(4)-Cu(1)	1.996(3)	O(1)-Cu(1)-O(1W)	96.69(12)
N(5)-Cu(1)	1.992(3)	O(1)-Cu(1)-O(3)	93.25(11)
O(1)-Cu(1)	1.908(3)	O(1)-Cu(1)-N(4)	91.92(12)
O(3)-Cu(1)	1.944(3)	O(1)-Cu(1)-N(5)	169.60(11)
O(1W)-Cu(1)	2.244(3)	O(3)-Cu(1)-O(1W)	93.54(11)
O(1)-C(1)	1.278(4)	O(3)-Cu(1)-N(4)	168.23(12)
O(3)-C(3)	1.277(4)	O(3)-Cu(1)-N(5)	92.24(11)
N(4)-C(19)	1.342(5)	N(4)-Cu(1)-O(1W)	96.35(11)
N(4)-C(23)	1.351(4)	N(5)-Cu(1)-O(1W)	91.77(11)
N(5)-C(24)	1.347(4)	N(5)- Cu(1)- N(4)	81.12(12)
N(5)-C(28)	1.333(4)	C(1)-O(1)-Cu(1)	128.3(2)
O(2)-C(1)	1.248(4)	C(3)-O(3)-Cu(1)	123.8(2)
F(1)-C(12)	1.350(4)	C(19)-N(4)-Cu(1)	114.9(2)
		C(24)-N(5)-Cu(1)	114.9(2)
		O(2)-C(1)-O(1)	122.3(3)

The bond distances of Cu-O [1.908(3) and 1.944(3) Å] for O(1)-Cu(1) and O(3)-Cu(1), respectively, and Cu-N [1.996(3) and 1.992(3) Å] for N(4)-Cu(1) and N(5)-Cu(1), respectively are similar to previously reported values (1.8-2.0 Å), while the bond O(1W)-Cu(1) [2.244(3) Å] is considerably

longer than O(1)-Cu(1) and O(3)-Cu(1) but similar to previously reported values [around 2.2 to 2.3 Å].<sup>84,92,109–113</sup>

Furthermore, the [CuN<sub>2</sub>O<sub>3</sub>] geometry is slightly distorted square pyramidal due to the unsymmetrical bond angles. O(1)-Cu(1)-O(3) = 93.25(11)°, O(1)-Cu(1)-N(5) = 169.60(11)°, O(3)-Cu(1)-N(4) = 168.23(12)°, O(1)-Cu(1)-N(4) = 91.92(12)°, O(1)-Cu(1)-O(1W) = 96.69(12)°, O(3)-Cu(1)-O(1W) = 93.54(11)°, N(5)-Cu(1)-N(4) = 81.12(12)°, N(4)-Cu(1)-O(1W) = 96.35(11)° and N(5)-Cu(1)-O(1W) = 91.77(11)°.

Table 15, shows the various types of H-bonding, bond distances in (Å) and bond angles (°).

Hydrogen bonding between molecules plays a key role in the complex geometry and in stabilizing the complex in the solid state.<sup>114,115</sup> The nitrate ion and lattice water molecules are involved in a series of strong and highly directional O–H···N and O–H···O bonding interactions.

Table 15: Hydrogen bond distances (Å) and bond angles (°) of complex **5**.

<b>D-H...A</b>	<b>d(D-H)/Å</b>	<b>d(H-A)/Å</b>	<b>d(D-A)/Å</b>	<b>D-H-A/°</b>
O1W-H1WA....O19W <sup>1</sup>	0.86	1.96	2.701(6)	143.1
O1W-H1WA....O18W <sup>1</sup>	0.86	1.92	2.773(8)	171.4
O1W-H1WB....O6W <sup>1</sup>	0.86	2.01	2.717(4)	138.4
O3W-H3WA....O11W	0.86	1.92	2.717(5)	155.1
O3W-H3WB....O10W	0.86	1.92	2.764(4)	169.8
C73A-H73B....F3	0.97	2.24	2.884(10)	122.6
O2W-H2WA....O9W <sup>2</sup>	0.85	1.96	2.714(4)	148.1
O2W-H2WB....O6N <sup>3</sup>	0.85	1.98	2.805(4)	162.5
O4W-H4WA....O11N	0.87	1.85	2.621(9)	147.5
O4W-H4WB....O5W <sup>2</sup>	0.87	1.94	2.686(5)	143.6
C98B-H98C....O16B	0.97	2.18	2.821(16)	122.1
O6W-H6WA....N8 <sup>4</sup>	0.85	1.96	2.769(4)	159.0
O6W-H6WB....O1N <sup>2</sup>	0.85	2.01	2.835(4)	164.6
O13W-H13A....N13B	0.85	2.03	2.739(9)	140.9
O8W-H8WA....O5N	0.85	1.96	2.791(4)	167.5
O8W-H8WB....O9W	0.85	2.22	2.823(4)	127.6
O12W-H12A....N13A	0.85	2.03	2.796(12)	150.0

Symmetry transformations used to generate equivalent atoms: <sup>1</sup>1+X,-1+Y,+Z; <sup>2</sup>1+X,+Y,+Z;

<sup>3</sup>1+X,-1+Y,+Z; <sup>4</sup>+X,1+Y,+Z

Although both complexes were adopted the same slightly distorted square pyramidal geometry, they have different space groups and different crystal types. The average equatorial Cu-O bond distances in complex **4** were

longer than those in complex **5**, this may be attributed to the presence of equatorial Cu-N bonds from the 2,2-bipy ligand in complex **5**. Whereas, the axial Cu-O bond distance in complex **5** is longer than those in the equatorial position in both complexes.

### **3.5 Anti-bacterial activity**

The solution stability of the Zn levo complexes was evaluated by  $^1\text{H}$  NMR before the screening of their anti-bacterial activity. The same DMSO solution of the complexes in the NMR tube was checked periodically at the same previous NMR experiment conditions and always gave the same data. In addition, the same samples were re-examined on two types of bacteria after being stored in the refrigerator for three days and similar previous results were obtained.

Zinc and copper levofloxacin complexes **1-5** were screened for their anti-bacterial activity against different types of  $G^-$  bacteria (*P. mirabilis*, *E. coli*, *P. aeruginosa* and *K. pneumonia*) and  $G^+$  bacteria (*S. aureus*, *S. epidermidis*, *B. subtilis* and *E. faecalis*) to show the synergistic anti-bacterial activity due to complexation. The results were obtained by the agar



diffusion method using a 6 mg/mL concentration (in DMSO) with a volume of 25  $\mu$ L per well. The average of three trials of the samples was stated as average  $\pm$  standard error. The IZD of complexes **1-5** and their parent ligands against  $G^-$  and  $G^+$  bacteria; 6 mg/ml of all species, 4 mg/ml of levo and 1.34 mg/ml of 2,2-bipy are shown in Figure 29, Figure 30, Figure 31, Figure 32, Table S 3 and Table S 4 (**Appendix D**) for gram-negative and gram-positive bacteria, respectively.

DMSO was used as negative control without showing any growth inhibition, whereas levofloxacin was used as positive control for both Gram negative and positive bacteria.  $ZnCl_2$ ,  $Cu(NO_3)_2$  and 2-ampy did not show any sensitivity toward all tested bacterial strains.

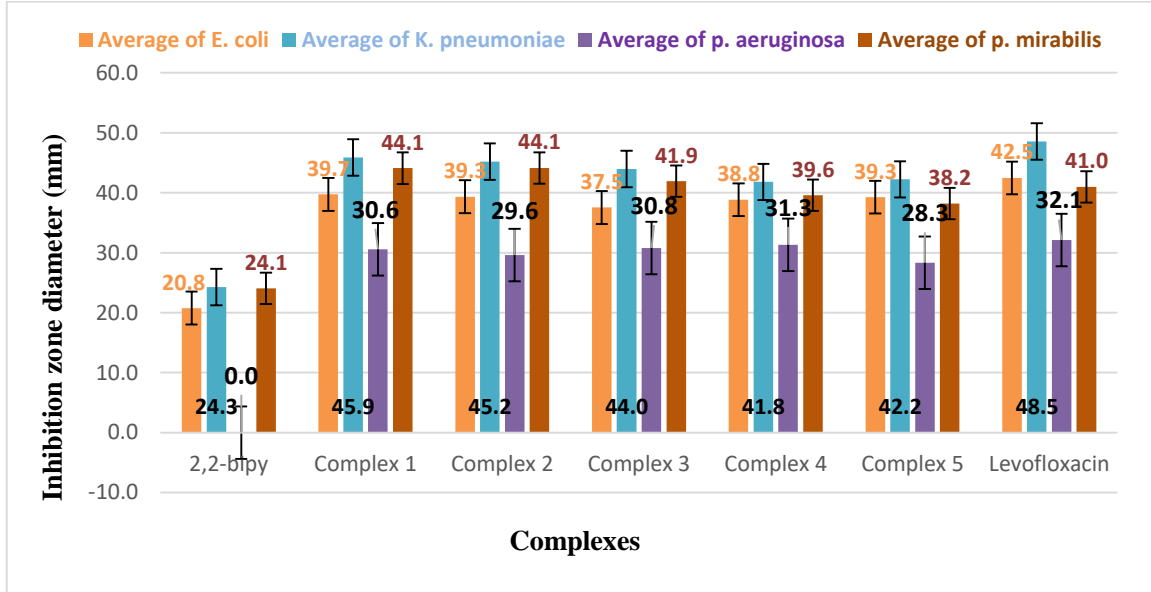


Figure 29: Inhibition zone diameter of complexes 1-5 and their parent ligands against  $G^-$  bacteria; the data stated as average  $\pm$  standard deviation (N = 3), 6 mg/ml of all species.

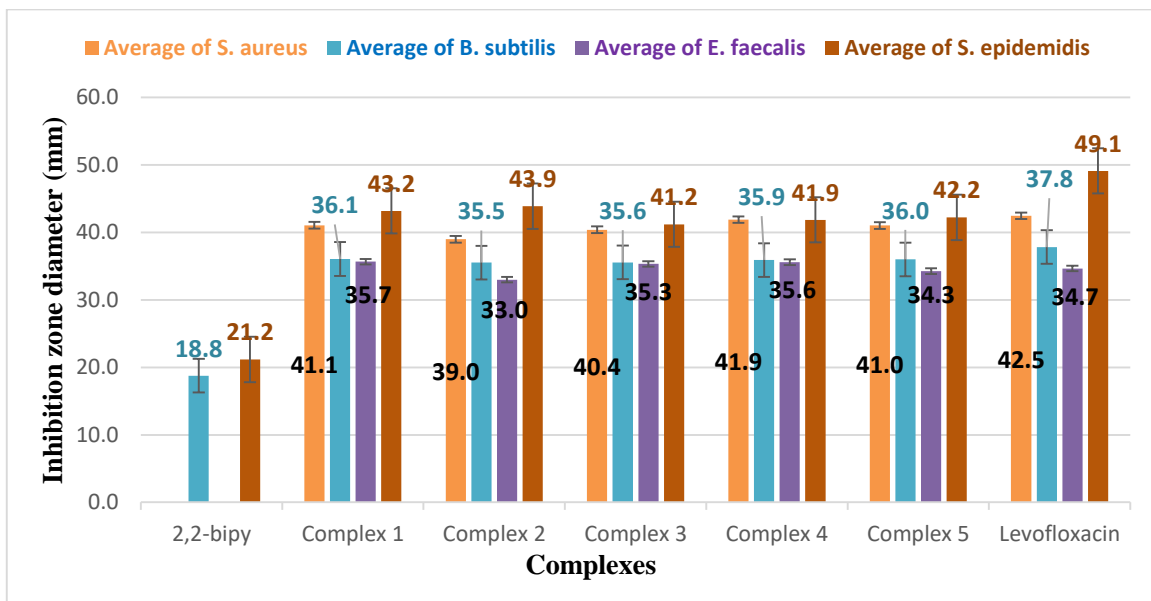


Figure 30: Inhibition zone diameter of complexes 1-5 and their parent ligands against  $G^+$  bacteria; the data stated as average  $\pm$  standard deviation (N = 3), 6 mg/ml of all species.

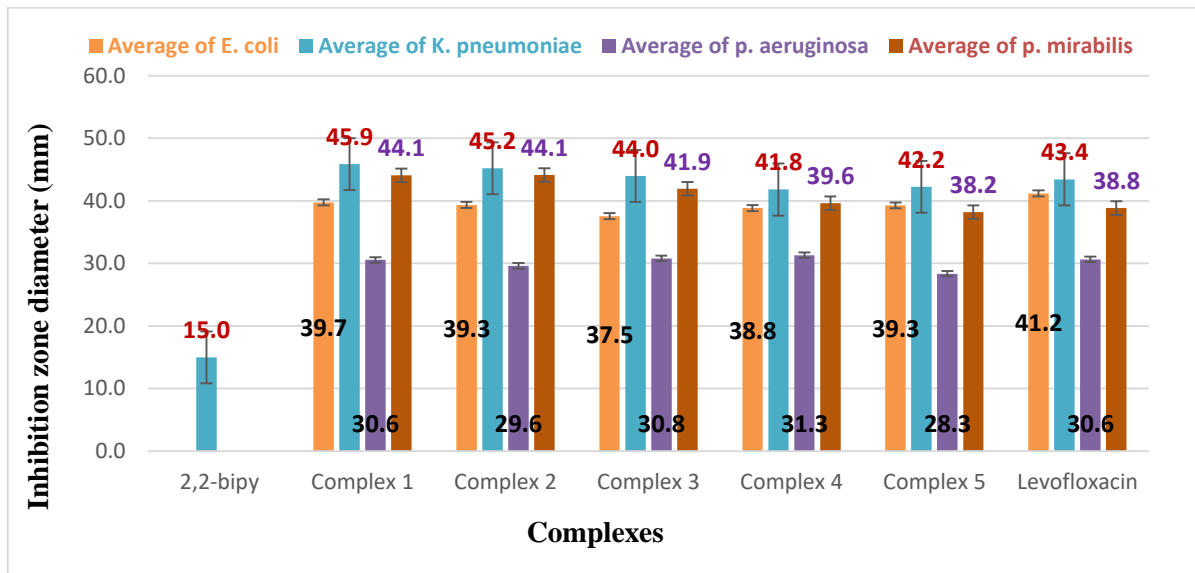


Figure 31: Inhibition zone diameter of complexes 1-5 and their parent ligands against  $G^-$  bacteria; the data stated as average  $\pm$  standard deviation (N = 3), 6 mg/ml of complexes 1-5, 4 mg/ml of levo and 1.34 mg/ml of 2,2-bipy.

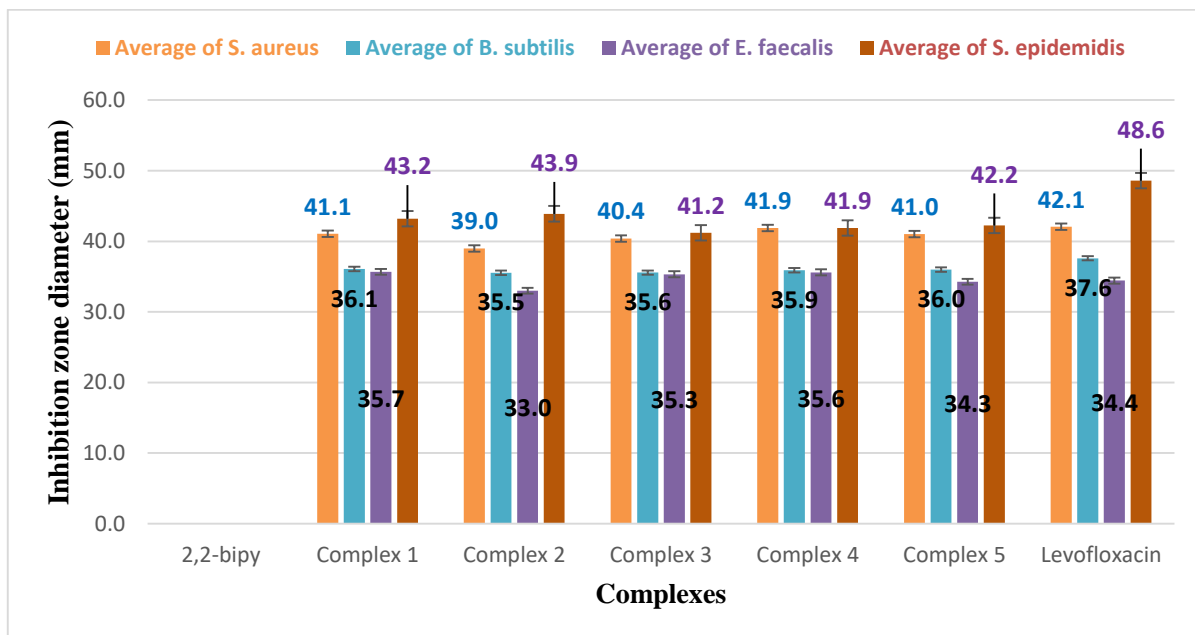


Figure 32: Inhibition zone diameter of complexes 1-5 and their parent ligands against  $G^+$  bacteria; the data stated as average  $\pm$  standard deviation (N = 3), 6 mg/ml of complexes 1-5, 4 mg/ml of levo and 1.34 mg/ml of 2,2-bipy.

All levofloxacin complexes were showed a broad sensitivity against all tested micro-organisms. Complex **1** showed high anti-bacterial activity against all tested bacterial strains except against *P. aeruginosa* showing lower sensitivity compared with other micro-organisms. The IZD values for complex **1** were found between 30-46 mm.

Complexes **2-5** showed high inhibition activity against all G<sup>-</sup> and G<sup>+</sup> bacteria with IZD values between 29-45.5 mm, 30-44 mm, 30-42 mm and 28-42.5 mm, respectively. The 2,2-bipy ligand with (6 mg/ml) showed low inhibition activity against all tested bacterial strains except for *P. aeruginosa*, *S. aureus* and *E. faecalis*, However, when the stoichiometric molar concentration (1.34 mg/ml) of the bipy ligand in the complex was used it showed no inhibition activity against all tested bacterial strains except a low inhibition activity for *K. pneumonia*. Complexes **1** and **2** showed slightly higher inhibition for *K. pneumonia* than free levofloxacin with the stoichiometric molar concentration (4 mg/ml).

All complexes showed slightly lower inhibition for *S. epidemidis* compared with free levofloxacin.

Different concentrations of levofloxacin were prepared and screened against two types of bacteria strains, *E. coli* and *S. aureus* as shown in Table 16. The results show good correlation between the concentration and the IZD values with slight difference between 3 mg/ml and 4 mg/ml levo concentrations as shown in Figure 33. Therefore, in a different experiment showed in Figures 31 and 32, the concentration of 4 mg/ml of the levo was used according to its percentage molar ratio in the complexes and the concentrations of the 2-amp and 2,2-bipy ligands were used according to their stoichiometric percentage in the complexes.

Table 16: Anti-bacterial activity data of different levo concentrations.

Compounds	<i>E. coli</i> G <sup>-</sup>	<i>S. aureus</i> G <sup>+</sup>
levo 1.0 mg/ml	31.3 ± 0.9	30.2 ± 0.7
levo 2.0 mg/ml	35.5 ± 0.5	35.4 ± 0.9
levo 3.08 mg/ml	39.9 ± 0.6	40.2 ± 0.4
levo 4.137 mg/ml	40.7 ± 0.7	41.1 ± 0.4
levo 5.0 mg/ml	41.3 ± 0.9	40.8 ± 0.5
levo 6.0 mg/ml	41.7 ± 1.0	41.4 ± 1.1
DMSO	-	-

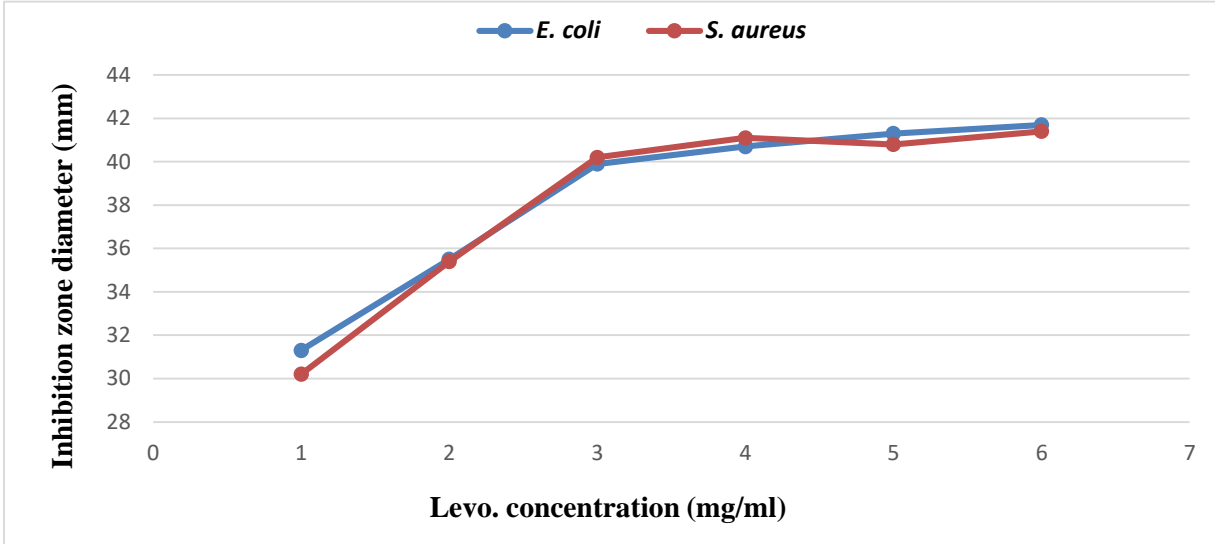


Figure 33: Correlation between inhibition zone diameter and different concentrations of levofloxacin.

Bacteria can be classified into two  $G^+$  or  $G^-$  depending on the structure of the bacterial cell walls. The main two different reasons in visualization properties of  $G^+$  and  $G^-$  bacteria are the thickness of the peptidoglycan layer and the presence or absence of the outer lipid membrane.  $G^-$  bacteria have a thin peptidoglycan layer with an outer lipid membrane. However,  $G^+$  bacteria have a thick peptidoglycan layer without outer lipid membrane.<sup>116</sup>

Levofloxacin has a broad spectrum against most  $G^-$  and  $G^+$  bacteria. The mechanism of action of levofloxacin is through inhibition of bacterial DNA replication and transcription as result of inhibition of the bacterial

topoisomerases.<sup>69</sup> Transition metals are involved in regulation of virulence and metabolism as a mechanism of host invasion, and many opportunistic pathogens.<sup>117</sup> In the treatment of bacteria, zinc and copper are mainly used to poison the bacterial pathogens.<sup>118</sup> The polarity of a metal ion may be reduced due to the partial sharing of positive charge upon chelating with the ligand donor groups, and thus the lipophilic nature of the central ion is increased by the delocalization of  $\pi$  electrons over the whole chelate ring. This enhances the penetration of the complex through the lipid cell membranes.<sup>80</sup>

In fact, metal complexes are active against a range of bacteria, fungi and viruses and can act as anti-microbial agents through various proposed mechanism of action, i.e. they can inhibit the synthesis of bacterial cell walls, causing irreversible inhibition of protein synthesis, altering protein synthesis leading to cell death and affecting the nucleic acid metabolism. In addition, Metal complexes anti-microbial activities depend on the nature of the metal ion, ligands, the chelate effect, the total charge of the complex and the nature of the outer ion.<sup>80</sup>

According to the results listed in Table S 3 and Table S 4 (**Appendix D**), the complexes gave similar results compared to the levofloxacin, when concentrations of 6 mg/ml and (4 mg/ml), the stoichiometric molar ratio in the complexes solutions of levofloxacin were used. In addition these complexes contain zinc and copper, which have biological activities.

The present results proposed that neither the changes of the chemical properties of complexed levofloxacin with Zn(II) and Cu(II) metal centers nor the increase in size of complex compared to the free levofloxacin, reduced its efficacy and inhibition bacterial activity.<sup>84</sup>



## 4. Conclusion

Zinc and copper complexes with the anti-biotic levofloxacin in the existence of N-based ligands were synthesized and characterized using various techniques such as IR, UV-Vis, <sup>1</sup>H-NMR, single crystal X-ray diffraction and other physical properties. The synthesized complexes were [Zn(levo)<sub>2</sub>(MeOH)<sub>2</sub>] (1), [Zn(levo)<sub>2</sub>(2-ampy)<sub>2</sub>] (2), [Zn(levo)<sub>2</sub>(2,2-bipy)].H<sub>2</sub>O (3), [Cu(levo)<sub>2</sub>(2-ampy)] .6.25H<sub>2</sub>O (4) and [Cu(levo)(H<sub>2</sub>O)(2,2-bipy)](NO<sub>3</sub>).2.5H<sub>2</sub>O (5)

The crystal structure of complexes 4 and 5 were determined using single crystal X-ray diffraction. Structure 4 and 5 revealed slightly distorted square pyramidal geometry with two bidentate chelating levofloxacin and one monodentate 2-ampy ligands of complex 4. Whereas in complex 5, the distorted square pyramidal geometry show the coordination of one bidentate chelating levofloxacin, one bidentate 2,2-bipy and one water molecule. Levofloxacin molecule was coordinated to metal through the pyridone oxygen atom and one of the oxygen atoms from the carboxylato group forming a six-membered ring.

All of the prepared levofloxacin complexes showed a broad sensitivity against all tested bacterial strains. Complex 1 showed high anti-bacterial activity against all tested bacteria except against *P. aeruginosa* which showed lower sensitivity compared to other micro-organisms. Whereas all complexes showed slightly lower inhibition for *S. epidemidis* compared to the free levofloxacin.

The present results showed that the zinc and copper complexes gave almost the same anti-bacterial activity.

## 5. References

- (1) Soetan, K. O.; Olaiya, C. O.; Oyewole, O. E. *African J. Food Sci.* **2010**, *4* (May), 200–222.
- (2) Jaishankar, M.; Tseten, T.; Anbalagan, N.; Mathew, B. B.; Beeregowda, K. N. *Interdiscip. Toxicol.* **2014**, *7* (2), 60–72. <https://doi.org/10.2478/intox-2014-0009>.
- (3) Koletzko, B.; Goulet, O.; Hunt, J.; Krohn, K.; Shamir, R. 1.. *J. Pediatr. Gastroenterol. Nutr.* **2005**, *41*. <https://doi.org/10.1097/01.mpg.0000181841.07090.f4>.
- (4) Rehder, D. *Introduction to Bioinorganic Chemistry Lecture Notes*.
- (5) Chopra, A.; Lineweaver, C. H. *The Major Elemental Abundance Differences between Life, the Oceans and the Sun*; **2008**; 49-55
- (6) *What Are Trace Elements? Osamu WADA*; 2004; Vol. 47.
- (7) Principles of bioinorganic chemistry: By S J Lippard and J M Berg. pp 411. University Science Books, Mill Valley, California. 1994. <https://onlinelibrary.wiley.com/doi/abs/10.1016/0307-4412%2895%2990685-1> (accessed Feb 25, 2020).
- (8) Sharma, R. K. *J. Environ. Biol.* **2014**, *26* (July 2005), 301–313. <https://doi.org/ISSN: 0254-8704>.
- (9) Hansen, A. M. K.; Bryan, C. E.; West, K.; Jensen, B. A. *Arch. Environ. Contam. Toxicol.* **2016**, *70* (1), 75–95. <https://doi.org/10.1007/s00244-015-0204-1>.
- (10) Stohs, S. J.; Bagchi, D. *Free Radical Biology and Medicine*. 1995, pp 321–336. [https://doi.org/10.1016/0891-5849\(94\)00159-H](https://doi.org/10.1016/0891-5849(94)00159-H).
- (11) Lynes, M. A.; Kang, Y. J.; Sensi, S. L.; Perdrizet, G. A.; Hightower, L. E. In *Annals of the New York Academy of Sciences*; 2007; Vol. 1113, pp 159–172. <https://doi.org/10.1196/annals.1391.010>.
- (12) Shils, M. E.; Olson, J. A.; Shike, M. *Modern Nutrition in Health and Disease*. Lea and Febiger 1994.
- (13) Salgueiro, M. J.; Zubillaga, M.; Lysionek, A.; Sarabia, M. I.; Caro, R.; De Paoli, T.; Hager, A.; Weill, R.; Boccio, J. *Nutrition Research*. Elsevier May 1, 2000, pp

- 737–755. [https://doi.org/10.1016/S0271-5317\(00\)00163-9](https://doi.org/10.1016/S0271-5317(00)00163-9).
- (14) Fraga, C. G. *Molecular Aspects of Medicine*. August 2005, pp 235–244. <https://doi.org/10.1016/j.mam.2005.07.013>.
- (15) Chemical and physical properties of zinc - MEL Chemistry <https://melscience.com/US-en/articles/chemical-and-physical-properties-zinc/> (accessed Mar 9, 2020).
- (16) Schläfer, H. B. N. Figgis: *Berichte der Bunsengesellschaft für Phys. Chemie* **1966**, 70 (8), 932–933. <https://doi.org/10.1002/bbpc.19660700841>.
- (17) Berg, J. M.; Shi, Y. *Science* (80-. ). **1996**, 271 (5252), 1081–1085.
- (18) Vallee, B. L.; Falchuk, K. H. *The Biochemical Basis of Zinc Physiology*; 1993; Vol. 73. <https://doi.org/10.1152/physrev.1993.73.1.79>.
- (19) Liu, Z.; Ng, Y. M.; Tiong, P. J.; Asyikin, R.; Talip, A.; Jasin, N.; Yi, V.; Jong, M.; Tay, M. G. *International Journal of Inorganic Chemistry*; **2017**, 2017 (Scheme 1).
- (20) Seyedmajidi, S. A.; Seyedmajidi, M.; Moghadamnia, A.; Khani, Z.; Zahedpasha, S.; Jenabian, N.; Jorsaraei, G.; Halalkhor, S.; Motallebnejad, M. *Int. J. Mol. Cell. Med.* **2014**, 3 (2), 81–87.
- (21) Zalewski, P. D.; Forbes, I. J.; Betts, W. H. *Biochem. J.* **1993**, 296 (2), 403–408. <https://doi.org/10.1042/bj2960403>.
- (22) Vallee, B. L.; Falchuk, K. H. *Physiological Reviews*. 1993, pp 79–118. <https://doi.org/10.1152/physrev.1993.73.1.79>.
- (23) Lim, K. H. C.; Riddell, L. J.; Nowson, C. A.; Booth, A. O.; Szymlek-Gay, E. A. *Nutrients* **2013**, 5 (8), 3184–3211. <https://doi.org/10.3390/nu5083184>.
- (24) Frassinetti, S.; Bronzetti, G. L.; Caltavuturo, L.; Cini, M.; Croce, C. Della. *Journal of Environmental Pathology, Toxicology and Oncology*. Begell House Inc. 2006, pp 597–610. <https://doi.org/10.1615/JEnvironPatholToxicolOncol.v25.i3.40>.
- (25) Osredkar, J. J. *Clin. Toxicol.* **2011**, s3 (01). <https://doi.org/10.4172/2161-0495.s3-001>.
- (26) Broadley, M. R.; White, P. J.; Hammond, J. P.; Zelko, I.; Lux, A. *New Phytologist*.

- John Wiley & Sons, Ltd March 1, 2007, pp 677–702. <https://doi.org/10.1111/j.1469-8137.2007.01996.x>.
- (27) Solomons, N. W. *Nutr. Rev.* **2009**, *56* (1), 27–28. <https://doi.org/10.1111/j.1753-4887.1998.tb01656.x>.
- (28) Prasad, A. S. In *Nutrition*; 1995; Vol. 11, pp 93–99.
- (29) SIMMER, K.; THOMPSON, R. P. H. *Acta Pædiatrica* **1985**, *74* (s319), 158–163. <https://doi.org/10.1111/j.1651-2227.1985.tb10126.x>.
- (30) McCarthy, T. J.; Zeelie, J. J.; Krause, D. J. *J. Clin. Pharm. Ther.* **1992**, *17* (1), 51–54. <https://doi.org/10.1111/j.1365-2710.1992.tb01265.x>.
- (31) Hershinkel, M.; Silverman, W. F.; Sekler, I. In *Molecular Medicine*; 2007; Vol. 13, pp 331–336. <https://doi.org/10.2119/2006-00038.Hershinkel>.
- (32) Tsugutoshi AOKI. *J. Japan Med. Assoc.* **2004**, *47* (8), 365–370.
- (33) Trumbo, P.; Yates, A. A.; Schlicker, S.; Poos, M. *J. Am. Diet. Assoc.* **2001**, *101* (3), 294–301. [https://doi.org/10.1016/S0002-8223\(01\)00078-5](https://doi.org/10.1016/S0002-8223(01)00078-5).
- (34) Guo, Z.; Sadler, P. J. *Angew. Chem. Int. Ed.* **1999**, *38*, 1512–1531.
- (35) Edited, C. *Chemistry and Biochemistry of a Leading Anticancer Drug Chemistry and Biochemistry of a Leading Anticancer Drug*; Verlag Helvetica Chimica Acta ; Zürich :, 1999. <https://doi.org/10.1002/9783906390420>.
- (36) Askary, V. R.; Jahan, N. A.; Sabbagh, A.; Jahani, F. S.; Dourandish, N.; Kamachali, A. R. K. *Clin. Biochem.* **2011**, *44* (13), S323–S324. <https://doi.org/10.1016/j.clinbiochem.2011.08.795>.
- (37) Dameron, C. T.; Howe, P.; *Copper*; World Health Organization, 1998.
- (38) Jutzi, P. *Chemie unserer Zeit* **1989**, *23* (1), 35–36. <https://doi.org/10.1002/ciuz.19890230108>.
- (39) Willis, M. S.; Monaghan, S. A.; Miller, M. L.; McKenna, R. W.; Perkins, W. D.; Levinson, B. S.; Bhushan, V.; Kroft, S. H. *Am. J. Clin. Pathol.* **2005**, *123* (1), 125–131. <https://doi.org/10.1309/V6GVYW2QTYD5C5PJ>.
- (40) Copper Essential for Human Health <https://copperalliance.org.uk/knowledge->

base/education/education-resources/copper-essential-human-health/ (accessed Mar 7, 2020).

- (41) Olivares, M.; Uauy, R. *Copper as an Essential Nutrient* 1,2; 1996; Vol. 63.
- (42) Panel, E.; Nda, A. *EFSA J.* **2015**, *13* (10), 1–51. <https://doi.org/10.2903/j.efsa.2015.4253>.
- (43) Hathaway, B. J.; Billing, D. E. *Coord. Chem. Rev.* **1970**, *5* (2), 143–207. [https://doi.org/10.1016/S0010-8545\(00\)80135-6](https://doi.org/10.1016/S0010-8545(00)80135-6).
- (44) Brewer, G. J. *J. Am. Coll. Nutr.* **2009**, *28* (3), 238–242. <https://doi.org/10.1080/07315724.2009.10719777>.
- (45) Öhrvik, H.; Thiele, D. J. *J. Trace Elem. Med. Biol.* **2015**, *31*, 178–182. <https://doi.org/10.1016/j.jtemb.2014.03.006>.
- (46) Iakovidis, I.; Delimaris, I.; Piperakis, S. M. *Mol. Biol. Int.* **2011**, *2011*, 1–13. <https://doi.org/10.4061/2011/594529>.
- (47) Melník, M. *SCoord. Chem. Rev.* **1982**, *42* (2), 259–293. [https://doi.org/10.1016/S0010-8545\(00\)80537-8](https://doi.org/10.1016/S0010-8545(00)80537-8).
- (48) Rardin, \* R Lynn; Tolman, W. B.; Lippard, S. J. *New J. Chem*; 1991; Vol. 15.
- (49) Batool, S. Department of Chemisrty. **2017**, No. Ii.
- (50) Curran, R. J.; McCann, D. M. *Dep. Chem.* **2009**, *Ph.D.* (October), 386.
- (51) Palacios, E. G.; Monhemius, A. J. *Hydrometallurgy* **2001**, *62* (3), 135–143. [https://doi.org/10.1016/S0304-386X\(01\)00187-6](https://doi.org/10.1016/S0304-386X(01)00187-6).
- (52) Palacios, E. G.; Juárez-López, G.; Monhemius, A. J. *Hydrometallurgy* **2004**, *72* (1–2), 139–148. [https://doi.org/10.1016/S0304-386X\(03\)00137-3](https://doi.org/10.1016/S0304-386X(03)00137-3).
- (53) Papageorgiou, S. K.; Kouvelos, E. P.; Favvas, E. P.; Sapalidis, A. A.; Romanos, G. E.; Katsaros, F. K. *Carbohydr. Res.* **2010**, *345* (4), 469–473. <https://doi.org/10.1016/j.carres.2009.12.010>.
- (54) Zelenák, V.; Vargová, Z.; Györyová, K. *Acta - Part A Mol. Biomol. Spectrosc.* **2007**, *66* (2), 262–272. <https://doi.org/10.1016/j.saa.2006.02.050>.
- (55) Spectroscopic Tools <http://www.science-and-fun.de/tools/> (accessed Mar 18,

- 2020).
- (56) Under, C.; Gugwad, V. M.; Ghanwat, A. A. Synthesis and Characterization of Transition Metal - Bidentate Ligand Complexes for the Construction of Functional Materials In. No. September 2017.
- (57) Sharma, J.; Singla, A. K.; Dhawan, S. *Int. J. Pharm.* **2003**, *260* (2), 217–227. [https://doi.org/10.1016/s0378-5173\(03\)00251-5](https://doi.org/10.1016/s0378-5173(03)00251-5).
- (58) Ali, H. A.; Darawsheh, M. D.; Rappocciolo, E. *Polyhedron* **2013**, *61*, 235–241. <https://doi.org/10.1016/j.poly.2013.06.015>.
- (59) Shahzadi, S.; Ali, S.; Jabeen, S.; Kanwal, N.; Rafique, U.; Khan, A. N. *Russ. J. Coord. Chem.* **2008**, *34* (1), 38–43. <https://doi.org/10.1134/s1070328408010077>.
- (60) Zhai, C.; Yan, F.-M.; Zhao, P.-Z. Phenanthroline-j 2 N,N 0 0 0 )Bis(2-Hydroxybenzoato-JO)-Copper(II). No. 2, 9–10. <https://doi.org/10.1107/S1600536808036283>.
- (61) Bon Kweon Koo. *Bull. Korean Chem. Soc.* **2001**, *22* (1), 113–116.
- (62) Kucková, L.; Jomová, K.; Švorcová, A.; Valko, M.; Segl’A, P.; Moncol’, J.; Kožíšek, J. *Molecules* **2015**, *20* (2), 2115–2137. <https://doi.org/10.3390/molecules20022115>.
- (63) Dasgupta, A. *Advances in Antibiotic Measurement*, 1st ed.; Elsevier Inc., 2012; Vol. 56. <https://doi.org/10.1016/B978-0-12-394317-0.00013-3>.
- (64) Reddy, V. P. In *Organofluorine Compounds in Biology and Medicine*; Elsevier, 2015; pp 133–178. <https://doi.org/10.1016/b978-0-444-53748-5.00005-8>.
- (65) Levaquin (Levofloxacin): Uses, Dosage, Side Effects, Interactions, Warning <https://www.rxlist.com/levaquin-drug.htm#description> (accessed Mar 22, 2020).
- (66) Hooper, D. C. *Kucers Use Antibiot. A Clin. Rev. Antibacterial, Antifung. Antiparasit. Antivir. Drugs, Seventh Ed.* **2017**, *88*, 2055–2084. <https://doi.org/10.1201/9781315152110>.
- (67) Noel, G. J. *Clin. Med. Ther.* **2009**, *1*, CMT.S28. [doi.org/10.4137/cmt.s28](https://doi.org/10.4137/cmt.s28).
- (68) Keam, S. J.; Croom, K. F.; Keating, G. M. *Drugs* **2005**, *65* (5), 695–724. <https://doi.org/10.2165/00003495-200565050-00007>.

- (69) Davis, R.; Bryson, H. M. *Drugs* **1994**, *47* (4), 677–700. <https://doi.org/10.2165/00003495-199447040-00008>.
- (70) Ahmadifar, M.; Vahidi-eyrisofla, N.; Fathi, R. The Study of Effect of Levofloxacin on Disorders of Female Hormones in Rats. **2014**, *11* (2), 71–74.
- (71) T, D. L. LEWIS ACIDIC ZN ( II ) SCHIFF BASE COMPLEXES IN HOMOGENEOUS CATALYSIS Daniele Anselmo. **2013**, No. ii.
- (72) Da Silva, C. M.; Da Silva, D. L.; Modolo, L. V.; Alves, R. B.; De Resende, M. A.; Martins, C. V. B.; De Fátima, Â. *J. Adv. Res.* **2011**, *2* (1), 1–8. <https://doi.org/10.1016/j.jare.2010.05.004>.
- (73) Selvaganapathy, M.; Raman, N. *J. Chem. Biol. Ther.* **2016**, *01* (02), 1–17. <https://doi.org/10.4172/2572-0406.1000108>.
- (74) Altaf, A. A.; Shahzad, A.; Gul, Z.; Rasool, N.; Badshah, A.; Lal, B.; Khan, E. *Http://Www.Sciencepublishinggroup.Com* **2015**, *1* (1), 1. <https://doi.org/10.11648/J.JDDMC.20150101.11>.
- (75) Scarborough, C. C.; Wieghardt, K. *Inorg. Chem.* **2011**, *50* (20), 9773–9793. <https://doi.org/10.1021/ic2005419>.
- (76) kumari, S. A.; babu, B. K.; Neeraja, G. *J. Chem. Pharm. Sci.* **2019**, *12* (02), 39–41. <https://doi.org/10.30558/jchps.20191202003>.
- (77) Constable, E. C.; Housecroft, C. E. *Molecules* **2019**, *24* (21). <https://doi.org/10.3390/molecules24213951>.
- (78) Erdemir, F.; Celepci, D. B.; Aktaş, A.; Gök, Y.; Kaya, R.; Taslimi, P.; Demir, Y.; Gulçin, İ. *Bioorg. Chem.* **2019**, *91* (June). <https://doi.org/10.1016/j.bioorg.2019.103134>.
- (79) Hooper, D. C. *Mechanisms of Action and Resistance of Older and Newer Fluoroquinolones*.
- (80) Uivarosi, V. *Molecules* **2013**, *18* (9), 11153–11197. <https://doi.org/10.3390/molecules180911153>.
- (81) Al-Khodir, F. A. I.; Refat, M. S. *Russ. J. Gen. Chem.* **2015**, *85* (3), 718–730. <https://doi.org/10.1134/S1070363215030317>.



- (82) Sultana, N.; Arayne, M. S.; Rizvi, S. B. S.; Haroon, U.; Mesaik, M. A. *Med. Chem. Res.* **2013**, *22* (3), 1371–1377. <https://doi.org/10.1007/s00044-012-0132-9>.
- (83) Sadeek, S. A.; Mohammed, S. F.; Rashid, N. G. *J. Chem. Pharm. Res.* **2018**, *10* (3), 33–42.
- (84) Sousa, I.; Claro, V.; Pereira, J. L.; Amaral, A. L.; Cunha-Silva, L.; De Castro, B.; Feio, M. J.; Pereira, E.; Gameiro, P. *J. Inorg. Biochem.* **2012**, *110*, 64–71. <https://doi.org/10.1016/j.jinorgbio.2012.02.003>
- (85) 1. Dolomanov, O.V., Bourhis, L.J., Gildea, R.J, Howard, J.A.K., Puschmann, H. *J. Appl. Cryst.* *42*, 339-341. **2009**, *42*, 339–341.
- (86) 2. Sheldrick, G. M. No Title. *Acta Cryst* **2015**, *A71*, 3-8.
- (87) 3. Sheldrick, G. M. No Title. *Acta Cryst.* **2015**, *C71*, 3–8.
- (88) Hudzicki, J. *Am. Soc. Microbiol.* **2016**, No. December 2009, 1–13.
- (89) Raymoni, G.; Abu Ali, H. *Appl. Organomet. Chem.* **2019**, *33* (1), 1–16. <https://doi.org/10.1002/aoc.4680>.
- (90) Zhang, X.; Yi, Z.-h.; Xue, M.; Xu, Y.; Yu, J.-h.; Yu, X.-y.; Xu, J. *Chem. Res. Chinese Univ.* **2007**, *23*, 631.
- (91) Yu, H.-l.; Yang, J.; Fu, Q.; Ma, J.-c.; Li, W.-. No Title. *Chem. Res. Chinese Univ.* **2008**, *24*, 123.
- (92) Turel, I. *Coord. Chem. Rev.* **2002**, *232* (1–2), 27–47. [https://doi.org/10.1016/S0010-8545\(02\)00027-9](https://doi.org/10.1016/S0010-8545(02)00027-9).
- (93) Rusu, A.; Hancu, G.; Tóth, G.; Vancea, S.; Toma, F.; Mare, A. D.; Man, A.; Nițulescu, G. M.; Uivarosi, V. *J. Mol. Struct.* **2016**, *1123*, 384–393. <https://doi.org/10.1016/j.molstruc.2016.07.035>.
- (94) Galani, A.; Efthimiadou, E. K.; Theodosiou, T.; Kordas, G.; Karaliota, A. *Inorganica Chim. Acta* **2014**, *423* (PB), 52–59. <https://doi.org/10.1016/j.ica.2014.09.034>.
- (95) Debnath, A.; Hussain, F.; Masram, D. T. *Bioinorg. Chem. Appl.* **2014**, *2014* (Iii), 2–3. <https://doi.org/10.1155/2014/457478>.
- (96) Huber, P. C.; Reis, G. P.; Amstalden, M. C. K.; Lancellotti, M.; Almeida, W. P.

- Polyhedron* **2013**, *57*, 14–19. <https://doi.org/10.1016/j.poly.2013.04.007>.
- (97) Qasim, A. *J. Dev. Res.* **2015**, No. June.
- (98) Debnath, A.; Hussain, F.; Masram, D. T. *Chem. Appl.* **2014**, *2014* (Iii). <https://doi.org/10.1155/2014/457478>.
- (99) Mimouni, F. Z.; Belboukhari, N.; Abdelkrim, C. *Der Pharma Chem.* **2018**, *10* (5), 31–35.
- (100) Alabdali, A. J.; Ibrahim, F. M. *journal of Applied Chemistry*; 2014; Vol. 6.
- (101) Galani, A.; Efthimiadou, E. K.; Mitrikas, G.; Sanakis, Y.; Psycharis, V.; Raptopoulou, C.; Kordas, G.; Karaliota, A. *Inorganica Chim. Acta* **2014**, *423* (PART A), 207–218. <https://doi.org/10.1016/j.ica.2014.08.005>.
- (102) Niven, M. L.; Percy, G. C. ) *K. Nakamoto, Ln]*'ared Spectra of Inorganic and Coordination Compounds; Wiley-Interscience, 1978; Vol. 3.
- (103) Lah, N.; Šegedin, P.; Leban, I. *Struct. Chem.* **2002**, *13* (3–4), 357–360. <https://doi.org/10.1023/A:1015824209616>.
- (104) García-Raso, Á.; Fiol, J. J.; Bádenas, F.; Lago, E.; Molins, E. *Polyhedron* **2001**, *20* (22–23), 2877–2884. [https://doi.org/10.1016/S0277-5387\(01\)00900-7](https://doi.org/10.1016/S0277-5387(01)00900-7).
- (105) Ren, P.; Su, N. P.; Qin, J. G.; Day, M. W.; Chen, C. T. C. *J. Struct. Chem* **2002**, *21*, 38–41.
- (106) Qin, J.; Su, N.; Dai, C.; Yang, C.; Liu, D.; Day, M. W.; Wu, B.; Chen, C. *Polyhedron* **1999**, *18*, 3461–3464.
- (107) Warad, I. *Res Chem Intermed* **2013**, *39* (3), 1481–1490.
- (108) Pace CN, Fu H, Lee Fryar K, Landua J, Trevino SR, Schell D, Thurlkill RL, Imura S, Scholtz JM, Gajiwala K, Sevcik J, Urbanikova L, Myers JK, Takano K, Hebert EJ, Shirley BA, G. G. *Protein Sci* **2014**, *5* (23), 652–661.
- (109) Ruíz, P.; Ortiz, R.; Perelló, L.; Alzuet, G.; González-Álvarez, M.; Liu-González, M.; Sanz-Ruíz, F. *J. Inorg. Biochem.* **2007**, *101* (5), 831–840. <https://doi.org/10.1016/j.jinorgbio.2007.01.009>.
- (110) Wallis, S. C.; Gahan, L. R.; Charles, B. G.; Hambley, T. W.; Duckworth, P. A. *J. Inorg. Biochem.* **1996**, *62* (1), 1–16. <https://doi.org/10.1016/0162->

0134(95)00082-8.

- (111) Hussain, A.; AlAjmi, M. F.; Rehman, M. T.; Amir, S.; Husain, F. M.; Alsalme, A.; Siddiqui, M. A.; AlKhedhairi, A. A.; Khan, R. A. *Sci. Rep.* **2019**, *9* (1), 1–17. <https://doi.org/10.1038/s41598-019-41063-x>.
- (112) Martins, D. A.; Gouvea, L. R.; Muniz, G. S. V.; Louro, S. R. W.; Batista, D. da G. J.; Soeiro, M. D. N. C.; Teixeira, L. R. *Bioinorg. Chem. Appl.* **2016**, *2016* (ii), 1–11. <https://doi.org/10.1155/2016/5027404>.
- (113) Feio, M. J.; Sousa, I.; Ferreira, M.; Cunha-Silva, L.; Saraiva, R. G.; Queirós, C.; Alexandre, J. G.; Claro, V.; Mendes, A.; Ortiz, R.; et al. *J. Inorg. Biochem.* **2014**, *138* (May), 129–143. <https://doi.org/10.1016/j.jinorgbio.2014.05.007>.
- (114) Abu Ali, H.; Abu Shamma, A.; Kamel, S. *J. Mol. Struct.* **2017**, *1142* (August), 40–47. <https://doi.org/10.1016/j.molstruc.2017.04.048>.
- (115) Abu Ali, H.; Jabali, B. *Polyhedron* **2016**, *107* (ii), 97–106. <https://doi.org/10.1016/j.poly.2016.01.010>.
- (116) Gram Positive vs Gram Negative | Technology Networks <https://www.technologynetworks.com/immunology/articles/gram-positive-vs-gram-negative-323007> (accessed Jul 23, 2020).
- (117) Buracco, S.; Peracino, B.; Andreini, C.; Bracco, E.; Bozzaro, S. *Front. Cell. Infect. Microbiol.* **2018**, *7* (JAN), 1–20. <https://doi.org/10.3389/fcimb.2017.00536>.
- (118) Weber, S.; Hilbi, H. *Methods Mol. Biol.* **2014**, *1197* (1), 153–167. [https://doi.org/10.1007/978-1-4939-1261-2\\_9](https://doi.org/10.1007/978-1-4939-1261-2_9).

## 6. Appendices

### Appendix A: Electronic spectra of complexes **1**, **3** and **4**.

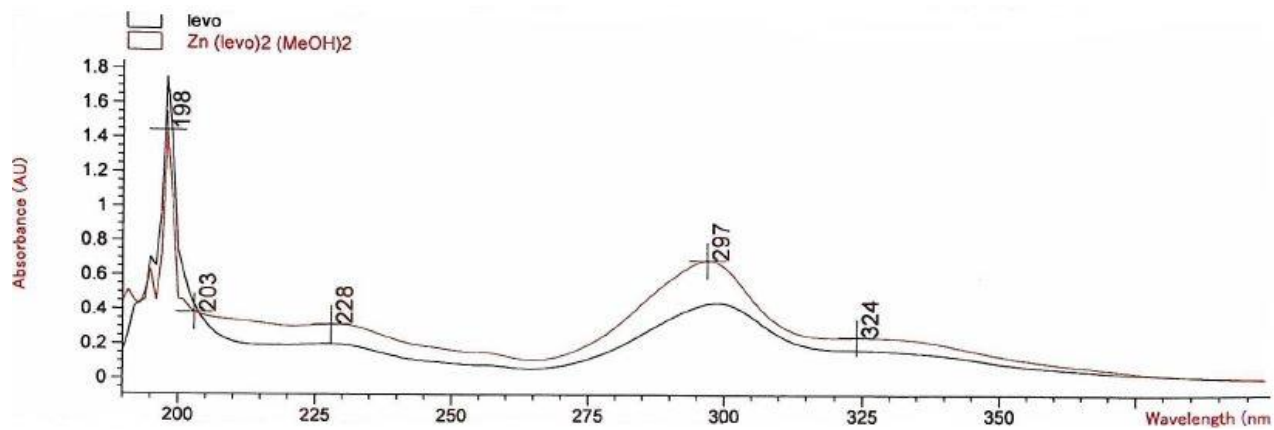


Figure S 1: UV-Vis. spectra of complex **1** with parent ligands.

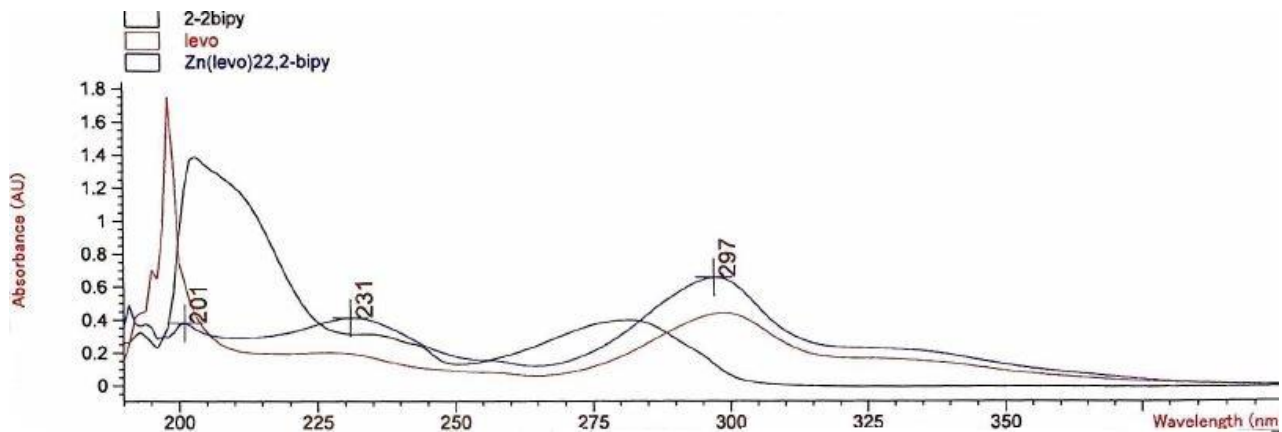


Figure S 2: UV-Vis. spectra of complex **3** with parent ligands.

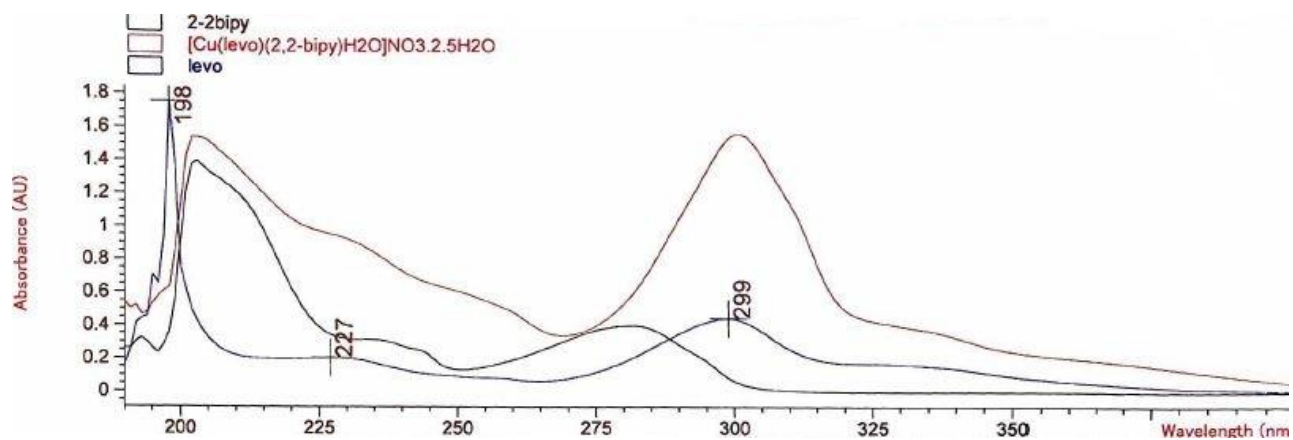


Figure S 3: UV-Vis. spectra of complex 4 with parent ligands.

## Appendix B: Infrared spectra of complexes 1, 3 and 4

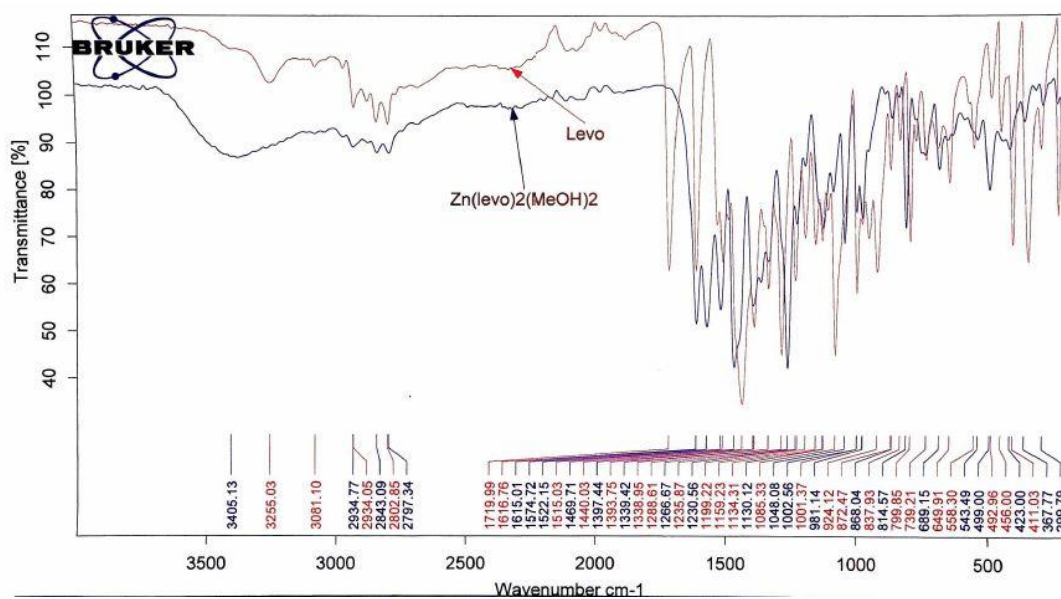
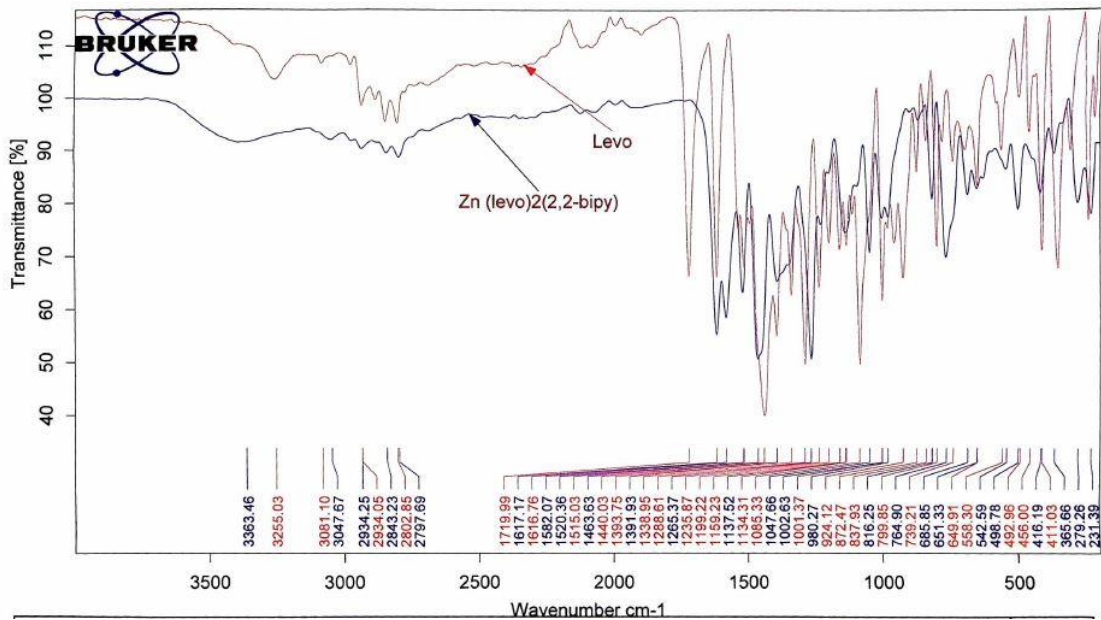
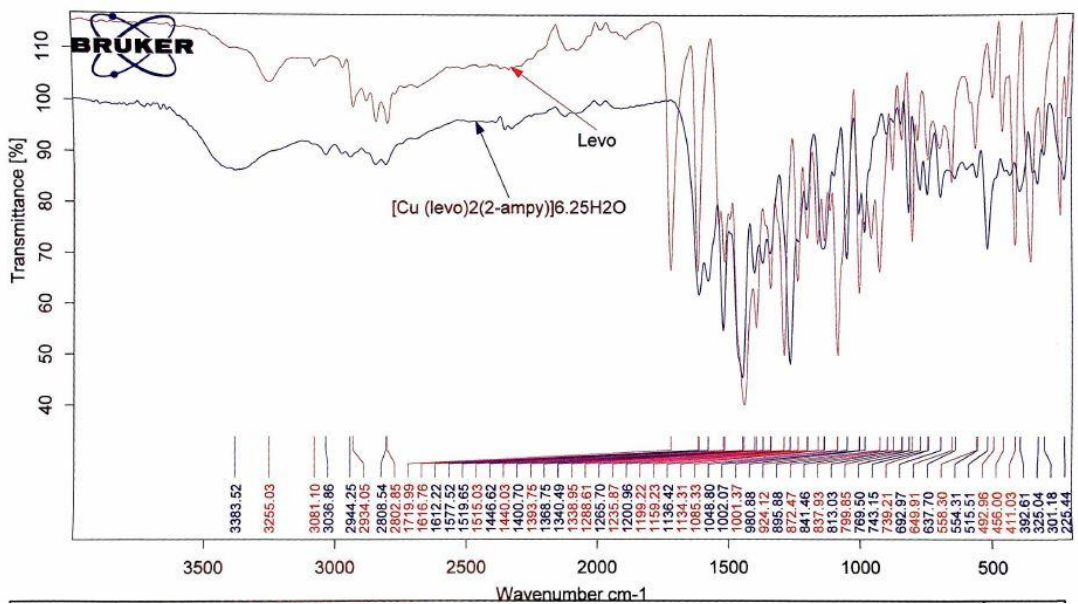


Figure S 4: IR spectra of complex 1 and levo ligand.

Figure S 5: IR spectra of complex **3** and levo ligand.Figure S 6: IR spectra of complex **4** and levo ligand.

**Appendix C:**  $^1\text{H-NMR}$  spectral data of complexes **1** and **2** and their parent ligands.

**Table S 1:**  $^1\text{H-NMR}$  spectral data of complex **1** and H-levo,  $\delta$  (ppm).

Complex 1	H-levo
1.39 (d, 3H, $\text{CH}_3$ , $^3J_{\text{H-H}} = 5.25$ Hz)	1.41 (d, 3H, $\text{CH}_3$ , $^3J_{\text{H-H}} = 6.9$ Hz)
2.22 (s, 3H, $\text{CH}_3$ )	2.19 (s, 3H, $\text{CH}_3$ )
2.42 (s, 4H, $\text{CH}_2$ )	2.39 (s, 4H, $\text{CH}_2$ , $^3J_{\text{H-H}} = 6.9$ Hz)
3.25 (s, 4H, $\text{CH}_2$ )	3.25 (s, 4H, $\text{CH}_2$ )
4.34 (d, 1H, $\text{OC}(\text{H}_a)\text{H}$ , $^3J_{\text{H-H}} = 10.11$ Hz)	4.32 (d, 1H, $\text{OC}(\text{H}_a)\text{H}$ , $^3J_{\text{H-H}} = 11.4$ Hz)
4.54 (d, 1H, $\text{OC}(\text{H}_b)\text{H}$ , $^3J_{\text{H-H}} = 10.94$ Hz)	4.54 (d, 1H, $\text{OC}(\text{H}_b)\text{H}$ , $^3J_{\text{H-H}} = 11.8$ Hz)
4.87 (bs, 1H, CH)	4.87 (bs, 1H, CH)
7.49 (d, 1H, CH, $^3J_{\text{H-H}} = 11.64$ Hz)	7.51 (d, 1H, CH, $^3J_{\text{H-H}} = 12.6$ Hz)
8.96 (s, 1H, CH)	8.92 (s, 1H, CH)
-121.62(d, 1F)	-122.24 (d, 1F, $^3J_{\text{H-F}} = 12.9$ Hz)

**Table S 2:**  $^1\text{H}$ -NMR spectral data of complex **2** and 2-ampy,  $\delta$  (ppm).

Complex <b>2</b>	2-ampy
1.33 (d, 3H, CH <sub>3</sub> , $^3J_{\text{H-H}} = 4.5$ Hz)	
2.18 (s, 3H, CH <sub>3</sub> )	
2.38 (s, 4H, CH <sub>2</sub> )	
3.21 (s, 4H, CH <sub>2</sub> )	
4.28 (d, 1H, OC(Ha)H, $^3J_{\text{H-H}} = 10.5$ Hz)	
4.48 (d, 1H, OC(Hb)H, $^3J_{\text{H-H}} = 10.8$ Hz)	
4.80 (bs, 1H, CH)	
5.88 (s, 2H, NH <sub>2</sub> )	
6.37 (d, 1H, CH <sub>ampy</sub> , $^3J_{\text{H-H}} = 7.8$ Hz)	6.77 d
6.50 (d, 1H, CH <sub>ampy</sub> , $^3J_{\text{H-H}} = 7.2$ Hz)	6.62 d
7.28 (t, 1H, CH <sub>ampy</sub> , $^3J_{\text{H-H}} = 5.7$ Hz)	7.55 t
7.44 (d, 1H, CH, $^3J_{\text{H-H}} = 10.2$ Hz)	
7.84 (d, 1H, CH <sub>ampy</sub> , $^3J_{\text{H-H}} = 4.2$ Hz)	8.07 d
8.85 (s, 1H, CH)	
-122.08 (d, 1F, $^3J_{\text{H-F}} = 10.2$ Hz)	



**Appendix D: *In-vitro*, anti-bacterial activity data for complexes 1-5.**

**Table S 3: *In-vitro*, anti-bacterial activity data for complexes 1-5 against Gram negative bacteria.**

Compounds	Gram-negative bacteria				
	Concentration	<i>E. coli</i>	<i>K. pneumoniae</i>	<i>P. mirabilis</i>	<i>P. aeruginosa</i>
DMSO	6 mg/ mL	-	-	-	-
ZnCl <sub>2</sub>	6 mg/ mL	-	-	-	-
Cu(NO <sub>3</sub> ) <sub>2</sub>	6 mg/ mL	-	-	-	-
Levofloxacin	4 mg/ mL	41.2 ± 0.9	43.5 ± 0.6	38.9 ± 0.9	30.6 ± 0.4
	6 mg/ml	42.5 ± 0.5	48.5 ± 0.7	40.9 ± 0.8	32.1 ± 0.7
2-ampy	1.1 mg/ml	-	-	-	-
	6 mg/ml	-	-	-	-
2,2-bipy	1.34 mg/ml	-	14.9 ± 1.1	-	-
	6 mg/ml	20.7 ± 0.9	24.2 ± 0.6	24.1 ± 1.3	-
Complex 1	6 mg/ mL	39.1 ± 0.9	45.8 ± 0.5	44.1 ± 0.4	30.5 ± 0.7
Complex 2	6 mg/ mL	39.3 ± 0.5	45.2 ± 0.4	44.1 ± 0.4	29.6 ± 1.2
Complex 3	6 mg/ mL	37.5 ± 0.5	43.9 ± 0.3	41.9 ± 0.7	30.8 ± 0.7
Complex 4	6 mg/ mL	38.8 ± 0.6	41.8 ± 0.9	39.6 ± 0.4	31.3 ± 0.4
Complex 5	6 mg/ mL	39.2 ± 0.3	42.1 ± 0.2	38.2 ± 0.6	28.3 ± 0.9

Inhibition zone diameter (millimeter (mm)) ± Standard error (N = 3)

**Table S 4:** *In-vitro*, anti-bacterial activity data for complexes **1-5** against Gram positive bacteria.

Compounds	Gram-positive bacteria				
	Concentration	<i>S. aureus</i>	<i>B. subtilis</i>	<i>E. faecalis</i>	<i>S. epidemidis</i>
DMSO	6 mg/ mL	-	-	-	-
ZnCl <sub>2</sub>	6 mg/ mL	-	-	-	-
Cu(NO <sub>3</sub> ) <sub>2</sub>	6 mg/ mL	-	-	-	-
Levofloxacin	4 mg/ mL	42.1 ± 1.3	37.6 ± 0.9	34.4 ± 0.5	48.5 ± 0.7
	6 mg/ml	42.4 ± 0.5	37.8 ± 1.5	34.6 ± 0.9	49.1 ± 0.3
2-ampy	1.1 mg/ml	-	-	-	-
	6 mg/ml	-	-	-	-
2,2-bipy	1.34 mg/ml	-	-	-	-
	6 mg/ml	-	18.7 ± 0.8	-	21.1 ± 0.4
Complex 1	6 mg/ mL	41.1 ± 0.2	36.0 ± 0.4	35.6 ± 1.1	43.2 ± 0.7
Complex 2	6 mg/ mL	39.1 ± 0.4	35.2 ± 0.6	34.2 ± 1.2	43.9 ± 0.3
Complex 3	6 mg/ mL	40.4 ± 1.3	35.5 ± 0.7	35.3 ± 1.2	41.2 ± 0.9
Complex 4	6 mg/ mL	41.9 ± 0.6	35.9 ± 0.3	35.6 ± 0.3	41.8 ± 0.8
Complex 5	6 mg/ mL	41.0 ± 0.8	36.0 ± 0.4	34.2 ± 0.6	42.2 ± 0.6

Inhibition zone diameter (millimeter (mm)) ± Standard error (N = 3)

**Appendix E:** Crystal structure data of [Cu(lev<sub>o</sub>)<sub>2</sub>(2-ampy)].6.25H<sub>2</sub>O (**4**)**Table 1:** Bond Lengths for complex **4**.

Atom		Length/Å	Atom		Length/Å
Cu1	O1	1.941(2)	Cu2	N15	2.300(3)
Cu1	O3	1.940(2)	F3	C49	1.351(3)
Cu1	O5	1.938(2)	F4	C67	1.351(4)
Cu1	O7	1.931(2)	O9	C42	1.270(4)
Cu1	N7	2.274(4)	O10	C42	1.247(4)
F1	C8	1.343(4)	O11	C44	1.272(3)
F2	C26	1.348(3)	O12	C51	1.375(3)
O1	C1	1.266(4)	O12	C52	1.435(4)
O2	C1	1.245(4)	O13	C60	1.271(4)
O3	C3	1.265(4)	O14	C60	1.244(4)
O4	C10	1.367(4)	O15	C62	1.271(4)
O4	C11	1.439(4)	O16	C69	1.367(4)
O5	C19	1.282(4)	O16	C70	1.449(4)
O6	C19	1.246(4)	N9	C46	1.393(4)
O7	C21	1.263(4)	N9	C47	1.328(4)
O8	C28	1.365(4)	N9	C53	1.488(4)
O8	C29	1.442(4)	N10	C50	1.384(4)
N1	C5	1.379(4)	N10	C55	1.466(5)
N1	C6	1.346(4)	N10	C58	1.471(5)

N1	C12	1.481(4)	N11	C56	1.435(5)
N2	C9	1.395(4)	N11	C57	1.425(5)
N2	C14	1.480(4)	N11	C59	1.432(5)
N2	C17	1.469(4)	N12	C64	1.395(4)
N3	C15	1.471(4)	N12	C65	1.330(4)
N3	C16	1.468(5)	N12	C71	1.491(4)
N3	C18	1.459(4)	N13	C68	1.400(4)
N4	C23	1.390(4)	N13	C73	1.468(5)
N4	C24	1.335(4)	N13	C76	1.476(4)
N4	C30	1.481(4)	N14	C74	1.477(5)
N5	C27	1.406(4)	N14	C75	1.467(5)
N5	C32	1.459(4)	N14	C77	1.466(5)
N5	C35	1.457(4)	N15	C78A	1.258(9)
N6	C33	1.459(4)	N15	C78B	1.332(8)
N6	C34	1.463(5)	N15	C82A	1.392(9)
N6	C36	1.470(5)	N15	C82B	1.436(8)
N7	C37	1.319(6)	N16A	C78A	1.352(12)
N7	C41	1.384(6)	N16B	C78B	1.373(10)
N8	C37	1.331(7)	C42	C43	1.491(4)
C1	C2	1.511(5)	C43	C44	1.434(4)
C2	C3	1.411(4)	C43	C47	1.381(4)
C2	C6	1.384(4)	C44	C45	1.447(4)

C3	C4	1.465(4)	C45	C46	1.410(4)
C4	C5	1.410(4)	C45	C48	1.414(4)
C4	C7	1.390(4)	C46	C51	1.407(4)
C5	C10	1.411(4)	C48	C49	1.358(4)
C7	C8	1.375(5)	C49	C50	1.425(4)
C8	C9	1.413(4)	C50	C51	1.393(4)
C9	C10	1.398(4)	C52	C53	1.502(5)
C11	C12	1.514(5)	C53	C54	1.531(5)
C12	C13	1.512(6)	C55	C56	1.468(6)
C14	C15	1.521(5)	C57	C58	1.483(6)
C16	C17	1.516(5)	C60	C61	1.503(4)
C19	C20	1.491(5)	C61	C62	1.418(4)
C20	C21	1.428(4)	C61	C65	1.382(4)
C20	C24	1.385(4)	C62	C63	1.457(4)
C21	C22	1.453(4)	C63	C64	1.406(4)
C22	C23	1.409(4)	C63	C66	1.398(4)
C22	C25	1.404(4)	C64	C69	1.415(5)
C23	C28	1.405(4)	C66	C67	1.367(5)
C25	C26	1.367(5)	C67	C68	1.407(4)
C26	C27	1.414(4)	C68	C69	1.390(4)
C27	C28	1.402(4)	C70	C71	1.503(5)
C29	C30	1.518(5)	C71	C72	1.525(6)

C30	C31	1.522(5)	C73	C74	1.510(5)
C32	C33	1.536(5)	C75	C76	1.493(5)
C34	C35	1.527(5)	C78A	C79A	1.401(14)
C37	C38	1.426(8)	C78B	C79B	1.399(13)
C38	C39	1.365(8)	C79A	C80A	1.384(14)
C39	C40	1.372(7)	C79B	C80B	1.399(13)
C40	C41	1.343(7)	C80A	C81A	1.355(13)
Cu2	O9	1.931(2)	C80B	C81B	1.399(12)
Cu2	O11	1.944(2)	C81A	C82A	1.390(13)
Cu2	O13	1.946(2)	C81B	C82B	1.380(11)
Cu2	O15	1.930(2)			

---

**Table 2:** Bond Angles for complex 4.

Atom	Atom	Atom	Angle/°	Atom	Atom	Atom	Angle/°
O1	Cu1	N7	92.24(12)	O13	Cu2	N15	97.19(11)
O3	Cu1	O1	92.62(10)	O15	Cu2	O9	85.00(9)
O3	Cu1	N7	99.65(13)	O15	Cu2	O11	165.47(12)
O5	Cu1	O1	171.22(14)	O15	Cu2	O13	92.27(9)
O5	Cu1	O3	86.57(10)	O15	Cu2	N15	98.80(11)
O5	Cu1	N7	96.51(12)	C42	O9	Cu2	130.6(2)
O7	Cu1	O1	85.29(10)	C44	O11	Cu2	126.25(19)
O7	Cu1	O3	166.35(13)	C51	O12	C52	112.0(2)

O7	Cu1	O5	93.44(10)	C60	O13	Cu2	130.7(2)
O7	Cu1	N7	93.92(12)	C62	O15	Cu2	126.5(2)
C1	O1	Cu1	130.6(2)	C69	O16	C70	113.2(3)
C3	O3	Cu1	126.5(2)	C46	N9	C53	119.5(3)
C10	O4	C11	113.0(3)	C47	N9	C46	119.9(2)
C19	O5	Cu1	129.3(2)	C47	N9	C53	120.4(2)
C21	O7	Cu1	125.6(2)	C50	N10	C55	121.7(3)
C28	O8	C29	113.3(2)	C50	N10	C58	118.9(3)
C5	N1	C12	118.9(3)	C55	N10	C58	112.0(3)
C6	N1	C5	120.4(3)	C57	N11	C56	113.6(3)
C6	N1	C12	120.6(3)	C57	N11	C59	113.9(3)
C9	N2	C14	114.7(3)	C59	N11	C56	115.2(4)
C9	N2	C17	119.5(3)	C64	N12	C71	118.5(3)
C17	N2	C14	111.1(3)	C65	N12	C64	120.0(3)
C16	N3	C15	108.2(3)	C65	N12	C71	121.5(3)
C18	N3	C15	110.5(3)	C68	N13	C73	118.1(3)
C18	N3	C16	111.8(3)	C68	N13	C76	120.8(3)
C23	N4	C30	117.7(3)	C73	N13	C76	110.0(3)
C24	N4	C23	120.9(3)	C75	N14	C74	109.0(3)
C24	N4	C30	121.1(3)	C77	N14	C74	110.8(3)
C27	N5	C32	116.0(3)	C77	N14	C75	112.0(3)
C27	N5	C35	120.5(3)	C78A	N15	Cu2	128.3(5)

C35	N5	C32	111.0(3)	C78A N15	C82A	120.8(7)
C33	N6	C34	108.9(3)	C78B N15	Cu2	134.9(4)
C33	N6	C36	110.9(3)	C78B N15	C82B	113.1(6)
C34	N6	C36	109.8(3)	C82A N15	Cu2	110.9(4)
C37	N7	Cu1	128.6(3)	C82B N15	Cu2	111.6(4)
C37	N7	C41	117.0(4)	O9	C42 C43	119.7(3)
C41	N7	Cu1	113.6(3)	O10	C42 O9	121.7(3)
O1	C1	C2	119.8(3)	O10	C42 C43	118.6(3)
O2	C1	O1	121.9(3)	C44	C43 C42	124.8(3)
O2	C1	C2	118.3(3)	C47	C43 C42	116.5(3)
C3	C2	C1	124.0(3)	C47	C43 C44	118.7(3)
C6	C2	C1	115.8(3)	O11	C44 C43	125.1(3)
C6	C2	C3	120.2(3)	O11	C44 C45	118.4(2)
O3	C3	C2	126.4(3)	C43	C44 C45	116.5(2)
O3	C3	C4	117.1(3)	C46	C45 C44	120.9(2)
C2	C3	C4	116.5(3)	C46	C45 C48	118.5(3)
C5	C4	C3	120.0(3)	C48	C45 C44	120.6(3)
C7	C4	C3	120.5(3)	N9	C46 C45	119.1(3)
C7	C4	C5	119.5(3)	N9	C46 C51	120.0(3)
N1	C5	C4	119.9(3)	C51	C46 C45	120.8(3)
N1	C5	C10	119.9(3)	N9	C47 C43	124.8(3)
C4	C5	C10	120.1(3)	C49	C48 C45	118.7(3)



N1	C6	C2	123.1(3)	F3	C49	C48	117.9(3)
C8	C7	C4	118.9(3)	F3	C49	C50	116.9(3)
F1	C8	C7	117.1(3)	C48	C49	C50	125.1(3)
F1	C8	C9	118.8(3)	N10	C50	C49	120.7(3)
C7	C8	C9	124.1(3)	N10	C50	C51	123.9(3)
N2	C9	C8	125.4(3)	C51	C50	C49	115.4(3)
N2	C9	C10	118.5(3)	O12	C51	C46	119.4(3)
C10	C9	C8	116.1(3)	O12	C51	C50	119.0(3)
O4	C10	C5	121.2(3)	C50	C51	C46	121.5(3)
O4	C10	C9	117.8(3)	O12	C52	C53	109.8(3)
C9	C10	C5	121.0(3)	N9	C53	C52	107.8(3)
O4	C11	C12	110.4(3)	N9	C53	C54	110.3(3)
N1	C12	C11	106.6(3)	C52	C53	C54	112.8(3)
N1	C12	C13	109.5(3)	N10	C55	C56	111.1(4)
C13	C12	C11	112.5(3)	N11	C56	C55	114.7(4)
N2	C14	C15	109.2(3)	N11	C57	C58	114.5(3)
N3	C15	C14	110.5(3)	N10	C58	C57	110.8(4)
N3	C16	C17	110.3(3)	O13	C60	C61	119.4(3)
N2	C17	C16	108.6(3)	O14	C60	O13	122.9(3)
O5	C19	C20	120.3(3)	O14	C60	C61	117.7(3)
O6	C19	O5	121.0(3)	C62	C61	C60	124.0(3)
O6	C19	C20	118.7(3)	C65	C61	C60	117.1(3)

C21	C20	C19	124.1(3)	C65	C61	C62	118.9(3)
C24	C20	C19	116.7(3)	O15	C62	C61	125.9(3)
C24	C20	C21	119.2(3)	O15	C62	C63	117.2(3)
O7	C21	C20	126.1(3)	C61	C62	C63	116.9(3)
O7	C21	C22	117.3(3)	C64	C63	C62	120.4(3)
C20	C21	C22	116.7(3)	C66	C63	C62	120.7(3)
C23	C22	C21	120.8(3)	C66	C63	C64	118.9(3)
C25	C22	C21	120.4(3)	N12	C64	C63	119.2(3)
C25	C22	C23	118.8(3)	N12	C64	C69	120.5(3)
N4	C23	C22	118.8(3)	C63	C64	C69	120.3(3)
N4	C23	C28	120.6(3)	N12	C65	C61	124.5(3)
C28	C23	C22	120.6(3)	C67	C66	C63	118.9(3)
N4	C24	C20	123.6(3)	F4	C67	C66	116.3(3)
C26	C25	C22	119.0(3)	F4	C67	C68	118.8(3)
F2	C26	C25	117.0(3)	C66	C67	C68	124.8(3)
F2	C26	C27	118.6(3)	N13	C68	C67	124.4(3)
C25	C26	C27	124.4(3)	C69	C68	N13	119.8(3)
N5	C27	C26	125.0(3)	C69	C68	C67	115.8(3)
C28	C27	N5	119.1(3)	O16	C69	C64	120.0(3)
C28	C27	C26	115.9(3)	O16	C69	C68	118.7(3)
O8	C28	C23	121.3(3)	C68	C69	C64	121.3(3)
O8	C28	C27	117.7(3)	O16	C70	C71	109.9(3)

C27	C28	C23	121.1(3)	N12	C71	C70	107.5(3)
O8	C29	C30	110.3(3)	N12	C71	C72	109.2(3)
N4	C30	C29	106.8(2)	C70	C71	C72	113.6(3)
N4	C30	C31	110.2(3)	N13	C73	C74	110.5(3)
C29	C30	C31	113.5(3)	N14	C74	C73	110.2(3)
N5	C32	C33	109.7(3)	N14	C75	C76	110.8(3)
N6	C33	C32	110.2(3)	N13	C76	C75	109.6(3)
N6	C34	C35	109.4(3)	N15	C78A	N16A	116.7(8)
N5	C35	C34	108.9(3)	N15	C78A	C79A	126.8(10)
N7	C37	N8	117.8(5)	N16A	C78A	C79A	116.5(9)
N7	C37	C38	122.0(5)	N15	C78B	N16B	114.3(7)
N8	C37	C38	120.2(5)	N15	C78B	C79B	129.7(8)
C39	C38	C37	117.7(5)	N16B	C78B	C79B	116.1(8)
C38	C39	C40	121.4(5)	C80A	C79A	C78A	109.8(9)
C41	C40	C39	117.4(5)	C80B	C79B	C78B	112.8(8)
C40	C41	N7	124.5(4)	C81A	C80A	C79A	128.4(10)
O9	Cu2	O11	92.65(9)	C81B	C80B	C79B	123.9(8)
O9	Cu2	O13	171.80(13)	C80A	C81A	C82A	115.1(9)
O9	Cu2	N15	90.87(11)	C82B	C81B	C80B	116.7(8)
O11	Cu2	O13	88.05(9)	C81A	C82A	N15	119.0(9)
O11	Cu2	N15	95.56(11)	C81B	C82B	N15	123.7(8)

---

**Appendix F:** Crystal structure data of [Cu(levo)(H<sub>2</sub>O)(2,2-bipy)](NO<sub>3</sub>).2.5H<sub>2</sub>O (**5**)**Table 1:** Bond Lengths for complex **5**.

Atom	Length/Å	Atom	Length/Å
Cu1 O1	1.908(3)	N8 C46	1.476(5)
Cu1 O1W	2.244(3)	N9 C47	1.352(4)
Cu1 O3	1.944(3)	N9 C51	1.334(4)
Cu1 N4	1.996(3)	N10 C52	1.350(4)
Cu1 N5	1.992(3)	N10 C56	1.337(4)
F1 C12	1.350(4)	C29 C30	1.495(4)
O1 C1	1.278(4)	C30 C31	1.433(4)
O2 C1	1.248(4)	C30 C34	1.383(4)
O3 C3	1.277(4)	C31 C32	1.452(4)
O4 C7	1.361(4)	C32 C33	1.409(4)
O4 C8	1.439(5)	C32 C39	1.413(4)
N1 C5	1.394(5)	C33 C35	1.403(4)
N1 C6	1.341(5)	C35 C41	1.393(4)
N1 C9	1.493(4)	C36 C37	1.513(4)
N2 C13	1.404(5)	C37 C38	1.525(5)
N2 C14	1.465(5)	C39 C40	1.358(5)
N2 C17	1.471(5)	C40 C41	1.414(4)
N3 C15	1.455(5)	C42 C43	1.516(5)
N3 C16	1.462(5)	C44 C45	1.533(5)

N3	C18	1.449(5)	C47	C48	1.386(4)
N4	C19	1.342(5)	C47	C52	1.483(4)
N4	C23	1.351(4)	C48	C49	1.389(5)
N5	C24	1.347(4)	C49	C50	1.387(5)
N5	C28	1.333(4)	C50	C51	1.399(5)
C1	C2	1.495(5)	C52	C53	1.390(4)
C2	C3	1.433(5)	C53	C54	1.401(5)
C2	C6	1.378(5)	C54	C55	1.390(5)
C3	C4	1.447(5)	C55	C56	1.386(4)
C4	C5	1.412(4)	Cu4	O4W	2.265(4)
C4	C11	1.409(5)	Cu4	O13A	1.862(5)
C5	C7	1.399(5)	Cu4	O13B	2.023(13)
C7	C13	1.403(6)	Cu4	O15	1.953(3)
C8	C9	1.500(6)	Cu4	N19	1.996(4)
C9	C10	1.538(6)	Cu4	N20	2.000(3)
C11	C12	1.375(5)	F4A	C96A	1.352(7)
C12	C13	1.400(5)	F4B	C96B	1.378(14)
C14	C15	1.518(5)	O13A	C85A	1.285(8)
C16	C17	1.501(5)	O13B	C85B	1.285(16)
C19	C20	1.388(5)	O14	C85A	1.307(7)
C19	C24	1.480(5)	O14	C85B	1.136(10)
C20	C21	1.394(6)	O15	C87A	1.296(7)

C21	C22	1.391(8)	O15	C87B	1.275(16)
C22	C23	1.372(6)	O16A	C91A	1.372(6)
C24	C25	1.387(5)	O16A	C92A	1.435(6)
C25	C26	1.386(5)	O16B	C91B	1.346(13)
C26	C27	1.384(5)	O16B	C92B	1.430(14)
C27	C28	1.395(5)	N16A	C89A	1.391(8)
Cu3	O3W	2.266(3)	N16A	C90A	1.309(10)
Cu3	O9	1.912(2)	N16A	C93A	1.481(7)
Cu3	O11	1.935(2)	N16B	C89B	1.394(17)
Cu3	N14	1.993(3)	N16B	C90B	1.310(15)
Cu3	N15	1.989(3)	N16B	C93B	1.441(17)
F3	C68	1.341(5)	N17A	C97A	1.386(7)
O9	C57	1.278(4)	N17A	C98A	1.460(8)
O10	C57	1.247(4)	N17A	C101	1.451(6)
O11	C59	1.277(4)	N17B	C1A	1.475(15)
O12	C63	1.365(5)	N17B	C97B	1.390(14)
O12	C64	1.425(5)	N17B	C98B	1.450(17)
N11	C61	1.379(5)	N18A	C99A	1.472(7)
N11	C62	1.324(5)	N18A	C100	1.464(9)
N11	C65	1.491(4)	N18A	C102	1.478(10)
N12A	C69	1.381(9)	N18B	C1B	1.451(18)
N12A	C70A	1.449(13)	N18B	C1C	1.45(2)

N12A C73A	1.461(15)	N18B C99B	1.430(18)
N12B C69	1.471(8)	N19 C103	1.350(5)
N12B C70B	1.475(13)	N19 C107	1.341(5)
N12B C73B	1.474(15)	N20 C108	1.355(5)
N13A C71A	1.472(13)	N20 C112	1.321(6)
N13A C72A	1.472(13)	C1A C1B	1.538(18)
N13A C74A	1.477(13)	C85A C86A	1.488(10)
N13B C71B	1.483(17)	C85B C86B	1.453(17)
N13B C72B	1.455(14)	C86A C87A	1.436(10)
N13B C74B	1.448(13)	C86A C90A	1.391(9)
N14 C75	1.343(4)	C86B C87B	1.417(19)
N14 C79	1.335(4)	C86B C90B	1.430(19)
N15 C80	1.353(4)	C87A C88A	1.460(12)
N15 C84	1.345(4)	C87B C88B	1.43(2)
C57 C58	1.500(4)	C88A C89A	1.423(11)
C58 C59	1.425(4)	C88A C95A	1.390(11)
C58 C62	1.385(4)	C88B C89B	1.41(2)
C59 C60	1.453(4)	C88B C95B	1.40(2)
C60 C61	1.407(4)	C89A C91A	1.393(9)
C60 C67	1.392(5)	C89B C91B	1.399(15)
C61 C63	1.413(5)	C91A C97A	1.394(7)
C63 C69	1.394(6)	C91B C97B	1.418(14)

C64 C65	1.516(6)	C92A C93A	1.517(8)
C65 C66	1.528(6)	C92B C93B	1.561(18)
C67 C68	1.376(5)	C93A C94A	1.506(11)
C68 C69	1.410(6)	C93B C94B	1.50(2)
C70A C71A	1.506(14)	C95A C96A	1.358(10)
C70B C71B	1.537(11)	C95B C96B	1.352(18)
C72A C73A	1.563(14)	C96A C97A	1.418(8)
C72B C73B	1.551(13)	C96B C97B	1.410(15)
C75 C76	1.393(4)	C98A C99A	1.519(9)
C75 C80	1.484(4)	C98B C99B	1.531(19)
C76 C77	1.393(5)	C100 C101	1.520(9)
C77 C78	1.388(5)	C103 C104	1.393(5)
C78 C79	1.383(5)	C103 C108	1.478(6)
C80 C81	1.395(4)	C104 C105	1.377(6)
C81 C82	1.385(5)	C105 C106	1.388(6)
C82 C83	1.391(5)	C106 C107	1.394(6)
C83 C84	1.387(5)	C108 C109	1.386(5)
Cu2 O2W	2.268(3)	C109 C110	1.380(6)
Cu2 O5	1.901(2)	C110 C111	1.388(6)
Cu2 O7	1.954(2)	C111 C112	1.389(5)
Cu2 N9	2.012(3)	O13 O22W	1.343(19)
Cu2 N10	1.994(3)	O13 O24W	1.64(3)



F2	C40	1.354(4)	O16W O17W	1.02(2)
O5	C29	1.277(4)	O1N N1N	1.249(4)
O6	C29	1.241(4)	O2N N1N	1.246(4)
O7	C31	1.271(4)	O3N N1N	1.253(5)
O8	C35	1.370(4)	O4N N2N	1.247(4)
O8	C36	1.436(4)	O5N N2N	1.250(4)
N6	C33	1.401(4)	O6N N2N	1.253(4)
N6	C34	1.330(4)	O21W O15W <sup>1</sup>	1.35(2)
N6	C37	1.492(4)	O7N N3N	1.352(12)
N7	C41	1.385(4)	O8N N3N	1.126(14)
N7	C42	1.460(4)	O9N N3N	1.335(11)
N7	C45	1.455(4)	O10N N4N	1.328(15)
N8	C43	1.463(5)	O11N N4N	1.248(13)
N8	C44	1.465(4)	O12N N4N	1.253(13)

<sup>1</sup>-1+X,-1+Y,-1+Z

**Table 2:** Bond Angles for complex **5**.

Atom			Angle/°	Atom			Angle/°
O1	Cu1	O1W	96.69(12)	C56	N10	Cu2	125.8(2)
O1	Cu1	O3	93.25(11)	C56	N10	C52	119.4(3)
O1	Cu1	N4	91.92(12)	O5	C29	C30	119.5(3)
O1	Cu1	N5	169.60(11)	O6	C29	O5	122.1(3)
O3	Cu1	O1W	93.54(11)	O6	C29	C30	118.4(3)

O3	Cu1	N4	168.23(12)	C31	C30	C29	124.6(3)
O3	Cu1	N5	92.24(11)	C34	C30	C29	116.3(3)
N4	Cu1	O1W	96.35(11)	C34	C30	C31	118.9(3)
N5	Cu1	O1W	91.77(11)	O7	C31	C30	125.3(3)
N5	Cu1	N4	81.12(12)	O7	C31	C32	118.4(3)
C1	O1	Cu1	128.3(2)	C30	C31	C32	116.4(3)
C3	O3	Cu1	123.8(2)	C33	C32	C31	121.1(3)
C7	O4	C8	113.4(3)	C33	C32	C39	117.9(3)
C5	N1	C9	118.9(3)	C39	C32	C31	121.1(3)
C6	N1	C5	120.6(3)	N6	C33	C32	118.9(3)
C6	N1	C9	120.3(3)	N6	C33	C35	119.7(3)
C13	N2	C14	117.2(3)	C35	C33	C32	121.4(3)
C13	N2	C17	119.7(3)	N6	C34	C30	124.6(3)
C14	N2	C17	112.0(3)	O8	C35	C33	121.3(3)
C15	N3	C16	109.8(3)	O8	C35	C41	117.9(3)
C18	N3	C15	111.4(3)	C41	C35	C33	120.8(3)
C18	N3	C16	110.5(3)	O8	C36	C37	110.4(3)
C19	N4	Cu1	114.9(2)	N6	C37	C36	107.3(2)
C19	N4	C23	119.7(3)	N6	C37	C38	110.9(3)
C23	N4	Cu1	125.4(3)	C36	C37	C38	112.5(3)
C24	N5	Cu1	114.9(2)	C40	C39	C32	119.2(3)
C28	N5	Cu1	125.5(2)	F2	C40	C39	118.1(3)

C28	N5	C24	119.4(3)	F2	C40	C41	117.3(3)
O1	C1	C2	119.8(3)	C39	C40	C41	124.6(3)
O2	C1	O1	122.3(3)	N7	C41	C35	119.7(3)
O2	C1	C2	117.9(3)	N7	C41	C40	124.2(3)
C3	C2	C1	124.4(3)	C35	C41	C40	116.0(3)
C6	C2	C1	116.6(3)	N7	C42	C43	109.0(3)
C6	C2	C3	118.8(3)	N8	C43	C42	110.0(3)
O3	C3	C2	125.2(3)	N8	C44	C45	110.2(3)
O3	C3	C4	118.0(3)	N7	C45	C44	108.1(3)
C2	C3	C4	116.8(3)	N9	C47	C48	121.8(3)
C5	C4	C3	121.2(3)	N9	C47	C52	114.2(3)
C11	C4	C3	120.8(3)	C48	C47	C52	124.0(3)
C11	C4	C5	118.0(3)	C47	C48	C49	118.9(3)
N1	C5	C4	118.4(3)	C50	C49	C48	119.1(3)
N1	C5	C7	120.0(3)	C49	C50	C51	119.1(3)
C7	C5	C4	121.6(3)	N9	C51	C50	121.5(3)
N1	C6	C2	124.2(3)	N10	C52	C47	115.0(3)
O4	C7	C5	121.6(3)	N10	C52	C53	122.0(3)
O4	C7	C13	118.0(3)	C53	C52	C47	123.0(3)
C5	C7	C13	120.4(3)	C52	C53	C54	118.3(3)
O4	C8	C9	112.0(3)	C55	C54	C53	119.1(3)
N1	C9	C8	107.6(3)	C56	C55	C54	119.0(3)

N1	C9	C10	110.7(3)	N10	C56	C55	122.1(3)
C8	C9	C10	112.3(4)	O13A	Cu4	O4W	97.2(2)
C12	C11	C4	119.0(3)	O13A	Cu4	O15	90.7(2)
F1	C12	C11	117.3(3)	O13A	Cu4	N19	93.2(2)
F1	C12	C13	118.3(3)	O13A	Cu4	N20	170.9(2)
C11	C12	C13	124.3(4)	O13B	Cu4	O4W	104.1(4)
C7	C13	N2	119.0(3)	O15	Cu4	O4W	93.42(13)
C12	C13	N2	124.4(4)	O15	Cu4	O13B	97.9(4)
C12	C13	C7	116.7(3)	O15	Cu4	N19	173.51(13)
N2	C14	C15	110.6(3)	O15	Cu4	N20	94.12(13)
N3	C15	C14	111.4(3)	N19	Cu4	O4W	91.21(13)
N3	C16	C17	110.4(3)	N19	Cu4	O13B	85.4(4)
N2	C17	C16	108.9(3)	N19	Cu4	N20	81.32(14)
N4	C19	C20	122.0(4)	N20	Cu4	O4W	90.17(14)
N4	C19	C24	114.6(3)	N20	Cu4	O13B	160.7(3)
C20	C19	C24	123.4(3)	C85A	O13A	Cu4	131.1(5)
C19	C20	C21	118.1(4)	C85B	O13B	Cu4	121.9(8)
C22	C21	C20	119.4(4)	C87A	O15	Cu4	127.5(4)
C23	C22	C21	119.3(4)	C87B	O15	Cu4	111.2(7)
N4	C23	C22	121.4(4)	C91A	O16A	C92A	113.1(4)
N5	C24	C19	114.3(3)	C91B	O16B	C92B	114.5(8)
N5	C24	C25	121.2(3)	C89A	N16A	C93A	117.9(6)

C25	C24	C19	124.5(3)	C90A N16A C89A	120.4(5)
C26	C25	C24	119.6(3)	C90A N16A C93A	121.2(5)
C27	C26	C25	118.9(3)	C89B N16B C93B	119.3(11)
C26	C27	C28	118.6(3)	C90B N16B C89B	119.7(11)
N5	C28	C27	122.3(3)	C90B N16B C93B	120.8(11)
O9	Cu3	O3W	95.34(10)	C97A N17A C98A	120.7(4)
O9	Cu3	O11	93.31(10)	C97A N17A C101	122.2(4)
O9	Cu3	N14	91.69(11)	C101 N17A C98A	112.2(5)
O9	Cu3	N15	169.55(11)	C97B N17B C1A	122.3(10)
O11	Cu3	O3W	93.58(10)	C97B N17B C98B	121.6(11)
O11	Cu3	N14	168.36(11)	C98B N17B C1A	107.9(10)
O11	Cu3	N15	92.44(11)	C99A N18A C102	108.9(6)
N14	Cu3	O3W	96.41(10)	C100 N18A C99A	109.6(5)
N15	Cu3	O3W	93.01(11)	C100 N18A C102	111.1(6)
N15	Cu3	N14	81.11(11)	C1C N18B C1B	111.4(12)
C57	O9	Cu3	128.2(2)	C99B N18B C1B	109.7(10)
C59	O11	Cu3	123.3(2)	C99B N18B C1C	110.7(13)
C63	O12	C64	113.9(3)	C103 N19 Cu4	114.9(3)
C61	N11	C65	118.3(3)	C107 N19 Cu4	125.4(3)
C62	N11	C61	120.5(3)	C107 N19 C103	119.7(4)
C62	N11	C65	121.0(3)	C108 N20 Cu4	114.6(3)
C69	N12A	C70A	129.9(8)	C112 N20 Cu4	126.1(3)

C69 N12A C73A	112.9(8)	C112 N20 C108	119.3(3)
C70A N12A C73A	115.3(8)	N17B C1A C1B	111.5(10)
C69 N12B C70B	108.8(7)	N18B C1B C1A	111.3(11)
C69 N12B C73B	125.7(8)	O13A C85A O14	117.1(6)
C73B N12B C70B	113.6(8)	O13A C85A C86A	119.9(6)
C71A N13A C72A	109.2(7)	O14 C85A C86A	123.0(5)
C71A N13A C74A	108.0(9)	O13B C85B C86B	118.6(11)
C72A N13A C74A	112.2(9)	O14 C85B O13B	133.7(12)
C72B N13B C71B	109.9(6)	O14 C85B C86B	107.7(10)
C74B N13B C71B	114.2(13)	C87A C86A C85A	125.0(6)
C74B N13B C72B	107.7(10)	C90A C86A C85A	116.6(6)
C75 N14 Cu3	115.2(2)	C90A C86A C87A	118.1(7)
C79 N14 Cu3	125.3(2)	C87B C86B C85B	127.5(13)
C79 N14 C75	119.5(3)	C87B C86B C90B	114.1(12)
C80 N15 Cu3	115.2(2)	C90B C86B C85B	118.4(12)
C84 N15 Cu3	125.4(2)	O15 C87A C86A	120.1(7)
C84 N15 C80	119.3(3)	O15 C87A C88A	123.1(7)
O9 C57 C58	119.4(3)	C86A C87A C88A	116.7(6)
O10 C57 O9	122.2(3)	O15 C87B C86B	132.9(13)
O10 C57 C58	118.4(3)	O15 C87B C88B	106.6(11)
C59 C58 C57	124.7(3)	C86B C87B C88B	120.5(14)
C62 C58 C57	116.7(3)	C89A C88A C87A	120.0(7)

C62	C58	C59	118.4(3)	C95A C88A C87A	121.8(8)
O11	C59	C58	125.1(3)	C95A C88A C89A	118.2(8)
O11	C59	C60	117.7(3)	C89B C88B C87B	120.0(13)
C58	C59	C60	117.2(3)	C95B C88B C87B	123.1(15)
C61	C60	C59	119.9(3)	C95B C88B C89B	116.8(13)
C67	C60	C59	120.1(3)	N16A C89A C88A	119.2(6)
C67	C60	C61	119.9(3)	N16A C89A C91A	119.7(6)
N11	C61	C60	119.6(3)	C91A C89A C88A	121.2(6)
N11	C61	C63	120.0(3)	N16B C89B C88B	118.9(12)
C60	C61	C63	120.4(3)	N16B C89B C91B	117.1(10)
N11	C62	C58	124.3(3)	C91B C89B C88B	123.4(12)
O12	C63	C61	121.4(4)	N16A C90A C86A	125.3(6)
O12	C63	C69	118.5(3)	N16B C90B C86B	126.5(12)
C69	C63	C61	120.2(3)	O16A C91A C89A	122.2(5)
O12	C64	C65	110.8(3)	O16A C91A C97A	116.9(4)
N11	C65	C64	106.8(3)	C89A C91A C97A	120.7(5)
N11	C65	C66	109.9(3)	O16B C91B C89B	123.4(10)
C64	C65	C66	112.8(4)	O16B C91B C97B	118.5(9)
C68	C67	C60	118.3(4)	C89B C91B C97B	117.9(10)
F3	C68	C67	118.0(4)	O16A C92A C93A	110.1(5)
F3	C68	C69	118.0(3)	O16B C92B C93B	108.1(10)
C67	C68	C69	124.0(4)	N16A C93A C92A	106.4(5)

N12A C69 C63	115.5(5)	N16A C93A C94A	110.3(6)
N12A C69 C68	125.5(5)	C94A C93A C92A	112.0(6)
C63 C69 N12B	123.9(5)	N16B C93B C92B	105.3(10)
C63 C69 C68	117.2(3)	N16B C93B C94B	109.9(12)
C68 C69 N12B	117.0(6)	C94B C93B C92B	114.2(12)
N12A C70A C71A	113.1(10)	C96A C95A C88A	119.2(7)
N12B C70B C71B	109.5(8)	C96B C95B C88B	119.7(14)
N13A C71A C70A	108.4(8)	F4A C96A C95A	118.6(6)
N13B C71B C70B	108.2(10)	F4A C96A C97A	116.6(6)
N13A C72A C73A	112.8(8)	C95A C96A C97A	124.8(6)
N13B C72B C73B	113.6(8)	F4B C96B C97B	118.9(10)
N12A C73A C72A	106.3(10)	C95B C96B F4B	116.2(11)
N12B C73B C72B	102.9(10)	C95B C96B C97B	124.7(12)
N14 C75 C76	122.0(3)	N17A C97A C91A	120.0(5)
N14 C75 C80	114.4(3)	N17A C97A C96A	124.2(5)
C76 C75 C80	123.6(3)	C91A C97A C96A	115.7(5)
C75 C76 C77	118.4(3)	N17B C97B C91B	118.7(10)
C78 C77 C76	118.9(3)	N17B C97B C96B	125.0(10)
C79 C78 C77	119.3(3)	C96B C97B C91B	116.3(10)
N14 C79 C78	121.9(3)	N17A C98A C99A	107.9(5)
N15 C80 C75	114.0(3)	N17B C98B C99B	111.3(11)
N15 C80 C81	121.5(3)	N18A C99A C98A	111.0(5)



C81	C80	C75	124.5(3)	N18B C99B C98B	112.3(13)
C82	C81	C80	119.1(3)	N18A C100 C101	110.8(5)
C81	C82	C83	119.0(3)	N17A C101 C100	107.8(5)
C84	C83	C82	119.3(3)	N19 C103 C104	121.4(4)
N15	C84	C83	121.8(3)	N19 C103 C108	114.6(3)
O5	Cu2	O2W	97.63(11)	C104 C103 C108	123.9(3)
O5	Cu2	O7	93.13(10)	C105 C104 C103	118.9(4)
O5	Cu2	N9	90.26(11)	C104 C105 C106	119.7(4)
O5	Cu2	N10	166.59(11)	C105 C106 C107	118.8(4)
O7	Cu2	O2W	91.52(10)	N19 C107 C106	121.5(4)
O7	Cu2	N9	173.25(11)	N20 C108 C103	114.6(3)
O7	Cu2	N10	94.33(10)	N20 C108 C109	121.6(4)
N9	Cu2	O2W	93.81(10)	C109 C108 C103	123.8(4)
N10	Cu2	O2W	93.29(10)	C110 C109 C108	118.7(4)
N10	Cu2	N9	81.24(11)	C109 C110 C111	119.6(3)
C29	O5	Cu2	129.5(2)	C110 C111 C112	118.3(4)
C31	O7	Cu2	124.0(2)	N20 C112 C111	122.5(4)
C35	O8	C36	113.1(2)	O22W O13 O24W	96.8(12)
C33	N6	C37	118.9(2)	O1N N1N O3N	119.6(3)
C34	N6	C33	120.1(3)	O2N N1N O1N	120.3(3)
C34	N6	C37	121.1(3)	O2N N1N O3N	120.2(3)
C41	N7	C42	120.0(3)	O4N N2N O5N	120.2(3)

C41	N7	C45	123.9(3)	O4N	N2N	O6N	120.6(3)
C45	N7	C42	111.7(3)	O5N	N2N	O6N	119.3(3)
C43	N8	C44	110.4(3)	O8N	N3N	O7N	119.4(10)
C43	N8	C46	108.1(3)	O8N	N3N	O9N	119.3(10)
C44	N8	C46	111.1(3)	O9N	N3N	O7N	115.4(7)
C47	N9	Cu2	114.6(2)	O11N	N4N	O10N	131.0(10)
C51	N9	Cu2	125.8(2)	O11N	N4N	O12N	121.2(10)
C51	N9	C47	119.6(3)	O12N	N4N	O10N	105.9(10)
C52	N10	Cu2	114.7(2)				

---